SUBSIDY PLAN MODELING AND OPTIMIZATION FOR THE PROMOTION OF GREEN TECHNOLOGIES IN MARITIME TRANSPORTATION

JINGWEN QI

MPhil

The Hong Kong Polytechnic University

2021

The Hong Kong Polytechnic University

Department of Logistics and Maritime Studies

Subsidy plan modeling and optimization for the promotion of green technologies in maritime transportation

JINGWEN QI

A thesis submitted in partial fulfillment of the requirements for the degree of Master of Philosophy

May 2021

CERTIFICATE OF ORIGINALITY

I hereby declare that this thesis is my own work and that, to the best of my knowledge and belief, it reproduces no material previously published or written, nor material that has been accepted for the award of any other degree or diploma, except where due acknowledgement has been made in the text.

____________________(Signed)

JINGWEN QI (Name of student)

Abstract

Environmental protection and sustainable development are recognized as one of the major issues in the maritime industry. Various green technologies have been developed to alleviate the ship emission problem. In this thesis, we focus on the promotion of two of the comparatively common technologies, namely shore power and using liquefied natural gas (LNG) as marine fuel. Government subsidies are powerful tools for the promotion, but existing studies on them stop at qualitative analysis or policy evaluating. In this thesis, we aim to fill the gap and study the subsidy plan modeling and optimization for the promotion of shore power and LNG as marine fuel. The thesis consists of three studies.

Chapter 2 focuses on the application of subsidies in the promotion of shore power and obtains the optimal subsidy design for the port to encourage ships to use shore power while berthing. The trade-off between the environmental benefits and subsidy expenses is the main issue to be addressed. Considering the characteristics of the port, including the unit environmental benefits of emission reduction, the electricity price, and the historical data of ship visits, a stochastic model was built to describe the problem. We make full use of existing data of ship visits to make an approximation of the visits in the coming year, which is a closer estimate than that of existing relevant studies. Taking advantage of the problem structure, we convert the model into a deterministic one by applying sample average approximation (SAA) and binomial distribution. Next, without the loss of generality, we reformulated the model and made the model tractable so that it could be solved by CPLEX. Abundant numerical experiments were conducted to validate the model and show the influence of values of crucial parameters on the optimal solution. We summarized useful

managerial insights from the numerical experiment results and sensitive analysis.

Chapter 3 investigates the government subsidy plan optimization for LNG as fuel for maritime transportation. In this problem, the government provides subsidies for ports and ship operators to cover part of the LNG bunkering station construction cost and ship conversion cost. With the aim to maximize the net benefit, namely the environmental benefit minus the subsidy expenditure, the government needs to decide the amount of subsidies to be offered. Given the relationships between different parties, we abstract the problem into a trilevel programming model that consists of the government, port, and ship levels. Taking advantage of the behavior rules of ship operators, we convert the bilevel (port level and ship level) problem into an equivalent single-level problem. Then, with a enumeration algorithm, we identify the optimal subsidy plan for the government. The proposed model and solution method were validated by a series of numerical experiments with realistic parameters.

Chapter 4 explores the LNG bunkering station deployment problem. Due to the limited annual budget, the government cannot build LNG bunkering stations at all ports in the area at a time. In practice, it will take several years to complete the building of LNG bunkering system. Despite that the ports at which LNG bunkering stations will be built are predetermined, the specific construction sequence are flexible, as well as the construction situation in each period. Considering that ship routes in the area have different port of calls, ship emission of each route also varies with the construction sequence. Therefore, this chapter aims to identify the optimal construction sequence that minimizes the total ship emission in the construction period. A two-stage method is proposed to solve the problem. In the first stage, we reduce the number of potential optimal solutions of each ship route, and in the second stage, decision matrices are adopted to indicate the choice of shipping lines and convert the bilevel problem into a single-level problem that can be solved by CPLEX after linearization. Comparison between the results of the two-stage method and a greedy algorithm shows the superiority of our method.

Keywords: Maritime transportation; Liner shipping; Multilevel programming; Government subsidy; Stochastic problem; Shore power; Liquefied natural gas (LNG)

Acknowledgements

I would like to express my gratitude to my supervisor Dr. Shuaian Wang for his invaluable support during the last two years in academic research as well as other aspects of life. All my works would not be possible without Dr. Wang's guidance. I would also like to thank Prof. Pengfei Guo, Prof. Li Jiang, Dr. Meifeng Luo, Dr. Achim I. Czerny, and many others, for their lectures offer essential knowledge and skills in conducting research. My friends in LMS also provide essential help.

Special thanks go to the staff in the General Office of LMS and the Research Office for their assistance in my study and life at PolyU. Finally, I would like to thank my parents for their endless love and support. I would never be able to finish my thesis and come to this point of life without their company and encouragement.

Table of Contents

List of Figures

List of Tables

Chapter 1

Introduction

Shipping has been playing the role of the backbone of both international and domestic trade. Although the annual growth rate of international maritime trade volume has dropped from 2.8% in 2018 to 0.5% in 2019, the volume has reached 11.08 billion tons in 2019 (UNCTAD 2020). On the other hand, traditional marine fuels are dirty and contain high levels of impurities, such as sulfur and nitrogen. Combining the two facts mentioned above, ship emissions have become a major social concern. According to the Fourth International Maritime Organization (IMO) Greenhouse Gas Study (Faber et al. 2020), the shipping industry is responsible for 15% of the nitrogen oxides (NO_X), 13% of the sulfur dioxide (SO_2), and 2.7% of the carbon dioxide (CO_2) emitted through human activities. The numbers are even higher in coastal areas. For example, ship emissions contribute heavily to air pollution in European countries, being responsible for up to 24% of nitrogen dioxide (NO_2) emissions in the Netherlands and 30% of sulfate (SO_4^{2-}) emissions in Italy (Viana et al. 2014). In the Review of Maritime Transport 2019 (UNCTAD 2019), commissioned by the United Nations, environmental concerns were recognized as a major issue in the maritime industry for 2019–2024. According to the estimates of Sofiev et al. (2018), maritime industry emissions, including SO_2, CO_2, NO_X, and particulate matter (PM_X), are to blame for at least 250,000 deaths and 6.4 million childhood asthma cases per year.

To reduce the air pollution caused by shipping emissions, stringent regulations on the quality of bunker fuels have recently come into effect. Since January 1, 2020, fuel oils used onboard have been required to contain no more than 0.5% of sulfur in mass, according to ship emission regulations under the IMO's International Convention for the Prevention of Pollution from Ships (MARPOL) Annex VI, unless emission reduction technologies capable of achieving an equivalent effect have been applied. Quality restrictions on bunker fuels used by vessels in emission control areas (ECAs) and inland river areas are even more stringent. At present, there are four main ECAs around the world: the Baltic Sea area, the North Sea area, the North American area and the United States Caribbean Sea area. In these ECAs ships have to burn fuel with 0.1% or less sulfur from 1 January 2015 (International Maritime Organization 2018). Besides, ships are required to use fuel with no more than 0.1% sulfur in mass while berthing at ports within the European Union (European Union 2016). Moreover, according to the Law of the People's Republic of China on the Prevention and Control of Atmospheric Pollution (The National People's Congress of the People's Republic of China 2018), ships that sail along China's inland rivers must use regular diesel oil available on the market, which contains no more than 0.005% sulfur; such oil is highly expensive.

In addition to lower-sulfur fuels, there are other approaches available for ship operators to obey relevant regulations, including shore power that is used while berthing, sulfur scrubbers that clean ship emissions before release, internal engine modifications that control the production of NO_X in the combustion process, and alternative energy sources such as biofuels, wind and solar power, LNG and hydrogen fuels as bunker fuel (New South Wales Environment Protection Authority of Australia 2015). Among all alternative methods, shore power and LNG as marine fuel can obviously reduce ship emissions and are relatively common.

Shore power, also known as "shore-side power," "on-shore power supply," "shore-to-ship power," "alternative maritime power," "cold-ironing," and "high-voltage shore connections (HVSC)," is the technology that allows ships to shut down their auxiliary engines and use the electricity provided by the port to power on-board machines. This approach moves the power production from dirty onboard sources to greener and more efficient large-scale power stations, and can therefore decrease ship emissions and bring environmental benefits. According to New South Wales Environment Protection Authority of Australia (2015), shore power can reduce ship emissions while berthing by up to 95%. In order to promote the use of shore power, governments of various countries and areas have approved regulations to support the installation of shore power facilities, including onboard facilities and onshore facilities. To be specific, some of the governments provide subsidies to ports and ships in order to cover part of the shore power system installation cost (The Government of Canada 2017, Ministry of Transport of the People's Republic of China 2017, Shenzhen Transportation Commission 2014, European Executive Agency for Competitiveness and Innovation 2009). However, the price of shore power are not competitive compared with the cost of using auxiliary engines, and the ship operator always choose the traditional way because its cheaper (Li 2019, European Commission 2019). Therefore, efficient government subsidies that encourage ship operators to use the shore power facility as much as possible are needed.

LNG is natural gas (predominantly methane with some admixture of ethane) that has been cooled to $-162°C$ and stored in liquid form for ease and safety during non-pressurized storage or transport (Aneziris et al. 2020). LNG has been recognized as the cleanest fossil energy for ship use on Earth. The products of the full combustion of pure LNG are CO_2 and water (H_2O). Compared with ships powered by traditional bunker fuel oil, LNG-fueled ships generate much lower emissions. Studies have found that LNG reduces SO_X and PM by nearly 100%, NO_X by up to 85–90%, and CO_2 by 15–20% (Wang and Notteboom 2014, New South Wales Environment Protection Authority of Australia 2015). Therefore, using LNG as bunker fuel can significantly reduce ship emissions and alleviate air pollution problems. However, the application of LNG-fueled ships are still quite limited. One of the main reasons is the lack of a complete LNG bunkering system (Wang and Notteboom 2014, Acciaro 2014).

Currently, the construction of LNG bunkering system is hindered by the "chicken and egg" problem faced by all alternative fuels (Lim and Kuby, Ko et al. 2017). Today, at an early stage in the introduction of LNG as bunker fuel, many ship operators refuse to retrofit their ships with LNG engines without adequate bunkering stations. At the same time, insufficient LNG refueling demand leaves bunkering stations idle, wasting the investment in building them. As the emission reductions brought by the adoption of LNG-fueled ships would improve air conditions along major shipping routes, governments have the motivation to provide subsidies to resolve the "chicken and egg" problem and encourage the adoption of LNG as bunker fuel.

Previous studies on the government subsidies used to encourage the adoption of these two green technologies stop at qualitative or rough quantitative analysis. The characteristics of different areas and ships sailing through them are not considered, and the specific form and amount have not been investigated in deep yet. To fill the gaps between academic research and the practical needs, this thesis investigates the subsidy plan modeling and optimization for the promotion of shore power and LNG as marine fuel in maritime transportation. In this thesis, we take the advantage of characteristics of different areas and aim to find out the optimal subsidy plan that can maximize the benefit or minimize the maritime emissions. Decisions of different parties in the application of shore power and LNG as marine fuel, namely port authorities, ship operators, and the government, are integrated.

This thesis consists of the following five parts:

(i) In Chapter 1, we introduce the background of the green technologies and issues that hinders the extensive use of them.

(ii) In Chapter 2, we address the optimal subsidy design problem for the port to encourage ships to use shore power while berthing with stochastic ship visits. Considering the characteristics of the port, a stochastic model was built to balance trade-off between the environmental benefits and subsidy expenses. A tailored solution method that is based on SAA and binomial distribution was applied to reformulated and make the model tractable without loss of generality. A great number of numerical experiments validate the model and solution method we proposed. Useful managerial insights are obtained from the sensitive analysis.

(iii) In Chapter 3, we consider that that the government provides subsidy for ports and ship operators to stimulate the LNG bunkering station construction and ship conversion. We propose a trilevel programming model that consists of the government, port, and ship levels to maximize the government's net profit. A tailored method is proposed to convert the bilevel (port level and ship level) problem into an equivalent single-level problem. Embedded in an enumeration algorithm, the method significantly reduces the difficulty of solving the problem. A series of numerical experiments with realistic parameters were conducted to show the significance of this study.

(iv) In Chapter 4, we figure how to arrange the LNG bunkering station construction works with a limit annual budget. A bilevel programming model with the objective to minimize the total ship emission through the planning period is presented. Based on the problem structure characteristics, a two-stage method is proposed to handle the bilevel structure and linearize the model. Numerical experiments based on real data were carried out to show the effectiveness of the model and bilevel method.

(v) In Chapter 5, we present main findings obtained from the three studies above and discuss future research directions.

Chapter 2

Optimal Subsidy Design for Clean Energy Usage in Berthing Operations

2.1 Introduction

2.1.1 Background

A generic shore power system consists of three elements: the shore-side power supply system, the shore-ship connecting system, and the ship-borne power receiving system (Chen et al. 2019). Figure 2.1 shows the structure of a generic shore power system. As we can see from the picture, the shore-side system receives electricity from the power grid and transfer it to the ship-side facility through the shore-ship connecting system that consists of cables joining the onshore power supply interface to the power receiving interface onboard.

Both shore-side and ship-side facilities are indispensable to the successful application of shore power. The willingness of ship operators to use shore power is the critical factor that decides how much environment benefits can be achieved and one of the barriers to the extensive use of shore power (Ballini and Bozzo 2015, Vaishnav et al. 2016, Qi et al. 2020). However, for economic reasons, ships with an on-board

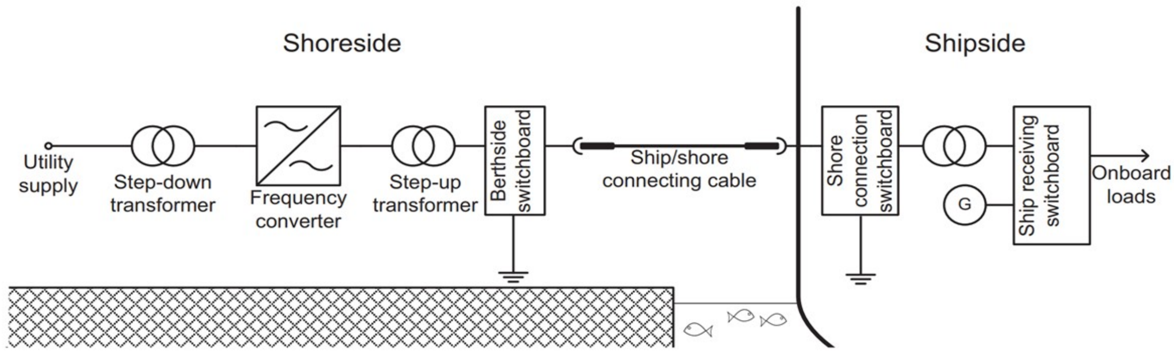

Figure 2.1: A generic shore power system (Sciberras et al. 2015)

shore power system are not always willing to use it. In areas with regulations aiming at reducing ship emissions at ports, for example the United Kingdom (Department of Transport 2019) and California (California Air Resources Board 2020), the utilization rate of shore power system is higher than that of areas without such regulations. In those areas, many ship operators refuse to use shore power because it is expensive, and as a result the emission reduction effect is not obvious. Economic subsidies are promising methods to promote the shore power usage, and they have been used by the government in other incentive programs under government policies (Zhuge et al. 2019, 2020). Hence, the introduction of subsidies that can make shore power more economical and increase the usage rate of existing shore power facilities is a pressing need (Ship Technology 2017, Chen et al. 2019, Radwan et al. 2019). At present, such policies are implemented in various forms. The first form is the preferential shore power price. This method is straightforward: it reduces the price of shore power and hence makes it more economical than the traditional method of electricity generation during the berthing period. Another measure is to subsidize ship operators for each time they use shore power. In this chapter, we consider the environmental impact as well as the economic gain and loss for ports in order to investigate the design of specific shore power incentive policies, including the shore power price and the subsidy amount.

2.1.2 Current Shore Power Subsidy Policies

For ports, the cost to provide shore power usually covers two parts: the electricity cost charged by the power company and the equipment maintenance cost. Marine diesel oil (MDO) is a low-sulfur fuel frequently used to abide by the 0.1% sulfur content regulation, and the cost of using it can be regarded as a standard by which to measure the cost-effectiveness of shore power for ship operators. As summarized in Li (2019), for ports along the coastline of China, shore power is provided at the rate of 1.2–1.4 CNY/kWh (approximately 0.17–0.2 USD/kWh), which is close to the cost of generating power by consuming MDO, 1.24–1.84 CNY/kWh (approximately 0.17–0.26 USD/kWh). Nevertheless, the price is not very attractive, considering the extra manpower and time for the cable connection and disconnection for ships to adopt shore power (Li 2019). Therefore, multiple local governments in China have established regulations to encourage the usage of shore power.

More specifically, ports in Shenzhen sell shore electricity to ships at the government guided price closely related to the MDO bunkering price (Shenzhen Municipal Committee of Communication 2019), which ensures that the cost of using shore power is a fraction(50% in 2020) of the cost of using MDO while berthing. In addition, for shipping companies that adopt shore power at more than 10% of their visits to ports in Shenzhen, a subsidy (800–2000 CNY, approximately 122–306 USD) will be granted for each visit that uses shore power. In Shanghai, ships from companies that have joined the Shanghai Port Green Convention and promised to use shore power can enjoy the shore power service at a favorable price while visiting international container terminals and cruise terminals. This favorable price is decided by the government and is positively related to the MDO marine fuel oil closing price at the end of the month in Singapore's Platts open market Shanghai Government (2019).

In the European Union, one of the main barriers to the promotion of shore power is related to taxation policies. Ships berthing at ports in the European Union have to pay taxes applied to electricity for shore power, while the electricity generated by the auxiliary engines onboard is tax-exempt. This difference makes electricity generation on-board cheaper than the shore power (European Commission 2019).

To remove this obstacle, some member states of the European Union, including Sweden, Germany and Denmark, have decided to apply a reduced tax rate on shore power for ships (Offshore Energy 2018). The reduction in tax rate lowers the cost of using shore power and increases its competitiveness.

However, the application of policies, including the shore power price, the subsidy amount, and the reduced tax rate, has not been covered by existing studies as an optimization problem from the standpoint of a single port. Most of the existing incentive policies are made by the government and all ports in the territory should follow the same policies. Since the decision of whether to use shore power is made for each ship visit, the operation situations of berthing ships are critical to the policy decision. Meanwhile, each port has its own location and strategy, as a result the distributions of berthing time and the emission volume of ship visits vary significantly. Therefore, not all ports can maximize their benefits minus their costs by applying such uniform policies. In this chapter we take the advantage of the historical data of a port to approximate the frequency of future visits and customize the optimal incentive policies for the port, namely the shore power price and subsidy amount for each time the shore power is used.

2.1.3 Literature Review

From the perspective of a port, it is an optimization problem to determine its shore power price, as well as the amount of subsidy to be provided. In order to obtain the optimal incentive measures, the port needs to maximize a function equal to the total benefits minus the costs, which can be calculated as environmental benefits plus shore power selling revenues, minus extra electricity cost and subsidies given to ship visits that use shore power. In existing studies focusing on the economic aspect of shore power (McArthur and Osland 2013, Song 2014, Wang et al. 2015, Winkel et al. 2015, Innes and Monios 2018), ship visits' berthing time, emission volumes, electricity demands and other related information are assumed to be known. However, details of coming visits are uncertain until the ship leaves, which involve stochastic parameters such as berthing times and emission volumes. As for the value of these parameters of visits, academic studies and technical reports usually make two types of assumptions. One is to use the average value for all visits (Song 2014, Song and Li 2017, Wang et al. 2015), the other is to divide ships into several categories of homogeneous vessels (McArthur and Osland 2013, Winkel et al. 2016, Innes and Monios 2018, Starcrest Consulting Group 2019) and use the same value for all vessels in the same category. However, in practice the parameters of future visits may differ substantially from those observed in the past. Therefore, the aforementioned assumptions about parameter values of visits are not sufficiently accurate to approximate reality.

This chapter aims to fill this research gap and figure out how to make use of the information of historical ship visits of the port to approximate the possible situations of future visits and determine suitable shore power incentive policies. The main contributions of this chapter are as follows:

- In this chapter, we take the uncertainty of visiting ships' operation situations into account. Unlike previous studies, we obtain the optimal subsidy amount that can maximize the port's net benefit, considering its characteristics.
- We develop a stochastic programming model to describe the problem. Then a tailored solution method based on SAA method and binomial distribution is proposed to convert the model and make it tractable.
- Extensive numerical experiments were conducted to demonstrate the necessity of the study. Useful managerial insights were summarized from the numerical experiment results and sensitive analysis.

The remainder of the chapter is organized as follows. Section 2.2 provides the formal problem description and the mathematical model. Section 2.3 describes how the stochastic model is converted into a small-scale mixed integer linear program. Numerical experiments and results are presented in Section 2.4. The thesis closes with conclusions in Section 2.5.

2.2 Mathematical Model

In this section, we first provide a general model for the problem. This is followed by a model based on historical data.

2.2.1 General Model

In this chapter we consider a port that has already installed shore power facilities and provides shore power service to ships. Some of the ships that visit the port are equipped with onboard shore power facilities, but not all of them use shore power at the port. To encourage these ships to use shore power as much as possible, the port has decided to provide shore power at an attractive price and a subsidy to ship operators for each visit that uses shore power. Therefore, the port focuses on determining the optimal shore power price and the subsidy amount. Because a ship visits various ports on its route, the shore power price and subsidy at a single port have little effect on the decision of the ship operator on whether to install onboard shore power facilities or not. In other words, the shore power subsidy policy has little effect on ships currently without shore power facilities. Therefore, this chapter only considers ships with shore power facilities. In the following, "ships" refers to ships that have onboard shore power facilities, and "ship visits" refers to visits made by ships with shore power facilities.

Considering that the trade volume and the port throughput are seasonal, we work with a one-year planning horizon. A port with a set $\mathcal{V}$ of ship visits in a year has to determine the subsidy amount s and the shore power price p. In order to obtain an optimal decision, the port needs to balance the environmental benefits of emission reduction, the revenue of selling electricity to ships, the cost of electricity purchasing, and the subsidy for visits using shore power. The port obtains B USD of environmental benefits per ton of emissions reduction. At the same time, it costs the port C_E USD per kWh to purchase the electricity consumed by ship visits as shore power.

Because some details of a ship visit are uncertain before departure from the port, they are represented by a series of random parameters. The i^{th} visit consumes $\tilde{E}_i$

kWh electricity, $i \in \mathcal{V}$. There are two options for the ship operator. One is to use auxiliary engines onboard to generate electricity, in which case $\tilde{Q}_i^F$ tons of MDO will be used to generate one kWh of electricity, and $\tilde{Q}_i^F \times \tilde{E}_i$ tons of MDO will be consumed during the berthing period. As a result, the visit will emit $\tilde{Q}_i$ tons of exhaust gases in total. The other option is to connect to the shore power system and use electricity provided by the port. The decision of the i^{th} visit whether to use shore power is denoted by a binary decision variable x_i. From the perspective of ship visits, besides the cost of shore power fee, there is also a disutility to use shore power due to the extra manpower and time needed for the cable connection and disconnection. Since the proficiency of crew members needed related to shore power usage varies from one visit to the next, the i^{th} visit chooses to use shore power only when the benefits of doing so is at least equal to the disutility $\tilde{D}_i$. In this section, we develop a mathematical model $[M1]$ to describe the stochastic problem. First we present the list of notations that will be used before giving the model.

Deterministic parameters

$\mathcal{V}$	the set of ship visits, $\mathcal{V} = \{1, ..., \lvert\mathcal{V}\rvert\}$, in which i represents the i^{th} ship visit;
B	the average environmental benefit of emissions reduction (USD/ton), equal to the economic value of emissions' environmental pollution;
P_F	the price of MDO (USD/ton);
C_E	the cost of providing electricity to ships (USD/kWh), equal to the electricity generating cost;
α, β	confidence parameters in chance constraint, which are determined by the port and represent the port's requirement on the ratio of the ship visits that use shore power;
M	a large positive number.

Random parameters

$\tilde{Q}_i$	the emission volume of the i^{th} ship visit when MDO is used during berthing (ton);
$\tilde{E}_i$	the electricity demand of the i^{th} ship visit while berthing (kWh);

$\tilde{Q}_i^F$	the MDO volume that is consumed during the i^{th} ship visit to generate one kWh of electricity (ton/kWh);
$\tilde{D}_i$	the disutility brought by the shore power usage (USD) for the i^{th} ship visit.

Decision variables

x_i	binary variable, equal to 1 when the i^{th} ship visit uses shore power, 0 otherwise;
s	the subsidy for each ship visit that uses shore power (USD);
p	the price of shore power (USD/kWh).

In the following model $[M1]$ we optimize the subsidy policy that consists of two parts: one is the subsidy awarded for each visit that uses shore power, and the other is the shore power price that is attractive to ship operators. Since the purpose is to stimulate ship operators to use their shore power facilities as much as possible, it is reasonable to set the price according to the cost incurred to generate power using MDO, like some existing policies do. However, the MDO volume required to generate one kWh of electricity varies from ship to ship. Meanwhile the shore power should be provided to all ship visits at the same price. Therefore, in $[M1]$ the shore power price is a decision variable but there is no fixed ratio of the shore power usage cost to the MDO cost. As the shore power utilization will lead to some disutility, for example the extra connection and disconnection processes, it is assumed that ship operators will put their shore power facilities to use when the economic benefit exceeds the disutility. Here we present the stochastic model $[M1]$:

$$[\boldsymbol{M1}] \quad \text{maximize } Z = \mathbb{E}\left\{\sum_{i\in\mathcal{V}} \left[\tilde{Q}_i B + \tilde{E}_i(p - C_E) - s\right] x_i\right\} \tag{2.1}$$

subject to

$$\Pr\left\{\left(\sum_{i\in\mathcal{V}} x_i \Big/ |\mathcal{V}|\right) \geq 1-\alpha\right\} \geq 1-\beta \tag{2.2}$$

$$\tilde{E}_i(\tilde{Q}_i^F P_F - p) + s - \tilde{D}_i - M x_i \leq 0, \quad \forall i \in \mathcal{V} \tag{2.3}$$

$$\tilde{D}_i - \tilde{E}_i(\tilde{Q}_i^F P_F - p) - s - M(1 - x_i) \leq 0, \quad \forall i \in \mathcal{V} \tag{2.4}$$

$$x_i = 0, 1, \quad \forall i \in \mathcal{V} \tag{2.5}$$

$$s \geq 0 \tag{2.6}$$

$$p \geq 0. \tag{2.7}$$

The objective function (2.1) maximizes the expected value of the profit from all ship visits, which equals the revenue minus the cost. Constraint (2.2) is a chance constraint which means that with a probability at least equal to $1 - \beta$, no less than a proportion $1 - \alpha$ of visits will chose to use shore power. Constraints (2.3) and (2.4) guarantee that ship visits only use shore power when the profit of using it exceeds the disutility. Constraints (2.5)–(2.7) define the domains of the variables.

One of the main challenges in solving $[M1]$ is that, in practice, the exact distributions of the parameters are unknown. Therefore, we use distributions summarized from existing ship visit data as surrogates for the actual unknown distribution of parameters.

2.2.2 Model Based on Historical Data

To obtain empirical distributions of the random parameters, the port collects data from a set of existing visits denoted by $\mathcal{V}'$. The known parameters associated with ship visits in $\mathcal{V}'$, indexed by l, are listed below:

Notations for historical visits

$\mathcal{V}'$	the set of existing visits;
Q'_l	the emission volume when MDO is used during berthing (ton) of the l^{th} existing visit;
E'_l	the electricity demand while berthing (kWh/visit) of the l^{th} existing visit;
${Q'}_l^F$	the MDO volume consumed to generate one kWh of electricity (ton/kWh) of the l^{th} existing visit.
D'_l	the disutility brought by the shore power usage (USD) for the l^{th} existing visit.

We apply the SAA method and consider each existing visit l as a set of possible values of random parameters in a future visit, which means that the random parameters in each future visit will be identical to one set of possible values, and all sets of values have the same probability. Then, the empirical distribution of the random parameters can be described as $\Pr\left(\left(\tilde{Q}_i, \tilde{E}_i, \tilde{Q}_i^F, \tilde{D}_i\right) = \left(Q'_l, E'_l, Q'^F_l, D'_l\right)\right) = 1/|\mathcal{V}'|, \forall l \in \mathcal{V}'$.

We further assume that for different ship visits i, $i \in \mathcal{V}$, the parameters $\left(\tilde{Q}_i, \tilde{E}_i, \tilde{Q}_i^F, \tilde{D}_i\right)$ have independent and identical distribution. As a result, there are $\left|\mathcal{V}'\right|^{|\mathcal{V}|}$ different scenarios for the parameters of all ship visits in the next year. We build $[M2]$ to maximize the expected value of the total port profit from future ship visits with constraints on the shore power usage ratio. Here we list new notations that will be used:

Parameters of scenarios

Ω	the set of possible scenarios of parameters of all ship visits in the next year, $\Omega = 1, ..., \left|\mathcal{V}'\right|^{|\mathcal{V}|}$;
$\hat{Q}_{ij}$	the emission volume of the i^{th} ship visit when MDO is used during berthing in the j^{th} scenario (ton), $\forall i \in \mathcal{V}, \forall j \in \Omega$;
$\hat{E}_{ij}$	the electricity demand of the i^{th} ship visit while berthing in the j^{th} scenario (kWh), $\forall i \in \mathcal{V}, \forall j \in \Omega$;
$\hat{Q}^F_{ij}$	the MDO volume that is consumed to generate one kWh of electricity of the i^{th} ship visit in the j^{th} scenario (ton/kWh), $\forall i \in \mathcal{V}, \forall j \in \Omega$;
$\hat{D}_{ij}$	the disutility brought by the shore power usage (USD) for the the i^{th} ship visit in the j^{th} scenario, $\forall i \in \mathcal{V}, \forall j \in \Omega$.

Decision variables

$\hat{x}_{ij}$	binary variable, equal to 1 when the i^{th} ship visit adopts shore power in the j^{th} scenario, 0 otherwise, $\forall i \in \mathcal{V}, \forall j \in \Omega$;
$\hat{y}_j$	binary variable, equal to 1 when the proportion of ship visits that use shore power in the j^{th} scenario is no less than $1-\alpha$, 0 otherwise, $\forall j \in \Omega$.

Adopting empirical distributions, we convert $[M1]$ into the following model:

$$[\boldsymbol{M2}] \ \text{maximize } Z = \frac{1}{|\Omega|}\sum_{j\in\Omega}\sum_{i\in\mathcal{V}}\left[\hat{Q}_{ij}B + \hat{E}_{ij}(p - C_E) - s\right]\hat{x}_{ij} \tag{2.8}$$

subject to

$$(2.6), (2.7)$$

$$\sum_{j\in\Omega}\hat{y}_j \Big/ |\Omega| \geq 1 - \beta \tag{2.9}$$

$$\sum_{i\in\mathcal{V}}\hat{x}_{ij} - |\mathcal{V}|(1-\alpha) < M\hat{y}_j, \ \ \forall j\in\Omega \tag{2.10}$$

$$|\mathcal{V}|(1-\alpha) - \sum_{i\in\mathcal{V}}\hat{x}_{ij} \leq M(1-\hat{y}_j), \ \ \forall j\in\Omega \tag{2.11}$$

$$\hat{E}_{ij}(\hat{Q}^F_{ij}P_F - p) + s - \hat{D}_{ij} - M\hat{x}_{ij} \leq 0, \ \ \forall i\in\mathcal{V}, \forall j\in\Omega \tag{2.12}$$

$$\hat{D}_{ij} - \hat{E}_{ij}(\hat{Q}^F_{ij}P_F - p) - s - M(1-\hat{x}_{ij}) \leq 0, \ \ \forall i\in\mathcal{V}, \forall j\in\Omega \tag{2.13}$$

$$\hat{x}_{ij} = 0, 1, \ \ \forall i\in\mathcal{V}, \forall j\in\Omega \tag{2.14}$$

$$\hat{y}_j = 0, 1, \ \ \forall j\in\Omega. \tag{2.15}$$

The objective function (2.8) maximizes the expected value of profit from all ship visits in the next year. Constraint (2.9) guarantees that in all scenarios, at least $(1-\beta)|\Omega|$ scenarios have at least $(1-\beta)|\mathcal{V}|$ visits using shore power. Constraints (2.10) and (2.11) state the relationship between the $\hat{y}_i$ and $\hat{x}_{ij}$ variables. Constraints (2.12) and (2.13) mean that in any scenario, a ship visit will adopt shore power only when the benefit of doing it exceeds the disutility. Constraints (2.14) and (2.15) define the domains of $\hat{y}_i$ and $\hat{x}_{ij}$.

Because the random variables in $[M1]$ are replaced by a series possible scenarios in $[M2]$, there exist some differences between the constraints of the two models. For the constraints on the number of ship visits using shore power, in $[M1]$ the lower limit of the probability that each ship visit adopts shore power with probability at least equal to $1-\alpha$ is defined by constraint (2.2). However, in $[M2]$ constraints (2.9)–(2.11) set the ratio of scenarios under which no fewer than $|\mathcal{V}|(1-\alpha)$ visits use shore power to be at least equal to $1-\beta$. The other difference is the ship visits' decision on shore power usage. In $[M2]$, the decision of each ship visit under each scenario is described by constraints (2.14) and (2.15).

To solve $[M2]$ exactly, we would have to enumerate all possible scenarios of the future visits. When $|\mathcal{V}| = 1000$ and $\left|\mathcal{V}'\right| = 100$ there are 100^{1000} scenarios in total, which is impossible to enumerate. Therefore, we need to devise another method to solve the problem.

2.3 Model Reformulation

In this section, we develop a tailored solution method to address the intractable model $[M2]$. We first use a binomial distribution to handle the constraints on the expected number of ship visits that use shore power, thus converting the model into a mixed integer nonlinear program, which is then linearized to be a mixed integer linear program that can be solved by an off-the-shelf solver CPLEX.

2.3.1 Model Conversion

The main difficulty in solving $[M2]$ is the very large number of possible scenarios, which makes the problem computationally intractable. In order to make the problem tractable, we reduce the problem scale without loss of generality. As mentioned, the total number of future visits that use shore power depends on the existing data set. Specifically, given p and s, we denote the number of visits in $\mathcal{V}'$ that use shore power as k, and the probability of a future visit to use shore power is calculated as $k/|\mathcal{V}'|$. We introduce an intermediate decision variable x'_l to denote the decision of visits with different sets of values to use shore power or not.

Intermediate decision variable

x'_l binary decision variable, equal to 1 when the visit with the l^{th} set of values adopts shore power, 0 otherwise.

Then we have

$$k = \sum_{l \in \mathcal{V}'} x'_l. \tag{2.16}$$

From constraint (2.16) we can see that k is closely related to the variables x'_l, which depend on the decision variables p and s. Therefore, k is a function of p and s. For all future visits, we denote the number of visits that use shore power as $\tilde{K}$. For each coming visit, it will adopt shore power with probability $k/|\mathcal{V}'|$ because k out of $\mathcal{V}'$ value sets will lead the visit to use shore power. Hence, the random variable $\tilde{K}$, which equals the sum of $|\mathcal{V}|$ identically and independently distributed binary random variables, is a binomial random variable: $\tilde{K} \sim B\left(|\mathcal{V}|, k/|\mathcal{V}'|\right)$. Constraint (2.9) sets the lower limit of the proportion of scenarios in which more than $|\mathcal{V}|\,(1-\alpha)$ coming visits will use shore power. In constraints (2.10) and (2.11), the variable $\hat{y}_j$ indicates whether the j^{th} scenario has enough visits using shore power or not. Introducing the intermediate decision variable x'_l, we can use $\tilde{K}$ to represent the number of coming visits that will use shore power, and $\hat{y}_j$ become unnecessary. Therefore, constraints (2.9) to (2.11) can be replaced by constraint (2.16) and

$$\sum_{u=\lceil (1-\alpha)|\mathcal{V}| \rceil}^{|\mathcal{V}|} \begin{pmatrix} |\mathcal{V}| \\ u \end{pmatrix} (k/|\mathcal{V}'|)^u [(1-(k/|\mathcal{V}'|)]^{(|\mathcal{V}|-u)} \geq 1-\beta. \tag{2.17}$$

We use $\lceil (1-\alpha)\,|\mathcal{V}| \rceil$ as the lower bound of the summation in constraint (2.17) because $(1-\alpha)\,|\mathcal{V}|$ could be fractional. As shown in constraint (2.17), the left-hand side is strictly monotonically increasing in k. Therefore, we denote the minimal value of k that satisfies constraint (2.17) as k_{min}, which can be obtained by applying a dichotomous search method. Before presenting the logic of this method, we define $f(k) = \sum_{u=\lceil (1-\alpha)|\mathcal{V}| \rceil}^{|\mathcal{V}|} \begin{pmatrix} |\mathcal{V}| \\ u \end{pmatrix} (k/|\mathcal{V}'|)^u [(1-(k/|\mathcal{V}'|)]^{(|\mathcal{V}|-u)} - (1-\beta)$.

Algorithm 1 Dichotomous method for k_{min}

Input: intermediate variable k_L, k_R, k_M, $term$. //k_L, k_R are the lower and upper limits of k_{min}, k_M is the arithmetic mean of k_L and k_R, $term$ is a binary variable that works as the termination condition of the algorithm.

Output: k_{min}

Initialization: initial variables $k_L = 0$, $k_R = |\mathcal{V}'|$, $term = 0$, initial solution $k_{min} = 0$.
while $term = 0$ **do**
    if $f(k_L)f(k_R) < 0$ **then**
        $k_M = \lceil (k_L + k_R)/2 \rceil$
        if $k_R = k_M$ **then**
            $k_{min} = k_R$
            $term = 1$
        else
            if $f(k_M) = 0$ **then**
                $k_{min} = k_M$
                $term = 1$
            else if $f(k_M) > 0$ **then**
                $k_R = k_M$
            else if $f(k_M) < 0$ **then**
                $k_L = k_M$
            end if
        end if
    end if
end while
return k_{min}

In Algorithm 1, we have $f(0) < 0$ and $f(|\mathcal{V}|) > 0$. Keeping $f(k_R) > 0$ and $f(k_L) < 0$, we can iteratively update the values of k_L and k_R by checking the value of $f(k_M)$ until the minimum value of k_R that makes $f(k_R) > 0$ is found. We will prove the following property.

Proposition 2.1. *All values of k that satisfy constraint (2.17) can be enumerated as: k_{min}, $k_{min}+1$, $k_{min}+2$,..., $|\mathcal{V}'|-1$, $|\mathcal{V}'|$.*

Proof. *The smallest value of k that satisfies constraint (2.17) is k_{min} because for $k = 0, 1, ..., k_{min}-1$ we have $f(k) < 0$, and constraint (2.17) is not satisfied. Considering that the left-hand side of constraint (2.17) is strictly monotonically increasing in k, for $k = k_{min}+1, k_{min}+2, ..., |\mathcal{V}'|$ we have $f(k) > f(k_{min}) \geq 0$, and constraint (2.17) is satisfied.*

Then constraint (2.17) can be replaced with

$$k \geq k_{min}. \tag{2.18}$$

In the objective function in $[M2]$, the two sum calculations can be swapped:

$$\text{maximize } Z = \sum_{i \in \mathcal{V}} \sum_{j \in \Omega} \frac{1}{|\Omega|} \left[\hat{Q}_{ij}B + \hat{E}_{ij}(p - C_E) - s\right] \hat{x}_{ij}. \tag{2.19}$$

For each ship visit, there are $|\Omega|/|\mathcal{V}'|$ out of $|\Omega|$ scenarios in which the values of parameters are identical to the l^{th} value set, $l \in \mathcal{V}'$. Therefore, the profit expectation that the port can get from the i^{th} coming visit, $\sum_{j \in \Omega} \frac{1}{|\Omega|} \left[\hat{Q}_{ij}B + \hat{E}_{ij}(p - C_E) - s\right] \hat{x}_{ij}$, can be rewritten as $\sum_{l \in \mathcal{V}'} \frac{|\Omega|}{|\mathcal{V}'|} \frac{1}{|\Omega|} \left[Q'_l B + E'_l(p - C_E) - s\right] x'_l$. Then the objective function (2.19) can be rewritten as

$$\text{maximize } Z = \sum_{i \in \mathcal{V}} \sum_{l \in \mathcal{V}'} \frac{1}{|\mathcal{V}'|} \left[Q'_l B + E'_l(p - C_E) - s\right] x'_l. \tag{2.20}$$

As shown in objective function (2.20), $[Q_l' B + E_l'(p - C_E) - s]\, x_l'$ is not related to i, namely $\sum_{l \in \mathcal{V}'} \frac{1}{|\mathcal{V}'|} [Q_l' B + E_l'(p - C_E) - s]\, x_l'$ equals the same value for different i. Therefore, objective function (2.20) can be rewritten as

$$\text{maximize } Z = \frac{|\mathcal{V}|}{|\mathcal{V}'|} \sum_{l \in \mathcal{V}'} [Q_l' B + E_l'\,(p - C_E) - s]\, x_l'. \tag{2.21}$$

In conclusion, the problem now becomes that of searching for a solution that maximizes the total profit of the port by providing shore power to ship visits with existing value sets, with the constraint that at least k_{min} visits with existing value sets choose to use shore power while berthing, as shown in $[M3]$:

$$[\boldsymbol{M3}] \quad \text{maximize } Z = \frac{|\mathcal{V}|}{|\mathcal{V}'|} \sum_{l \in \mathcal{V}'} [Q_l' B + E_l'\,(p - C_E) - s]\, x_l' \tag{2.22}$$

subject to

$$E_l'(Q_l'^F P_F - p) + s - D_l' - M x_l' \leq 0, \quad \forall l \in \mathcal{V}' \tag{2.23}$$

$$D_l' - E_l'(Q_l'^F P_F - p) - s - M(1 - x_l') \leq 0, \quad \forall l \in \mathcal{V}' \tag{2.24}$$

$$x_l' = 0, 1, \quad \forall l \in \mathcal{V}' \tag{2.25}$$

$$(2.6), (2.7), (2.16), (2.18).$$

The model $[M3]$ is a mixed integer nonlinear program whose size is much smaller than that of $[M2]$.

We denote by p^* and s^* the optimal solution of $[M3]$. We assume that at least one historical visit l satisfies $E_l'(Q_l'^F P_F - p^*) + s^* - D_l' > 0$ because otherwise no subsidy program is needed. We also assume that at least one of p^* and s^* is strictly greater than 0, because otherwise the problem becomes trivial as the port does not need to provide any incentives. After analyzing $[M3]$, we establish the property following:

Proposition 2.2. *For any set of historical ship visits* $\mathcal{V}'$*, at least one visit* l *satisfies* $E_l'(Q_l'^F P_F - p^*) + s^* - D_l' = 0$.

Proof. *Suppose that* $E_l'(Q_l'^F P_F - p^*) + s^* - D_l' \neq 0$, $\forall l \in \mathcal{V}'$. *The objective function of* $[M3]$ *can be rewritten as*

$$\text{maximize } Z = \frac{|\mathcal{V}|}{|\mathcal{V}'|} \sum_{l \in \mathcal{V}'} (Q_l' B + E_l' p - E_l' C_E - s) x_l'. \tag{2.26}$$

As shown in (2.26)*, the objective function consists of four parts, namely the environmental benefits of emissions reduction, the revenue of selling power to ships, minus the cost of power generation, and the subsidy for each visit using shore power. First we define* $\mathcal{V}^*$ *as the set of ship visits that adopt shore power under the optimal solution* s^*, p^**, that is* $\mathcal{V}^* = \{l \in \mathcal{V}' | E_l'(Q_l'^F P_F - p^*) + s^* - D_l' \geq 0\}$.

We construct another solution denoted by $\widehat{s}^*, \widehat{p}^*$ *as follows:* $\widehat{s}^* = s^*$ *and* $\widehat{p}^* = \min\left\{Q_l'^F - (D_l' - s^*)/E_l', l \in \mathcal{V}^*\right\}$. *Note that we have* $\widehat{p}^* > p^* \geq 0$. *With the new solution, all ship visits stick to their decisions to adopt shore power. Therefore, the environmental benefits, the cost of generating shore power and the subsidy amount do not change. At the same time, the total revenue from selling shore power increases by an amount equal to* $\sum_{l \in \mathcal{V}^*} E_l'(\widehat{p}^* - p^*)$. *Overall, the objective function value increases, which contradicts with the assumption that* s^*, p^* *is an optimal solution. Therefore, we must have at least one visit* $l \in \mathcal{V}'$ *that makes* $E_l'(Q_l'^F P_F - p^*) + s^* - D_l' = 0$.

Based on Property 2.2, when the shore power price p (subsidy s) is predetermined as p_{Pre} (s_{Pre}), we can enumerate all possible optimal solutions $\{(p_{pre}, s_l) | E'_l(Q_l'^F P_F - p_{Pre}) + s_l - D_l' = 0, \forall l \in \mathcal{V}'\}$ ($\{(p_l, s_{Pre}) | E'_l(Q_l'^F P_F - p_l) + s_{Pre} - D_l' = 0, \forall l \in \mathcal{V}'\}$) and the objective function value of each solution, denoted by Z_l^s (Z_l^p). After comparing $Z_l^s, \forall l \in \mathcal{V}'$ ($Z_l^p, \forall l \in \mathcal{V}'$), we can obtain the optimal objective function value and the corresponding optimal solution.

2.3.2 Model Linearization

The objective function of $[M3]$ contains the product of decision variables, namely $[Q_l'B + E_l'(p - C_E) - s]\, x_l'$. Therefore, we linearize $[M3]$ by introducing a series of parameters and decision variables before solving it.

Parameter

M_l' the parameter that is large enough, equal to $2(Q_l'B + 2E_l'C_E)$.

Decision variable

z_l' the overall profit the port obtains from a ship visit with the values of the l^{th} set, equal to $Q_l'B + E_l'(p - C_E) - s$ when the visit uses shore power, 0 otherwise.

Then the objective function is converted to

$$[\boldsymbol{M3}] \text{ maximize } Z = \frac{|\mathcal{V}|}{|\mathcal{V}'|} \sum_{l \in \mathcal{V}'} z_l' \tag{2.27}$$

with two sets of constraints added:

$$z_l' - M_l'(1 - x_l') - [Q_l'B + E_l'(p - C_E) - s] \le 0, \quad \forall l \in \mathcal{V}' \tag{2.28}$$

$$z_l' - M_l' x_l' \le 0, \quad \forall l \in \mathcal{V}'. \tag{2.29}$$

The value of M in constraints (2.28) and (2.29) is a sufficiently large number. For any z_l', $l \in \mathcal{V}'$, when $x_l' = 0$, namely the ship visit with the l^{th} set of values does not adopt shore power, constraint (2.28) for l is slack, and constraint (2.29) is equivalent to $z_l' \le 0$. Because the objective function is to find the maximum value, we have $z_l' = 0$. Similarly, when $x_l' = 1$, namely the ship visit does adopt shore power in the l^{th} scenario, constraint (2.29) for l is slack, and constraint (2.28) is equal to $z_l' = Q_l'B + E_l'(p - C_E) - s$.

After the linearization, we obtain a mixed integer linear program with $|\mathcal{V}'| + 2$ decision variables, which can be solved by a generic solver such as CPLEX.

2.4 Numerical Experiments

To validate the model, we conducted multiple numerical experiments with different values of crucial parameters, including α, β, B, C_E, and P_F. CPLEX 12.10 was used to solve the model. Sensitive analyses were carried out to show the influence of different parameters on the optimal objective value.

2.4.1 Parameter Settings

The parameters were determined on the basis of existing studies and reports. We assumed that the following numerical experiments have $10,000$ future ship visits in the next year but only 100 different possible sets of values for random parameters. In this subsection we show how we collected and prepared the parameters and data. Here we give parameters other than the possible value sets of random variables. First, for the average environmental benefit of emission reduction (B), we benefit from existing studies that have researched the social cost factor of emissions from shipping to estimate a general value. According to Nunes et al. (2019) and Song (2014), the social cost factor of different emissions, namely $NO_X, SO_2, PM_{2.5}$, and CO_2, are $6,282$ USD/ton, $11,123$ USD/ton, $61,179$ USD/ton, and 33 USD/ton, respectively. From multiple reports that investigate ship emissions (European Commission 2002, Cooper and Gustafsson 2004, International Maritime Organization 2012, Ng et al. 2016, Smith et al. 2014), we know that exhaust gases from berthing ships contain approximately 2% of NO_X, 0.3% of SO_2, 0.04% of $PM_{2.5}$, and 97.66% of CO_2. Therefore, the overall average environmental benefit of emission reduction (B) equals 216 USD/ton. Considering that the social costs vary widely base on the port location, sensitive analysis on B will be conducted. Referring to the market price, we set the price of MDO at 400 USD/ton ($P_F = 400$ USD/ton). According to Sascha (2017), it costs around 0.18 USD for the power station to generate one kWh of power ($C_E = 0.18$ USD/kWh), using hard coal as the fuel. For the confidence parameters in chance constraints, we set $\alpha = 0.05$ and $\beta = 0.1$.

To validate the model and the algorithm, we constructed two groups of possible value sets, one including 100 sets and the other including 1000 sets, based on the data from the technical report prepared by Starcrest Consulting Group (2019) for the Port of Los Angeles. The ships use their auxiliary engines to generate power by consuming MDO while berthing. We assume that 217 grams of MDO are required for one kWh of power (Cooper and Gustafsson 2004). In other words, we have ${Q'}_l^F = 2.17 \times 10^{-4}$ ton/kWh ($\forall l \in \mathcal{V}'$). The emission volume ($Q'_l$) and electricity demand (E'_l) of the l^{th} historical visit are related to the vessel type, ship capacity and berthing time (Starcrest Consulting Group 2019). Winkel et al. (2015) state that shore power is the most popular among cruise ships, container ships, tankers, reefers, and RORO ships (cargo ships and ferries). In this chapter, we generate a set of historical ship visits on the basis of the ship visit record of the Port of Los Angeles in 2018 (Starcrest Consulting Group 2019) because it is one of the ports with the most developed shore power system (more recent records are not available). In the report, the ship visit data are sorted by vessel type and capacity level, including the power requirement and the berthing time information (minimal, maximal and average values). In this chapter, five different ship types are considered as potential shore power consumers, and we further assume that in each category the number of visits that are equipped with shore power system is proportional to the total number of visits. We generated two groups of possible values for random variables, one with 100 sets and the other with 1000 sets, the number of value sets with each vessel type and each capacity level is proportional to ship visit data from Starcrest Consulting Group (2019), and the electricity demands of visits in each capacity level in the report are also used. Within each capacity level, we generate a series of berthing times that satisfy the minimal, maximal and average values. Considering European Commission (2002), Cooper and Gustafsson (2004), International Maritime Organization (2012), Ng et al. (2016), Smith et al. (2014), we determined that the vessel emits 712.1 grams of exhaust gases to generate one kWh of electricity while berthing for all visits. Then through simple calculations, we obtain Q'_l and E'_l, $l \in \mathcal{V}'$. The disutility brought by the shore power usage is hard to quantify, and there are no existing papers that focus on this problem, so we generated D'_l randomly between 50 to 200 USD.

2.4.2 Results and Sensitive Analysis

Computational experiments were conducted on a LENOVO XiaoXinPro-13IML 2019 laptop with i7-10710U CPU, 1.10 GHz processing speed and 16 GB of memory. The model and the algorithm were implemented in C++ programming. The mixed integer linear model [$M3$] was solved by CPLEX 12.10, and all numerical experiments with 100 value sets were completed within a few seconds, and the numerical experiment with 1000 value sets was completed within 11.5 seconds. We conducted sensitive analysis with the group of possible values with 100 sets, and the details are stated in the following.

We conducted the numerical experiment $N1$ with the data collected and the result shows that the optimal solution is $s_1^* = 200.06$ USD, $p_1^* = 0.087$ USD/kWh, and the port will gain $Z_1^* = 39,398,700$ USD in a year for providing shore power service to ships. In this numerical experiment, k_{min}^1 in constraint (2.18) equals 96 and visits with all possible value sets will opt to use shore power with such shore power price and subsidy amount. We also conducted other numerical experiments with the same parameters, namely $N2$ that the port provides only the favorable shore power price ($s = 0$, $p \geq 0$), $N3$ that the port gives only subsidy to visits that use shore power ($s \geq 0$, $p = C_E$), and $N4$ that the port provides no incentive policies ($s = 0$, $p = C_E$). In addition, the constraint (2.18) on the number of historical visits that use shore power was also removed from $N2$, $N3$, and $N4$. The results of all four numerical experiments are listed in Table 2.1, in which we use the $g_q = \left(Z_q^* - Z_1^*\right)/Z_1^* \times 100\%, q = 2, 3, 4$ to represent the gap between the optimal solution value of $N2$, $N3$, $N4$ and the optimal solution value of $N1$.

From Table 2.1 we can see that the incentive policies have an obvious influence on the port side shore power facilities' usage ratio. With both the favorable shore power price and subsidy for visits that use shore power, visits with all possible value sets choose to use shore power and the port can earn $39,398,700$ USD by providing shore power to ships. Meanwhile, the port can earn $35,902,000$ USD, $982,141$ USD, and 0 USD with only the favorable shore power price, only the subsidy, and no incentive policy applied, respectively. These numbers demonstrate the necessity of

Table 2.1: Results of $N1$, $N2$, $N3$, and $N4$

	$N1$	$N2$	$N3$	$N4$
s_q^* (USD)	200.09	N/A	$2,735.75$	N/A
p_q^* (USD/kWh)	0.087	0.08	N/A	N/A
k_q^* (visit)	100	84	31	0
Z_q^* (USD)	$39,398,700$	$35,902,000$	$982,141$	0
Incentive policy	Favorable shore power price, subsidy	Favorable shore power price	Subsidy	None
Remarks	N/A	$s = 0$	$p = C_E$	$s = 0$, $p = C_E$
g_q	N/A	8.9%	97.5%	100%

the incentive policies and the relevance of our problem.

In $[M2]$, constraints (2.9)–(2.11) reflect the port's expectation of the percentage of ship visits that use shore power. To better understand how this expectation influences the optimal solution, we calculated the value of k_{min} with different values of α and β. And Table 2.2 shows that the value of k_{min} is closely related to the value of α. For a numerical experiment (N), we denote the optimal value of Z by Z^*; for the numerical experiment with the same parameters but without constraints (2.9)–(2.11) (N'), which means that the port focus on the maximization of the total profit and does not care about the shore power usage rate, we denote the optimal value of Z and k as Z_0^* and k_0^*. When the value of k_{min} in $N1$ is higher than k_0^*, the optimal objective value Z^* is most likely to be lower than Z_0^*, and sometimes Z^* can be negative. For example, for a port with $B = 150$ USD, $C_E = 0.18$ USD/kWh and when the price of MDO $P_F = 350$ USD/ton, the optimal solution value without constraints (2.9)–(2.11) is $Z^* = 655,922$ USD with $s^* = 62.25$ USD, $p^* = 0.075$ USD/kWh, and $k^* = 47$. When $\alpha \geq 0.6$ ($k_{min} \leq 41$), the optimal solution remains unchanged, and when $\alpha < 0.6$, namely $k > 50$, there will be a negative correlation between Z^* and α. With $\alpha = 0.2$, $0.1 \leq \beta \leq 0.4$ the port can still earn $295,924$ USD, but the optimal profit becomes negative ($Z^* = -26,822.9$ USD) when $\alpha = 0.05$ and $0.1 \leq \beta \leq 0.4$. Therefore, ports should evaluate the environmental benefits B of emission reduction and the electricity purchasing price C_E to determine the expected proportion of ship visits that use shore power. An unrealistic high expected value may yield a negative profit, which is undesirable.

The environmental benefits B and the electricity cost C_E differ from port to

Table 2.2: k_{min} with different values of α and β

β	α									
	0.05	0.1	0.2	0.3	0.4	0.5	0.6	0.7	0.8	0.9
0.1–0.4	96	91	81	71	61	51	41	31	21	11
0.5–0.9	95	90	80	70	60	50	40	30	20	10

port, and the MDO price P_F also fluctuates, so we conducted sensitive analysis to understand how these parameters affect the optimal solution. A series of numerical experiments with different parameters, as shown in Table 2.3, were conducted to demonstrate the influence of these parameters on the optimal profit (Z^*).

Table 2.3: Ranges of parameter values

Parameter	Range of values
B (USD/ton)	150, 180, 210, 216, 240
C_E (USD/kWh)	0.05,0.1,0.15,0.18,0.2
P_F (USD/ton)	200, 250, 300, 350, 400, 450, 500
k_{min}	10, 11, 20, 21, 30, 31, 40, 41, 50, 51, 60, 61, 70, 71, 80, 81, 90, 91, 95, 96

Specifically, $3,500$ ($= 5 \times 5 \times 7 \times 20$) numerical experiments were conducted. Because it would be tedious to list results of all numerical experiments, we selected two groups of them to show the correlations between the parameters and the objective value. In group 1, denoted by [$G1$], the experiments are conducted with the base case values $B = 150$ USD, $C_E = 0.18$ USD/kWh, and $P_F = 350$ USD/ton. The optimal solution value of the basic numerical experiment without constraints (2.9)–(2.11) is $Z^* = 655,922$ USD with $s^* = 62.25$ USD, $p^* = 0.075$ USD/kWh, and $k^* = 47$. In group 2, denoted by [$G2$], the experiments are conducted with the base case values $B = 210$ USD, $C_E = 0.2$ USD/kWh, and $P_F = 250$ USD/ton. The optimal solution value of the basic numerical experiment without constraints (2.9) to (2.11) is $Z^* = 1,153,180$ USD with $s^* = 61.52$ USD, $p^* = 0.053$ USD/kWh, and $k^* = 46$. For both basic numerical experiments, we changed one parameter at a time and observed the variation of the objective value. In Figure 2.2(a) we only show the results for $k_{min} \geq 50$ because the value of k^* in two numerical experiments was 46 and 47. Figure 2.2(a) shows that Z^* decreases with the value of k_{min}, which is understandable because a higher value of k_{min} means a stricter constraint on k. Figure 2.2(b) shows that there is a positive correlation between Z^* and P_F. The reason is that for a higher P_F, ship visits will be willing to adopt shore power at a higher price p, which leads to a higher shore power selling revenue as well as a higher total profit $Z*$. Meanwhile, Z^* decreases with C_E because the electricity cost of the port goes up with C_E. The correlation is shown in Figure 2.2(c). Lastly, the port tends to earn more with a higher value of B, and this result is also intuitive because B has a positive influence on the environmental benefits for the port.

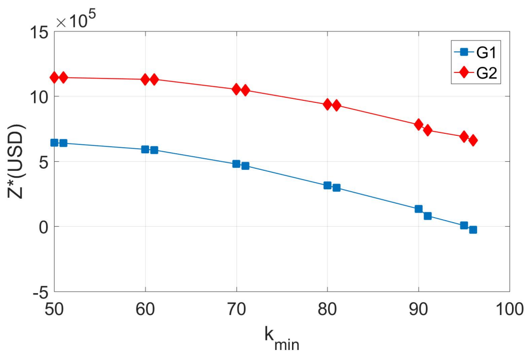

(a)

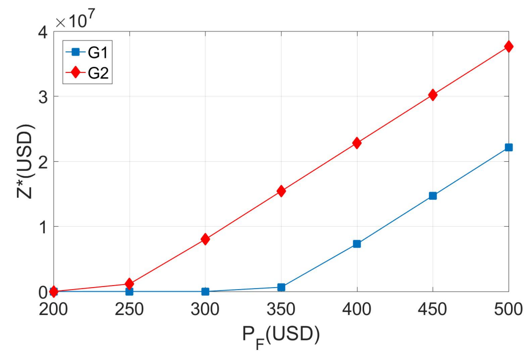

(b)

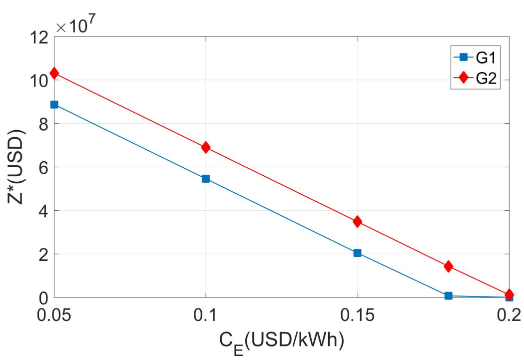

(c)

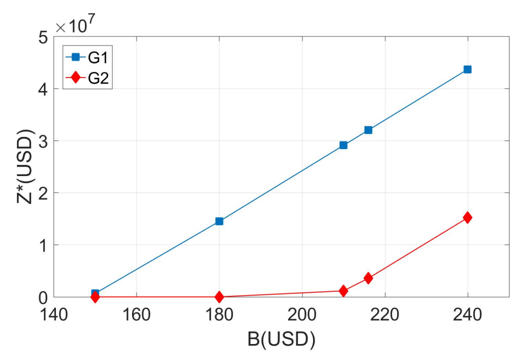

(d)

Figure 2.2: Sensitivity analysis of the parameters

We also found that in some numerical experiments, such as the instance with B = 150 USD/ton, C_E = 0.18 USD/kWh, and P_F = 250 USD/ton, an optimal objective value $Z^* = 0$ was obtained without constraints (2.9)–(2.11). This means that the port cannot gain through the shore power project; also with an expectation of positive shore power usage rate the port will suffer a loss. One of the approaches to reducing emissions from berthing ships and avoiding loss is to lower the electricity price C_E. The port authority could request a government subsidy on the electricity price (Dai et al. 2019). When the electricity is reduced to 0.15 USD/kWh, as the numerical experiment shows, the port could earn $5,574,730$ USD and 99% of the historical ship visits will choose to use shore power and reduce ship emissions.

2.5 Conclusions

Shore power is a practical method for the reduction of ship emissions at berth. However, the existing shore power systems are not frequently used by ships because they are not economical in some scenarios. In order to encourage ships to use their shore power facilities onboard, governments of various countries and regions have implemented incentive policies. In this chapter, we have investigated the problem of shore power incentive policies design, including the shore power price and subsidy amount determination, which has not yet been studied as an optimization problem from the standpoint of a single port. Considering the characteristics of ports, such as the environmental benefits of emission reduction, the electricity price, and the historical data of ship visits, a stochastic model was built to describe the problem. The SAA was applied to the original model. We took the advantage of the existing data of ship visits to make an approximation of the visits in the coming year, which is a closer estimate than that of existing relevant studies. At the same time, binomial distribution was adopted to handle the chance constraint. However, the great number of scenarios of ship visits in a year makes the model computationally intractable. Then, without the loss of generality, we reformulated the model and made the model tractable so that it could be solved by CPLEX.

A large number of numerical experiments with different parameters were conducted to validate the model. Using a comparison based on results obtained when both a favorable shore power price and subsidy are applied, only one of them, and no incentives at all, we have demonstrated that a favorable shore power price and subsidy for visits that use shore power are effective in encouraging ship visits to use shore power and hence reducing ship emissions while berthing. Sensitive analysis has shown that the total profit of the port increases with the environmental benefits of one tonnage of emission reduction and with MDO price; it decreases with the expected number of value sets with which visits would use shore power and with the electricity purchasing price. Our results also suggest that an unreasonably high requirement on shore power usage rate can lead to a negative total profit, so the port should take this fact into consideration when setting the shore power usage ratio requirements. In addition, for ports that cannot benefit from shore power when there is no requirements on usage ratio, government subsidies on electricity price could help encourage shore power usage and reduce ship emissions at berth.

Chapter 3

Government Subsidy Plan Modeling and Optimization for Liquefied Natural Gas as Fuel for Maritime Transportation

3.1 Introduction

3.1.1 Background

The shipping industry plays an important role in international trade, as it is responsible for transporting approximately 90% of the global cargo volume (International Maritime Organization 2019). With the continuous development of maritime transportation, ship emissions, as the by product of that, become a major issue in the maritime industry for 2021–2024 (UNCTAD 2019). Multiple methods haves been developed to alleviate the problem of ship emissions, including low sulfur fuels, sulfur scrubbers, internal engine modifications, and alternative energy sources such as biofuels, wind and solar power, LNG and hydrogen fuels as bunker fuel. LNG is an excellent choice for alternative marine fuels because of its low emission level (nearly no SO_X and PM, 10%–15% of NO_X, and 80%–85% of CO_2 compared to MDO) and high calorific value (13.7 MWh/ton, compared to MDO's 11.6 MWh/ton) (Wang and Notteboom 2014, New South Wales Environment Protection Authority of Australia 2015).

In addition, LNG can lower the operating costs of ships, which encourages ship operators to invest in LNG-fueled ships. LNG is priced more competitively than MDO and marine gas oil (MGO), which are usually adopted by ships to satisfy regulations concerning the sulfur content of marine fuels (International Maritime Organization 2020). According to a study conducted by the IMO (International Maritime Organization 2016), the bunkering price of MDO/MGO is about 25USD/mmBTU[3.1], while the bunkering price of LNG is about 15.5USD/mmBTU. Apart from the bunkering cost, the adoption of LNG as marine fuel can also reduce a ship's maintenance cost, because LNG-fueled engines and related equipment require less maintenance and have a longer service life than traditional ship engines (Oxford Institute for Energy Studies 2018). Given these benefits, several attempts have been made to develop and use LNG-fueled ships. For example, the CMA CGM Group, a world leader in transport and logistics that is committed to energy transition, planned to have 22 LNG fueled container ships in its fleet by 2022. Twelve have been delivered so far, including the world's first 23,000 TEU container ship powered by LNG (CMA CGM Group 2020). However, much remains to be done in terms of developing LNG-fueled ships, and multiple factors still hinder the adoption of LNG as bunker fuel, including the high cost of LNG engines, the extra space required for LNG fuel tank, potential gas leakages and the absence of a complete LNG bunkering infrastructure (Wang and Notteboom 2014, Acciaro 2014). Due to the limited capacity of LNG fuel tanks, a complete bunkering system is necessary for LNG fueled ships.

However, the construction of LNG bunkering stations is hindered by the "chicken and egg" problem faced by all alternative fuels (Lim and Kuby, Ko et al. 2017). Today, at an early stage in the introduction of LNG as bunker fuel, many ship

[3.1] BTU is the abbreviation of "British thermal unit", which is the amount of heat needed to raise the temperature of one pound of water by one degree Fahrenheit. The abbreviation mmBTU means one million BTUs.

operators refuse to retrofit their ships with LNG engines without adequate bunkering stations. At the same time, insufficient LNG refueling demand leaves bunkering stations idle, wasting the investment in building them. As the emission reductions brought by the adoption of LNG-fueled ships would improve air conditions along major shipping routes, governments have the motivation to provide subsidies to resolve the "chicken and egg" problem and encourage the adoption of LNG as bunker fuel. Therefore, in this chapter, we focus on how government subsidies can help popularize the adoption of LNG as bunker fuel and identify the optimal subsidy plan.

In practice, there are two types of LNG-fueled vessels. The first is powered purely by LNG; it is also an LNG carrier and can use natural gas produced during transportation for power (Schinas and Butler 2020). The other is equipped with dual-fuel engines that can switch between traditional bunker fuel oil and LNG during a trip (Fokkema et al. 2017). We consider only dual-fueled ships in this chapter because ships powered purely by LNG are self-sufficient.

3.1.2 Literature Review

Alternative marine fuels are promising methods of alleviating ship emissions (Deng et al. 2021, Ytreberg et al. 2021, Deng et al. 2021). The literature on the application of LNG as marine fuel can be divided into a stream addressing technical problems (Lim and Choi 2020, Aneziris et al. 2020, Milioulis et al. 2021) and a stream addressing management problems (Lim and Kuby, Ko et al. 2017). Studies of technical problems mainly focus on safety issues (Zheng et al. 2017, Park et al. 2018, Aneziris et al. 2020) and efficiency issues (Guan et al. 2017, Altosole et al. 2018, Lim and Choi 2020). The literature on management problems can be further subdivided into studies from the ship perspective and from the bunkering station perspective. From the ship perspective, whether and when to invest in ship retrofitting are common topics (Schinas and Butler 2020). Yoo (2017) focuses on specific ship types and assesses the economic applicability of LNG as a marine fuel for CO_2 carriers. Xu and Yang (2020) study the economic feasibility of LNG-fueled container ships on the Northern

Sea Route under the assumption that an LNG refueling station will be constructed in Sabetta Russia, and evaluate the CO_2 reduction compared with deploying ships powered by conventional fuels on this route. Kana and Harrison (2017) adopt Monte Carlo simulations to extend the ship-centric Markov decision process (Kana et al. 2015) and capture the impact of uncertainties in the economic parameters, ECA regulations, and LNG supply chain on the decision whether to retrofit a container ship as an LNG-fueled vessel. From the bunkering station perspective, studies focus on the bunkering network design and the layout of bunkering stations. Network design studies mainly aim to determine the optimal number and positions of bunkering stations in an area (Ursavas et al. 2020). As for the layout of bunkering stations, bunkering method selection (Tam 2020) and safety zone settling (Park et al. 2018) are frequently discussed. For a detailed review of this literature, please refer to Peng et al. (2021).

The two perspectives focus on either the demand side of LNG (LNG-fueled ships) or the supply side (LNG bunkering stations). However, in practice, the adoption of LNG as marine fuel is still in its infancy, and the two sides are interdependent due to the "chicken and egg" problem (Lim and Kuby, Ko et al. 2017). Therefore, this problem should be investigated from a systematic perspective. Such a perspective is adopted in several papers that investigate the problem of locating stations for alternative fuel vehicles; please refer to Ko et al. (2017) for a detailed review of this literature. Nevertheless, papers that study this problem focus on road transport, which is different from the problem discussed in this chapter for several reasons. First, in road transportation the selection of potential bunkering station positions are more flexible. Second, the vehicles that refuel at bunkering stations are more unpredictable since a large proportion do not travel according to a predetermined schedule. Third, in the problem of locating stations for alternative fuel vehicles, the decision maker try to cover as many paths as possible with estimated alternative fuel demands, rather than taking the interaction between supply side and demand side decisions into consideration. Fourth, in studies that focus on road transport government subsidies are not considered.

In maritime transportation, government subsidies are considered a practical method of promoting the use of green technologies, such as shore power (Wu and Wang 2020). Wu and Wang (2020) consider the interaction between the decisions of port authorities in constructing a shore power system and ship operators in installing onboard shore power facilities. They integrate government subsidies into the problem as a method of encouraging the application of shore power. However, there are several differences between the work of Wu and Wang (2020) and this chapter. First, the objective functions are different. Wu and Wang (2020) aim to maximize the total environmental benefit when the total subsidy amount may not exceed a predetermined budget. In this chapter, we do not have a budget for subsidies, and we maximize the net benefit for the government, namely the environmental benefit minus the subsidy expenditure. Second, subsidy policies are different. In Wu and Wang (2020), the government selects particular ports and ship routes and covers all of their construction or retrofitting costs. In this chapter, the government provides one subsidy rate for all ports and another for all ships, and port authorities and ship operators independently decide whether to conduct the construction or retrofitting. Third, due to the nature of shore power and LNG as marine fuel, the ports in Wu and Wang (2020) make decisions independently, while in this chapter the refueling volumes at different bunkering stations interact with each other. Therefore, in this chapter, all ports are managed by a port group that aims to maximize its total profit. These characteristics lead to essential differences between the model proposed in this chapter and the model used in Wu and Wang (2020), and the solution method proposed by Wu and Wang (2020) is not applicable to the problem in this chapter. In conclusion, although the backgrounds and problem structure of the two papers are similar, this chapter is substantially different from Wu and Wang (2020).

The scientific contribution of this chapter is threefold.

- This is the first study that aims to investigate the subsidy policy optimization problem for LNG as marine fuel. As far as we can determine, papers on the topic to date are limited to qualitative analysis or policy evaluation (Wan et al. 2019).
- We propose a new trilevel model to describe the problem. Decisions of the three

most interested parties involved in the application of LNG are integrated. This model can also be adapted to other alternative marine fuels, such as biofuels.

- A tailored solution method is developed to convert and solve the model. Based on port authorities' and ship operators' behavior, the bilevel problem involving the port-level and ship-level decisions is converted into an equivalent single-level problem, which significantly reduces the difficulty of solving the problem. Then an enumeration algorithm is applied to identify the optimal subsidy plan.

The remainder of this chapter is organized as follows: Section 3.2 gives the problem description and presents the model. Section 3.3 shows how the model is converted and then solved. Our numerical experiments and their results are presented in Section 3.4. Last, Section 3.5 presents our conclusions.

3.2 Model Formulation

A trilevel model that consists of the government, port, and ship levels is proposed in this section. The interrelationships among decisions considered at different levels are clearly described through the trilevel structure.

3.2.1 Problem Description

In this chapter, we consider a river under a government's regulatory regime. A set of physical ports, denoted by $\mathcal{P}$, all of which are managed by a port group, are located along the river. Within the set $\mathcal{P} = \{1, 2, ..., |\mathcal{P}|\}$, 1 represents the physical port farthest downstream and $|\mathcal{P}|$ represents the physical port farthest upstream.

There is a set $\mathcal{V}$ of vessels that sail on this river and fulfill transportation demands between the ports in $\mathcal{P}$. Each ship has its own route, and ships stick to their routes during the time span under consideration. We denote the physical port farthest downstream (the physical port farthest upstream) on the route of ship $j \in \mathcal{V}$ as $MD_j\,(MU_j)$. As shown in Figure 3.1, a route is a closed loop: ship j on its route starts from MD_j, visits ports upstream until MU_j, then reverses direction and finally goes back to MD_j. After returning to MD_j, the ship repeats the route. Because the route along the river is nearly linear, to complete a route, ship j will either visit or pass each physical port between MD_j and MU_j in the order $MD_j, MD_j + 1, ..., MU_j - 1, MU_j, MU_j - 1, ..., MD_j + 1$. We denote these as a new set $\mathcal{P}'_j$ and $k \in \mathcal{P}'_j$ represents the k^{th} port along the route, $k = 1, ..., 2(MU_j - MD_j)$. We further define a binary parameter T_{jk} that equals 1 if the k^{th} port along the route of ship j is visited by the ship and 0 otherwise, and we set a binary parameter B_{jki} that equals 1 if the k^{th} port (no matter whether it is visited or passed) corresponds to physical port $i \in \mathcal{P}$, and 0 otherwise. In the example given in Figure 3.1, the line represents a river along which five physical ports are located; the right-hand side is the downstream end and the left-hand side is the upstream end. The arcs represent the sailing directions of ship j between physical ports; for example, the arc from physical port 2 to physical port 4 means that ship j visits physical port 2 and then sails upstream to visit physical port 4. Physical port 1 is the most downstream port that ship j visits ($MD_j = 1$) and physical port 4 is the most upstream port that ship j visits ($MU_j = 4$). Then, the set of ports along the route of ship j consists of six elements; that is, $\mathcal{P}'_j = \{1, 2, 3, 4, 5, 6\}$. Because ship j does not visit physical port 3 when it sails upstream, we have $T_{j1} = 1, T_{j2} = 1, T_{j3} = 0, T_{j4} = 1, T_{j5} = 1$, and $T_{j6} = 1$. As the corresponding physical ports of the first, second, third, fourth, fifth, and sixth ports on the route are port 1, port 2, port 3, port 4, port 3, and port 2, respectively, we further have $B_{j11} = B_{j22} = B_{j33} = B_{j44} = B_{j53} = B_{j62} = 1$.

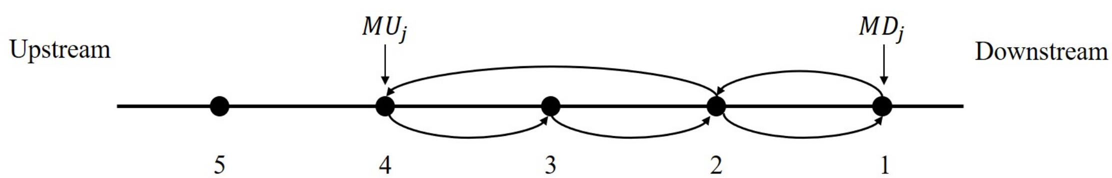

Figure 3.1: An example of the route of ship j

Ship $j \in \mathcal{V}$ sails at the speed of H_j knots (nautical miles per hour). The distance of the voyage from the k^{th} port along the route to the next is denoted by L_{jk}, $k \in \mathcal{P}'_j$. For $k = 1, 2, ..., |\mathcal{P}'_j| - 1$, L_{jk} is the sailing distance from the k^{th} port to the $(k+1)^{\text{th}}$, while $L_{j|\mathcal{P}'_j|}$ represents the sailing distance from the $|\mathcal{P}'_j|^{\text{th}}$ port to the first (i.e., from physical port $MD_j + 1$ to physical port MD_j). Therefore, the total sailing time for the ship to complete a whole route is $\sum_{k\in\mathcal{P}'_j} L_{jk}/H_j$. Other than the sailing time, ship j has to berth for m_{jk} hours at the k^{th} port for cargo handling (if the k^{th} port is not visited, then $m_{jk} = 0$). With a total of S hours of operation time per year, the ship finishes $O_j := S \Big/ \left[\left(\sum_{k\in\mathcal{P}'_j} L_{jk} \Big/ H_j\right) + \sum_{k\in\mathcal{P}'_j} T_{jk} m_{jk}\right]$ trips in a year.

We assume that currently all ships in $\mathcal{V}$ use MDO as the bunker fuel. The price of MDO is U_{MDO} USD/ton, and the combustion of one ton of MDO has a negative environmental impact of E_{MDO} USD. Ship j consumes R^j_{MDO} tons of MDO while sailing one nautical mile and consumes R'^j_{MDO} tons of MDO during berthing for one hour. Apart from the bunker cost, ship j has to pay $\bar{C}^j_{\text{MDO}}$ USD per year for the maintenance of the diesel engine. We denote by G_j the annual revenue of ship j from transporting cargo. Then, the annual profit for ship j is $G_j - \left[\bar{C}^j_{\text{MDO}} + O_j U_{\text{MDO}} \left(R^j_{\text{MDO}} \sum_{k\in\mathcal{P}'_j} L_{jk} + R'^j_{\text{MDO}} \sum_{k\in\mathcal{P}'_j} T_{jk} m_{jk}\right)\right]$, which is assumed to be positive, as otherwise the ship would be likely to exit the market.

Ship j may be retrofitted into dual-fueled, which incurs a fixed retrofitting cost denoted by $\hat{C}^{\mathcal{V}}_j$ (without government subsidy). The annual maintenance cost of the dual-fuel engine is denoted by $\bar{C}^j_{\text{Dual}}$. Ship j, after retrofitting, can switch between MDO and LNG for power. It will require R^j_{LNG} tons of LNG to sail one nautical mile and R'^j_{LNG} tons of LNG to berth for one hour. We assume that the consumption rates of LNG and MDO are proportional; that is, $R'^j_{\text{MDO}} \big/ R'^j_{\text{LNG}} = R^j_{\text{MDO}} \big/ R^j_{\text{LNG}} = R$, $j \in \mathcal{V}$. Therefore, for a ship, consuming 1 ton of LNG means reducing the consumption of MDO by R tons. For instance, according to International Maritime Organization (2016), the net calorific value of MDO is 11.6 MWh/ton and the net calorific value of LNG is 13.7 MWh/ton, and hence $R = 13.7/11.6 \approx 1.18$. Note that ships are not retrofitted yet because of the high retrofitting cost, a lack of LNG bunkering stations at ports, or an insignificant price difference between MDO and LNG.

The negative environmental impact of LNG is much lower than that of MDO. Denote by E_{LNG} the negative environmental impact of one ton of LNG. Since consuming one ton of LNG means reducing the consumption of MDO by R tons, the environmental benefits of consuming one ton of LNG can be calculated as $\Delta_E := R \cdot E_{\text{MDO}} - E_{\text{LNG}}$. Because using LNG as bunker fuel is a promising method of reducing the environmental impact of ship emissions along the river, the government tries to promote the adoption of LNG as bunker fuel by providing subsidies for ports that construct LNG bunkering stations and ships retrofitted as dual-fueled ships. The government's subsidies affect the decisions of the port group on the ports at which to construct LNG bunkering stations, and both the government subsidies and the port group's decisions affect the ship operators' decisions on whether to retrofit their ships as dual-fueled. We model the problem at three levels, namely the government level, the port level, and the ship level, as shown in Figure 3.2 and elaborated in the next three subsections.

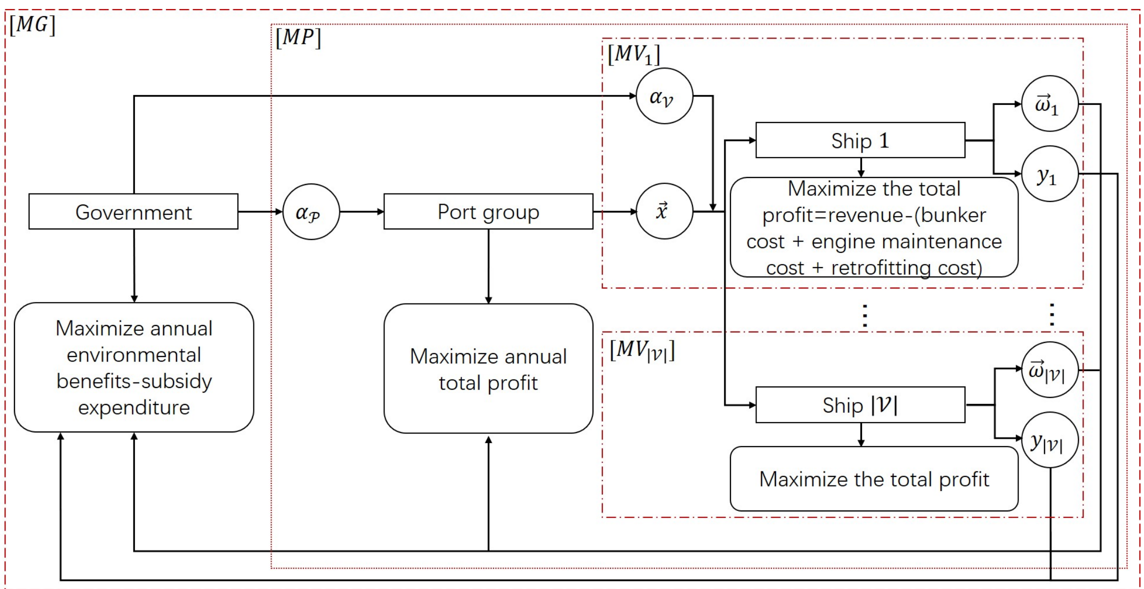

Figure 3.2: Demonstration of the problem structure

Government Level

The government makes decisions at the first level, aiming to maximize its annual total benefits, which equal the annual environmental benefits of emission reduction minus annual average subsidy expenses. Specifically, the government needs to determine the proportion of the bunkering station building cost to subsidize, denoted by $\alpha_{\mathcal{P}}$, and the proportion of the ship retrofitting cost to subsidize, denoted by $\alpha_{\mathcal{V}}$. To insure convenient policy implementation, we assume that the government chooses the values of $\alpha_{\mathcal{P}}$ and $\alpha_{\mathcal{V}}$ from a set of alternatives 0%, 5%, ..., 95%, and 100%. The purpose of the government subsidies is to stimulate the port group to build LNG bunkering stations and to encourage the retrofitting of ships as dual-fueled, so that a significant amount of LNG will be consumed to replace MDO, thus providing environmental benefits.

Port Level

At the port level, given the subsidy proportion $\alpha_{\mathcal{P}}$, the port group decides whether or not to construct an LNG bunkering station at each physical port $i \in \mathcal{P}$, denoted by the binary decision variable x_i, with the aim of maximizing its average annual profits. The construction of an LNG bunkering station at physical port $i \in \mathcal{P}$ costs $\hat{C}_i^{\mathcal{P}}$ (without government subsidy), which is a one-off cost. We convert $\hat{C}_i^{\mathcal{P}}$ into an annualized cost $C_i^{\mathcal{P}}$, which applies after depreciation and interest are considered. With the government subsidy, the port group needs to pay an annual cost of $(1 - \alpha_{\mathcal{P}})\, C_i^{\mathcal{P}}$. The port group purchases LNG from a supplier at a fixed price of $\tilde{U}_{\text{LNG}}$. The selling price to ships, namely, the LNG bunkering price, denoted by $\hat{U}_{\text{LNG}}$, is predetermined by the government to ensure that LNG is a more economical option for bunker fuel than MDO. Therefore, the port group could gain $\hat{U}_{\text{LNG}} - \tilde{U}_{\text{LNG}}$ by selling one ton of LNG. The total amount of LNG that the port group can sell depends on the ship operators' decisions, which are affected by the government's subsidy proportion $\alpha_{\mathcal{V}}$ and the availability of LNG bunkering stations at the ports in $\mathcal{P}$.

Ship level

Given the government's subsidy proportion $\alpha_{\mathcal{V}}$ at the first level and the locations of LNG bunkering stations determined at the second level, the operator of each ship $j \in \mathcal{V}$ decides whether to retrofit the ship or not and the refueling volume at each port if the ship is retrofitted (the ship may not refuel at ports that are passed by rather than visited, because the refueling would incur extra cost), to maximize its annual profit. The ship operators' refueling volume decisions affect the government's environmental benefits at the first level and the port group's revenue at the second level.

We denote by y_j a binary decision variable equal to 1 if and only if ship j is retrofitted. We convert the one-off retrofitting cost $\hat{C}_j^{\mathcal{V}}$ into an annualized cost $C_j^{\mathcal{V}}$. Then, benefiting from the government subsidy, the ship operator needs to pay an annual cost of $(1 - \alpha_{\mathcal{V}})\, C_j^{\mathcal{V}}$ for the retrofitting. If the ship is retrofitted, it will be equipped with an LNG tank with a capacity of q_j tons, and the original diesel engine will be replaced by a dual-fuel engine that has an annual maintenance cost of $\bar{C}_{\text{Dual}}^j$ USD. Because consuming one ton of LNG means reducing the consumption of MDO by R tons, the consumption of one ton of LNG implies a fuel cost reduction of $\Delta_U := R \cdot U_{\text{MDO}} - \hat{U}_{\text{LNG}}$ USD for the ship operator.

As the LNG bunkering price is the same at all available ports, if ship j visits a port with an LNG bunkering station, it will fill up its LNG tank. If the ship passes a port rather than visiting it, the ship may stop at the port for LNG refueling, at an extra cost of f_j USD. We define a binary decision variable θ_{jk} that equals 1 if and only if ship j refuels with LNG at port $k \in \mathcal{P}'_j$. We then have $\theta_{jk} = 1$ if $T_{jk} = 1$; a cost f_j will be incurred if $\theta_{jk} = 1$ and $T_{jk} = 0$.

For simplicity, it is assumed that a ship refuels just before leaving a port; that is, LNG purchased at the k^{th} port cannot be used to generate power for the ship when it is berthing at the port. To formulate the amount of LNG consumed by ship j, we define decision variables π_{jk}^{Finish} and π_{jk}^{Leave} as follows. (i) If ship j visits the k^{th} port for cargo handling (i.e., $T_{jk} = 1$), then π_{jk}^{Finish} is the volume of LNG remaining in the LNG tank of ship j when it has just finished cargo handling (before refueling, if any) and π_{jk}^{Leave} is the volume of LNG remaining in the LNG tank of ship j when it leaves the k^{th} port (after refueling, if any). (ii) If ship j stops at the k^{th} port just for refueling (i.e., $T_{jk} = 0$ and $\theta_{jk} = 1$), then π_{jk}^{Finish} represents the volume of LNG remaining in the LNG tank of ship j before refueling and π_{jk}^{Leave} represents the volume after refueling, and we have $\pi_{jk}^{Finish} < \pi_{jk}^{Leave}$. In both cases, $\pi_{jk}^{Finish} \leq \pi_{jk}^{Leave}$. Specifically, if ship j does not refuel at the k^{th} port along its route ($\theta_{jk} = 0$), $\pi_{jk}^{Finish} = \pi_{jk}^{Leave}$. If ship j refuels at the k^{th} port ($\theta_{jk} = 1$), we have $\pi_{jk}^{Finish} < \pi_{jk}^{Leave} = q_j$, because every time the ship refuels the LNG tank will be filled up.

The annual LNG refueling volume of ship j at physical port i, denoted by decision variable ω_{ji}, can now be calculated: $\omega_{ji} = O_j \sum_{k \in \mathcal{P}'_j} B_{jki} \left(\pi_j^{Leave} - \pi_j^{Finish}\right)$, for all $j \in \mathcal{V}$, $i \in \mathcal{P}$. The values of ω_{ji} affect the government's decisions and the port group's decisions: the annual environmental benefit for the government is $\Delta_E \sum_{j \in \mathcal{V}} \sum_{i \in \mathcal{P}} \omega_{ji}$, and the annual gain for the port group from selling LNG is $\left(\hat{U}_{\text{LNG}} - \tilde{U}_{\text{LNG}}\right) \sum_{j \in \mathcal{V}} \sum_{i \in \mathcal{P}} \omega_{ji}$.

3.2.2 Mathematical Model

Before presenting the mathematical model, we list the notations used in this chapter.

Sets and parameters

$\mathcal{P}$	the set of physical ports along the river, $\mathcal{P} = \{1, 2, ..., \lvert\mathcal{P}\rvert\}$, indexed by i;
$\mathcal{V}$	the set of ships sailing along the river, $\mathcal{V} = \{1, 2, ..., \lvert\mathcal{V}\rvert\}$, indexed by j;
$C_i^{\mathcal{P}}$	the annualized construction cost (USD) of LNG bunkering station at physical port $i, \forall i \in \mathcal{P}$;
$C_j^{\mathcal{V}}$	the annualized retrofitting cost (USD) of ship $j, \forall j \in \mathcal{V}$;
G_j	the annual revenue (USD/year) for ship j, $\forall j \in \mathcal{V}$;
Δ_E	the increment in environmental benefits (USD/ton) when one ton of LNG is consumed to replace MDO;
R_{LNG}^j	the LNG consumption rate (ton/nm) of ship j while sailing, if it is retrofitted, $\forall j \in \mathcal{V}$;
U_{MDO}	the MDO bunkering price (USD/ton) paid by ship operators;
$\hat{U}_{\text{LNG}}$	the LNG bunkering price (USD/ton) paid by ship operators;
$\tilde{U}_{\text{LNG}}$	the LNG purchasing price (USD/ton) paid by the port group;
Δ_U	the fuel cost reduction (USD/ton) brought by using one ton of LNG;
$\mathcal{P}'_j$	the set of ports along the route of ship j, $\mathcal{P}'_j = \{1, 2, ..., 2\left(MU_j - MD_j\right)\}$, indexed by k;
T_{jk}	binary parameter, equal to 1 if the k^{th} port along the route is visited by ship j, 0 otherwise, $\forall j \in \mathcal{V}, \forall k \in \mathcal{P}'_j$;

L_{jk} the sailing distance (nm, nautical mile) from the k^{th} port along the route of ship j to the $(k+1)^{\text{th}}$ port along the route, $k = 1, 2, ..., |\mathcal{P}'_j| - 1, \forall j \in \mathcal{V}$;

$L_{j|\mathcal{P}'_j|}$ the sailing distance (nm) from the $|\mathcal{P}'_j|^{\text{th}}$ port along the route of ship j to the 1^{st} port along the route, $\forall j \in \mathcal{V}$;

m_{jk} the berthing time (hour) of ship j at the k^{th} port along the route, $\forall j \in \mathcal{V}, \forall k \in \mathcal{P}'_j$;

R'^{j}_{LNG} the LNG consumption rate (ton/hour) of ship j while berthing, $\forall j \in \mathcal{V}$;

$\bar{C}^{j}_{\text{MDO}}$ the annual maintenance cost (USD/year) of the diesel engine of ship j if it is not retrofitted;

$\bar{C}^{j}_{\text{Dual}}$ the annual maintenance cost (USD/year) of the dual-fuel engine of ship j if it is retrofitted;

O_j the number of trips that ship j finishes in a year, $\forall j \in \mathcal{V}$;

f_j the extra cost (USD) of ship j refueling at a port that is located along the route but not visited by the ship, $\forall j \in \mathcal{V}$;

q_j the LNG tank capacity (ton) of ship j if it is retrofitted, $\forall j \in \mathcal{V}$;

B_{jki} binary parameter, equal to 1 if the k^{th} port along the route of ship j is physical port i, 0 otherwise, $\forall j \in \mathcal{V}, \forall k \in \mathcal{P}'_j, \forall i \in \mathcal{P}$;

M_i a large constant, $\forall i \in \mathcal{P}$.

Decision variables

$\alpha_{\mathcal{P}}$ the proportion of LNG bunkering station construction cost that will be covered by the government subsidy;

$\alpha_{\mathcal{V}}$ the proportion of ship retrofitting cost that will be covered by the government subsidy;

x_i binary variable, equal to 1 when an LNG bunkering station is constructed at physical port i, 0 otherwise, $\forall i \in \mathcal{P}$;

y_j binary variable, equal to 1 when ship j is retrofitted into a dual-fueled ship, 0 otherwise, $j \in \mathcal{V}$;

ω_{ji} the LNG refueling volume (ton) of ship j at physical port i each year if it is retrofitted, $\forall j \in \mathcal{V}$, $\forall i \in \mathcal{P}$;

θ_{jk}	binary variable, equal to 1 when ship j refuels LNG at the k^{th} port along its route if it is retrofitted, 0 otherwise, $\forall k \in \mathcal{P}'_j, \forall j \in \mathcal{V}$;
π_{jk}^{Finish}	the LNG remaining volume (ton) of the ship j when it finished cargo handling at the k^{th} port along the route and before refueling, $\forall j \in \mathcal{V}, \forall k \in \mathcal{P}'_j$;
π_{jk}^{Leave}	the LNG remaining volume (ton) of the ship j when it leaves the k^{th} port along the route after refueling, $\forall j \in \mathcal{V}$, $\forall k \in \mathcal{P}'_j$.

Vectors

$\vec{x}$	the vector of x_i, $\vec{x} = \left(x_1, ..., x_{\lvert\mathcal{P}\rvert}\right)$;
$\vec{y}$	the vector of y_j, $\vec{y} = \left(y_1, ..., y_{\lvert\mathcal{V}\rvert}\right)$;
$\vec{\omega}_j$	the vector of ω_{ji}, $\vec{\omega}_j = \left(\omega_{j1}, ..., \omega_{j\lvert\mathcal{P}\rvert}\right)$, $\forall j \in \mathcal{V}$;
$\vec{\omega}$	the vector of $\vec{\omega}_j$, $\vec{\omega} = \left(\vec{\omega}_1, ..., \vec{\omega}_{\lvert\mathcal{V}\rvert}\right)$;
$\vec{\pi}_j^{Leave}$	the vector of π_{jk}^{Leave}, $\vec{\pi}_j^{Leave} = \left(\pi_{j1}^{Leave}, ..., \pi_{j\lvert\mathcal{P}'_j\rvert}^{Leave}\right)$, $\forall j \in \mathcal{V}$;
$\vec{\pi}_j^{Finish}$	the vector of π_{jk}^{Finish}, $\vec{\pi}_j^{Finish} = \left(\pi_{j1}^{Finish}, ..., \pi_{j\lvert\mathcal{P}'_j\rvert}^{Finish}\right)$, $\forall j \in \mathcal{V}$;
$\vec{\theta}_j$	the vector of θ_{jk}, $\vec{\theta}_j = \left(\theta_{j1}, ..., \theta_{j\lvert\mathcal{P}'_j\rvert}\right)$, $\forall j \in \mathcal{V}$.

Then the problem faced by the government can be described as the following trilevel optimization model $[MG]$:

$$[\boldsymbol{MG}] \quad \text{maximize } \Delta_E \sum_{j\in\mathcal{V}} \sum_{i\in\mathcal{P}} \omega_{ji} - \alpha_{\mathcal{P}} \sum_{i\in\mathcal{P}} C_i^{\mathcal{P}} x_i - \alpha_{\mathcal{V}} \sum_{j\in\mathcal{V}} C_j^{\mathcal{V}} y_j \tag{3.1}$$

subject to

$$\alpha_{\mathcal{P}} \in \{0\%, 5\%, ..., 100\%\} \tag{3.2}$$

$$\alpha_{\mathcal{V}} \in \{0\%, 5\%, ..., 100\%\} \tag{3.3}$$

and

$$(\vec{x}, \vec{\omega}, \vec{y}) \in \Psi^{\mathcal{P}}\left(\alpha_{\mathcal{P}}, \alpha_{\mathcal{V}}\right) \tag{3.4}$$

where $\Psi^{\mathcal{P}}\left(\alpha_{\mathcal{P}}, \alpha_{\mathcal{V}}\right)$ is determined by the following model:

$$[\boldsymbol{MP}] \quad \Psi^{\mathcal{P}}\left(\alpha_{\mathcal{P}}, \alpha_{\mathcal{V}}\right) = \underset{\vec{x},\vec{\omega},\vec{y}}{\arg\max} \sum_{i\in\mathcal{P}} \left[-\left(1-\alpha_{\mathcal{P}}\right) C_i^{\mathcal{P}} x_i + \sum_{j\in\mathcal{V}} \left(\hat{U}_{\text{LNG}} - \tilde{U}_{\text{LNG}}\right) \omega_{ji} y_j \right] \tag{3.5}$$

subject to

$$x_i = 0, 1, \forall i \in \mathcal{P} \tag{3.6}$$

and

$$\left(y_j, \vec{\omega}_j\right) \in \Phi_j^{\mathcal{V}}\left(\alpha_{\mathcal{V}}, \vec{x}\right), \forall j \in \mathcal{V} \tag{3.7}$$

where $\Phi_j^{\mathcal{V}}\left(\alpha_{\mathcal{V}}, \vec{x}\right)$ is the projection of $\hat{\Phi}_j^{\mathcal{V}}\left(\alpha_{\mathcal{V}}, \vec{x}\right)$ on y_j and $\vec{\omega}_j$ (in other words, $\left(y_j, \vec{\omega}_j\right) \in \Phi_j^{\mathcal{V}}\left(\alpha_{\mathcal{V}}, \vec{x}\right)$ if and only if there exists $\left(\vec{\theta}_j, \vec{\pi}_j^{Leave}, \vec{\pi}_j^{Finish}\right)$ such that $\left(y_j, \vec{\omega}_j, \vec{\theta}_j, \vec{\pi}_j^{Leave}, \vec{\pi}_j^{Finish}\right) \in \hat{\Phi}_j^{\mathcal{V}}\left(\alpha_{\mathcal{V}}, \vec{x}\right)$), where $\hat{\Phi}_j^{\mathcal{V}}\left(\alpha_{\mathcal{V}}, \vec{x}\right)$ is determined by the following model:

$$[\boldsymbol{MV_j}] \quad \hat{\Phi}_j^{\mathcal{V}}\left(\alpha_{\mathcal{V}}, \vec{x}\right) = \underset{y_j,\vec{\omega}_j,\vec{\theta}_j,\vec{\pi}_j^{Leave},\vec{\pi}_j^{Finish}}{\arg\max} G_j - \left\{ y_j \left[C_j^{\mathcal{V}}\left(1-\alpha_{\mathcal{V}}\right) + O_j \sum_{k\in\mathcal{P}'_j} f_j\left(1-T_{jk}\right)\theta_{jk} \right.\right.$$
$$\left.\left. + \bar{C}_{\text{Dual}}^{j} - \Delta_U \sum_{i\in\mathcal{P}} \omega_{ji} \right] + \left(1-y_j\right)\bar{C}_{\text{MDO}}^{j} \right\} \tag{3.8}$$

subject to

$$\pi_{jk}^{Leave} = \pi_{jk}^{Finish} + \theta_{jk}\left(q_j - \pi_{jk}^{Finish}\right), \forall k \in \mathcal{P}'_j \tag{3.9}$$

$$\pi_{jk}^{Finish} = \max\left\{0, \pi_{j,k-1}^{Leave} - L_{j,k-1} R_{\text{LNG}}^{j} - m_{jk} {R'}_{\text{LNG}}^{j}\right\}, k = 2, 3, ..., \left|\mathcal{P}'_j\right| \tag{3.10}$$

$$\pi_{j1}^{Finish} = \max\left\{0, \pi_{j\left|\mathcal{P}'_j\right|}^{Leave} - L_{j\left|\mathcal{P}'_j\right|} R_{\text{LNG}}^{j} - m_{j1} {R'}_{\text{LNG}}^{j}\right\} \tag{3.11}$$

$$\omega_{ji} = O_j \sum_{k\in\mathcal{P}'_j} B_{jki}\left(\pi_{jk}^{Leave} - \pi_{jk}^{Finish}\right), \forall i \in \mathcal{P} \tag{3.12}$$

$$\theta_{jk} \leq \sum_{i \in \mathcal{P}} B_{jki} x_i, \forall k \in \mathcal{P}'_j \tag{3.13}$$

$$\sum_{i \in \mathcal{P}} B_{jki} T_{jk} x_i \leq \theta_{jk}, \forall k \in \mathcal{P}'_j \tag{3.14}$$

$$0 \leq \pi_{jk}^{Finish} \leq \max\left\{0, q_j - L_{j,k-1} R_{\text{LNG}}^{j} - m_{jk} R'^{j}_{\text{LNG}}\right\}, k = 2, ..., \left|\mathcal{P}'_j\right| \tag{3.15}$$

$$0 \leq \pi_{j1}^{Finish} \leq \max\left\{0, q_j - L_{j,\left|\mathcal{P}'_j\right|} R_{\text{LNG}}^{j} - m_{j1} R'^{j}_{\text{LNG}}\right\} \tag{3.16}$$

$$\theta_{jk} = 0, 1, \forall k \in \mathcal{P}'_j \tag{3.17}$$

$$y_j = 0, 1 \tag{3.18}$$

$$0 \leq \pi_{jk}^{Leave} \leq q_j, \forall k \in \mathcal{P}'_j. \tag{3.19}$$

The objective function (3.1) at the government level aims to maximize the annual environmental benefits of the reduction in ship emissions minus annual average subsidy expenses. Constraints (3.2) and (3.3) specify the domains of the subsidy proportions. In model $[MG]$, some of the parameters, namely ω_{ji}, x_i, and y_j, are not constants; the values of these parameters depend on the decisions of the port group and ship operators, which are described in the port-level and ship-level models. We use the set $\Psi^P(\alpha_P, \alpha_V)$ to denote them.

At the port level, because all physical ports are under the management of the port group, here we present the model $[MP]$ to describe the problem faced by the port group. The objective function (3.5) aims to maximize the annual total profits of the port group, equal to the annual profit of selling LNG, minus the annual average LNG bunkering station construction cost. Constraints (3.6) define the domain of decision variable x_i. In model $[MP]$, parameters y_j and ω_{ji} are not constants, and their values depend on ship operators' choices, which are described in ship-level models. We use the set $\Psi_j^V(\alpha_V, \vec{x})$ to denote them.

Because different ships at the ship level make their decisions independently, we build $[MV_j]$ for ship j. In objective function (3.8), the first part is the annual revenue G_j. Next, the objective functions for when ship j is retrofitted or not are listed separately. If ship j is retrofitted, the objective function equals the annual average retrofitting cost, plus the extra cost of refueling at ports that the ship does not visit, plus the annual maintenance cost of the dual-fuel engine minus the annual bunkering cost saving. If ship j is not retrofitted, the objective function equals the annual maintenance cost of the diesel engine. Constraints (3.9) give the relationship between the remaining LNG volume when the ship finishes cargo handling and other operations at the k^{th} port along the route and the remaining volume when it leaves the port. Constraints (3.10) and (3.11) state that the retrofitted ship will consume LNG while sailing from one port to the next and berthing there, and that MDO will be used if LNG is in short supply. Constraints (3.12) calculate the annual LNG bunkering volume of ship j at physical port i if the ship is retrofitted. Constraints (3.13) state that ship j can refuel with LNG at the k^{th} port along the route only if the port group decides to construct an LNG bunkering station at the port. Constraints (3.14) indicate that ship j will refuel at every port with an LNG bunkering station that it visits. Constraints (3.15) and (3.16) states the upper limits of the remaining LNG volume when ship j finishes cargo handling and before LNG refueling, if any, at the k^{th} port. The limit will be reached only if the ship refuels at the last port along the route before the k^{th} port. Constraints (3.17)–(3.19) define the domains of the decision variables.

3.3 Solution Method

The main difficulty in solving this problem is its trilevel structure, which leads to interdependence among the decisions of different decision makers. At the government level, subsidy rates $\alpha_{\mathcal{P}}$ and $\alpha_{\mathcal{V}}$ are determined. To handle the government-level problem, we enumerate all possible situations for the values of $\alpha_{\mathcal{P}}$ and $\alpha_{\mathcal{V}}$; then the problem becomes bilevel. In a bilevel problem, there is a leader who first makes a decision and a follower who makes a decision after the leader, and they each make decisions based on their own interests. The leader's decisions will influence the follower's decisions, which in turn, have an impact on the leader's objective function value. In our bilevel problem, the port group that manages all ports is the leader;

ship operators who control their own ships are followers who decide independently. In the following subsection, we convert the bilevel problem into an equivalent single-level problem $[SP]$, which can be solved by an off-the-shelf CPLEX solver after model linearization.

3.3.1 Model Conversion

At the ship level, all ship operators make decisions on whether to retrofit ships independently, because the capacity of bunkering stations is assumed to be infinite. The only factor that influences the ship operator's decision is the net profit from retrofitting the ship; the ship will be retrofitted if and only if the benefit exceeds the cost. Therefore, the decision-making process at the ship level can be represented by the two sets of binary variables z_j and ξ_j, as follows:

Variables

z_j binary variable, equal to 1 when ship j can benefit from being retrofitted into a dual-fueled ship, 0 otherwise, $\forall j \in \mathcal{P}$;

ξ_j parameter used to indicates the difference between z_j and y_j, equal to 0 when $z_j = y_j$, 1 otherwise.

With z_j and ξ_j, the bilevel programming model that consists of the port level and the ship level can be converted to a single-level programming model $[SP]$ as follows:

$$[\boldsymbol{SP}] \quad \max \sum_{i \in \mathcal{P}} \left[-(1-\alpha_{\mathcal{P}})\, C_i^{\mathcal{P}} x_i + \sum_{j \in \mathcal{V}} \left(\hat{U}_{\text{LNG}} - \tilde{U}_{\text{LNG}} \right) \omega_{ji} y_j \right] - \sum_{j \in \mathcal{V}} \hat{M}_j \xi_j \quad (3.20)$$

subject to constraint (3.6), constraints (3.9)–(3.19) for all $j \in \mathcal{V}$, and the following constraints:

$$z_j - y_j \leq \xi_j, \forall j \in \mathcal{V} \quad (3.21)$$

$$y_j - z_j \leq \xi_j, \forall j \in \mathcal{V} \quad (3.22)$$

$$\bar{C}_{\text{MDO}}^{j} - \left[C_j^{\mathcal{V}} \left(1 - \alpha_{\mathcal{V}}\right) + O_j \sum_{k \in \mathcal{P}_j'} f_j \left(1 - T_{jk}\right) \theta_{jk} + \bar{C}_{\text{Dual}}^{j} - \Delta_U \sum_{i \in \mathcal{P}} \omega_{ji} \right] \leq M_j z_j,$$

$$\forall j \in \mathcal{V} \tag{3.23}$$

$$\left[C_j^{\mathcal{V}} \left(1 - \alpha_{\mathcal{V}}\right) + O_j \sum_{k \in \mathcal{P}_j'} f_j \left(1 - T_{jk}\right) \theta_{jk} + \bar{C}_{\text{Dual}}^{j} - \Delta_U \sum_{i \in \mathcal{P}} \omega_{ji} \right] - \bar{C}_{\text{MDO}}^{j} \leq M_j \left(1 - z_j\right),$$

$$\forall j \in \mathcal{V} \tag{3.24}$$

$$\xi_j \geq 0, \forall j \in \mathcal{V}. \tag{3.25}$$

In $[SP]$, $\hat{M}_j$ and M_j are parameters that are large enough, and the values of $\hat{M}_j$ and M_j are listed below.

Parameters

- $\hat{M}_j$ parameter used in the objective function (3.20), equal to $\left(\hat{U}_{\text{LNG}} - \tilde{U}_{\text{LNG}}\right) \sum_{k \in \mathcal{P}_j'} L_{jk} R_{\text{LNG}}^{j} + m_{jk} {R'}_{\text{LNG}}^{j}$, $\forall j \in \mathcal{P}$;
- M_j parameter used in constraints (3.23) and (3.24), equal to $\max \left\{ C_j^{\mathcal{V}} \left(1 - \alpha_{\mathcal{V}}\right) + O_j \sum_{k \in \mathcal{P}_j'} f_j \left(1 - T_{jk}\right) + \bar{C}_{\text{Dual}}^{j}, \bar{C}_{\text{MDO}}^{j} + \Delta_U \sum_{k \in \mathcal{P}_j'} L_{jk} R_{\text{LNG}}^{j} + m_{jk} {R'}_{\text{LNG}}^{j} \right\}, \forall j \in \mathcal{V}$.

In $[SP]$, constraints (3.21) and (3.22) combined with the second part of objective function (3.20), $\sum_{j \in \mathcal{V}} \hat{M}_j \xi_j$, ensure that $z_j = y_j, j \in \mathcal{V}$. The left-hand side of constraints (3.23) is the benefit of retrofitting ship j. Constraints (3.23) and (3.24) guarantee that $z_j = 1$ if and only if ship j can benefit from being retrofitted. Therefore, the bilevel problem is converted to the equivalent single-level problem $[SP]$, which is a mixed integer nonlinear programming problem, and should be linearized before being solved. The linearization process is given in Appendix A. Solving $[SP]$, we obtain the corresponding government profit $OptG(\alpha_{\mathcal{P}}, \alpha_{\mathcal{V}}) = \Delta_E \sum_{j \in \mathcal{V}} \sum_{i \in \mathcal{P}} Opt\omega_{ji} - \alpha_{\mathcal{P}} \sum_{i \in \mathcal{P}} C_i^{\mathcal{P}} Optx_i - \alpha_{\mathcal{V}} \sum_{j \in \mathcal{V}} C_j^{\mathcal{V}} Opty_j$, in which $Optx_i$, $Opty_j$, and $Opt\omega_{ji}$ are the optimal solution of $[SP]$ with $\alpha_{\mathcal{P}}$ and $\alpha_{\mathcal{V}}$. Based on $[SP]$, the trilevel model $[MG]$

can be solved as follows:

$$\text{maximize}_{\alpha_{\mathcal{P}}\in\{0\%,5\%,\ldots,100\%\},\alpha_{\mathcal{V}}\in\{0\%,5\%,\ldots,100\%\}} OptG(\alpha_{\mathcal{P}}, \alpha_{\mathcal{V}}). \tag{3.26}$$

3.4 Numerical Experiments

The algorithm was programmed in C++ with Visual Studio 2019, and we used CPLEX 12.10 to solve $[SP]$ with different values of $\alpha_{\mathcal{P}}$ and $\alpha_{\mathcal{V}}$. Multiple numerical experiments were conducted to validate the model and the algorithm. Computational experiments were conducted on a LENOVO XiaoXinPro-13IML 2019 laptop with i7-10710U CPU, 1.10 GHz processing speed and 16 GB of memory.

3.4.1 Parameter settings

The parameters used in the numerical experiments were collected from previous studies and related reports. First we estimated the environmental benefits of consuming one ton of LNG, $\Delta_E := R \cdot E_{\text{MDO}} - E_{\text{LNG}}$. Ship emissions contain various pollutants, of which four are considered in this chapter: SO_X, NO_X, CO_2, and $PM_{2.5}$. Based on the Fourth Greenhouse Gas Study conducted by the IMO (Faber et al. 2020), we estimated that a traditional ship will emit 0.0001 ton of SO_X, 0.167 ton of NO_X, 3.206 tons of CO_2, and 0.00203 ton of $PM_{2.5}$ while consuming one ton of MDO, and a dual-fueled ship will emit 3.17×10^{-5} ton of SO_X, 0.0466 ton of NO_X, 2.75 tons of CO_2, and 1.26×10^{-4} ton of $PM_{2.5}$ while consuming one ton of LNG. These four pollutants make up more than 99% of ship emissions, and have a significant impact on social welfare. As summarized in Nunes et al. (2019) and Song (2014), the social costs associated with the emissions of SO_X, NO_X, CO_2, and $PM_{2.5}$ are 11,123 USD/ton, 6,282 USD/ton, 33 USD/ton, and 61,179 USD/ton, respectively. As a result, we obtained the values $E_{\text{MDO}} = 1,280.31$ USD/ton, $E_{\text{LNG}} = 391.43$ USD/ton, and $\Delta_E = R \cdot E_{\text{MDO}} - E_{\text{LNG}} = 1,119.33$ USD/ton. Next, we calculated the fuel cost reduction of the ship operator when 1 ton of LNG is consumed, $\Delta_U := R \cdot U_{\text{MDO}} - \hat{U}_{\text{LNG}}$. According to market information, the bunkering price of regular diesel is set at 950 USD/ton and the bunkering price of LNG, $\hat{U}_{\text{LNG}}$, is about 800 USD/ton. Therefore, $\Delta_U = 321$ USD/ton. The LNG purchasing cost of bunkering stations is around 650 USD/ton; thus, $\tilde{U}_{\text{LNG}} = 650$ USD/ton.

To numerically validate the model and algorithm proposed in this chapter, we generated a port set of 10 ports and a ship set of 25 ships. According to the International Maritime Organization (2016), the annualized construction cost of an LNG bunkering station is about $4,088,000$ USD per year. On this basis, we randomly generated the values of $C_i^{\mathcal{P}}$, $i \in \mathcal{P}$, between $3,270,400$ USD ($= 0.8 \times 4,088,000$) and $4,905,600$ USD ($= 1.2 \times 4,088,000$).

For ship operators, the total cost of retrofitting a large container ship of 15,000 TEU capacity as a dual-fueled ship is about 25 million to 30 million USD (International Maritime Organization 2016, Freight Waves 2019). However, due to waterway conditions, inland river ships have a smaller dead weight tonnage than seagoing vessels do. Therefore, we considered ships with a capacity of around 2000 TEU, whose retrofitting cost ranges from 15 million USD to 20 million USD. We randomly generated the values of $\hat{C}_j^{\mathcal{V}}, j \in \mathcal{V}$. After considering the 8% interest rate and 20 years' depreciation time, the cost was annualized into $C_j^{\mathcal{V}}$. The LNG tank capacity of ship j ranges from 6.39 to 8.52 tons, namely 15 to 20 m^3. The extra cost to ship j of refueling at a port that is not visited by the ship, f_j, ranges from 50 USD to 100 USD. Regarding maintenance costs, a ship that is retrofitted will need less maintenance and repair work, but such work will cost more (International Maritime Organization 2016). Consequently, we assumed that the annual cost for maintenance and repair is similar for traditional ships and dual-fueled ships; that is, $\bar{C}^j_{\text{Dual}} = \bar{C}^j_{\text{MDO}}, j \in \mathcal{V}$.

We assumed that each ship works for 330 days per year, including sailing and berthing for cargo handling, giving $S = 330 \times 24 = 7920$. The specific amount of annual revenue will not influence the optimal solution as long as the profit of each ship is positive, and we assumed that $G_j = C_j^{\mathcal{V}} + O_j \sum_{k \in \mathcal{P}'_j} f_j(1 - T_{jk}), j \in \mathcal{V}$, which is large enough to keep the profit positive. Ship j visits some of the ports along its route, and which ports the ship visits is randomly generated. The sailing speeds of different ships are randomly generated in the range of 15 to 20 knots, and the LNG consumption rate while sailing, R^j_{LNG}, is closely related to the sailing speed. Meanwhile, the LNG consumption rate while berthing, R'^{j}_{LNG}, is set to be the same for different ships due to their similar sizes. Considering the small capacity of container ships sailing along the inland river, the berthing time at each port varies from two to five hours.

3.4.2 Results and Sensitivity Analysis

All of the numerical experiments involved 10 ports along the river and 25 ships sailing among them, and were completed within 2000 seconds. We conducted sensitive analysis with different values of crucial parameters including $C_i^{\mathcal{P}}$, $C_j^{\mathcal{V}}$, Δ_E, U_{MDO}, $\hat{U}_{\mathrm{LNG}}$, and $\tilde{U}_{\mathrm{LNG}}$ to show their influence on the optimization results. Details of the sensitivity analysis are as follows.

First, we conducted the numerical experiment with the parameters given in Subsection 3.4.1, which is denoted as the basic case ($CBasic$). Next, we solved $[SP]$ with $\alpha_{\mathcal{P}} = \alpha_{\mathcal{V}} = 0$ to represent the scenario without government subsidy, denoted by $CWithout$. The results are presented in Table 3.1.

Table 3.1: Results of $CBasic$ and $CWithout$

	$CWithout$	$CBasic$
$OptG$ (USD)	0	79,681,000
$Opt\alpha_{\mathcal{P}}$	N/A	0.4
$Opt\alpha_{\mathcal{V}}$	N/A	0.55
Number of ports with bunkering stations	0	5
Number of ships retrofitted	0	25
Subsidy expenditure (USD)	0	32,846,100
LNG usage (ton)	0	100,531.65
Environmental revenue (USD)	0	112,527,000
Solution time (second)	N/A	687.824

From Table 3.1 we can see that without the subsidy from the government, no LNG bunkering station will be constructed due to the high cost of investment, and no ship will be retrofitted because of the high cost of investment and the lack of bunkering stations. With the optimal government subsidy plan, an environmental revenue of $112,527,000$ USD can be achieved by providing $32,846,100$ USD of subsidy in total, which yields a net benefit of $79,681,000$ USD. The comparison shows the huge benefit of using LNG as marine fuel and demonstrates the necessity and efficiency of a well-thought-out government subsidy.

Showing how the subsidy rates $\alpha_{\mathcal{P}}$ and $\alpha_{\mathcal{V}}$ influence the net government profit $ObjG$ and the consumption volume of LNG as marine fuel, the two sets of results for different values of $\alpha_{\mathcal{P}}$ and $\alpha_{\mathcal{V}}$ are displayed in Figure 3.3 and Figure 3.4.

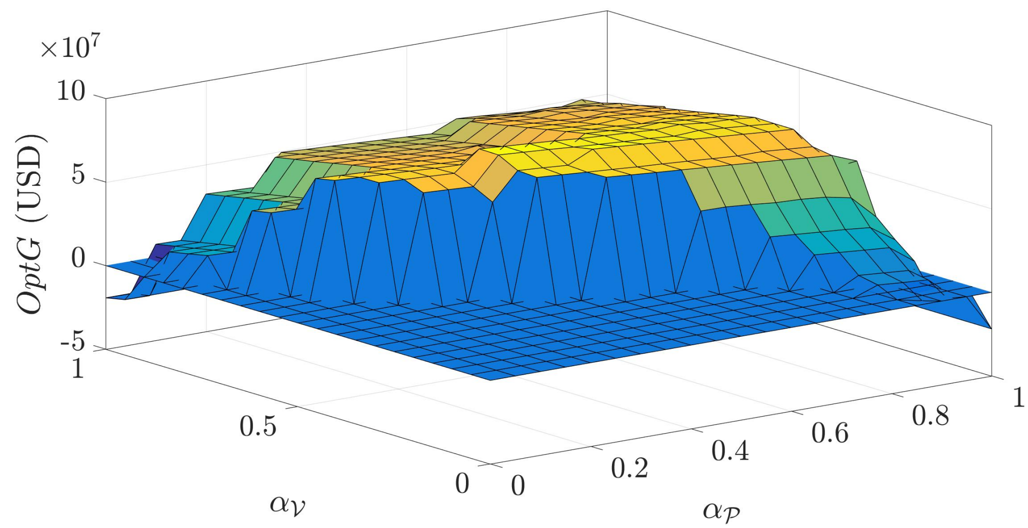

Figure 3.3: $OptG$ under different values of $\alpha_{\mathcal{P}}$ and $\alpha_{\mathcal{V}}$

From Figure 3.3 we can see that a higher $\alpha_{\mathcal{P}}$ and $\alpha_{\mathcal{V}}$ do not necessarily lead to higher government net profit; the government must balance environmental revenue and subsidy expenditure to obtain the optimal government subsidy plan. Generally, $ObjG$ is larger when the values of $\alpha_{\mathcal{P}}$ and $\alpha_{\mathcal{V}}$ are relatively close. In some extreme scenarios, $ObjG$ becomes negative; this phenomenon occurs when there is a wide gap between the values of $\alpha_{\mathcal{P}}$ and $\alpha_{\mathcal{V}}$, such as when $\alpha_{\mathcal{P}} = 1, \alpha_{\mathcal{V}} = 0$ or $\alpha_{\mathcal{P}} = 0, \alpha_{\mathcal{V}} = 1$. This indicates that it is important to determine the subsidy amount wisely, and subsidizing at both the port and ship levels is more efficient than focusing on just one of them. From Figure 3.4 we can see that with the same value of $\alpha_{\mathcal{P}}\,(\alpha_{\mathcal{V}})$, a larger $\alpha_{\mathcal{V}}\,(\alpha_{\mathcal{P}})$ does not always lead to a larger LNG consumption volume. This phenomenon is due to the multi-level structure and different objectives at each level.

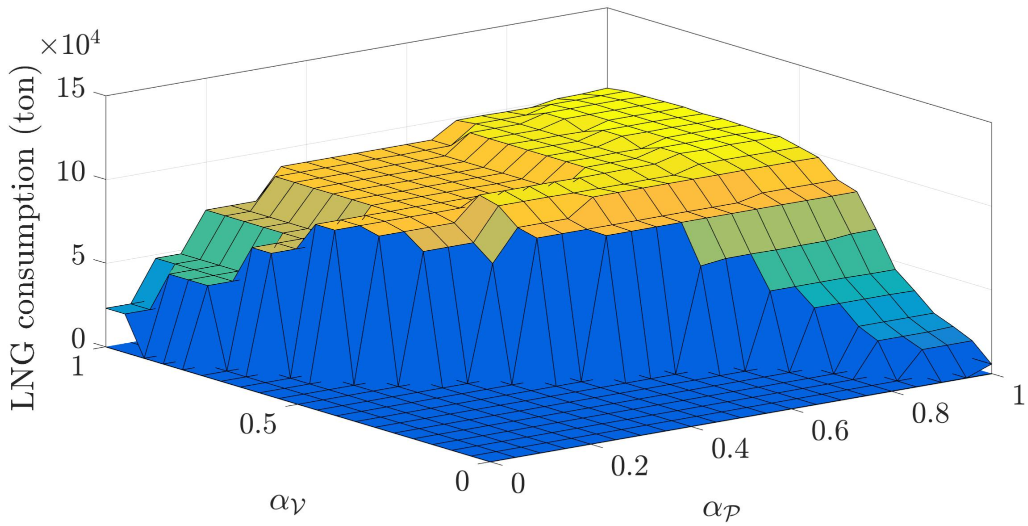

Figure 3.4: LNG consumption volume under different values of $\alpha_{\mathcal{P}}$ and $\alpha_{\mathcal{V}}$

Table 3.2 shows the results of numerical experiments with different values of $C_{\mathcal{P}}^i$, $C_{\mathcal{V}}^j$, Δ_E, U_{MDO}, $\hat{U}_{\text{LNG}}$, and $\tilde{U}_{\text{LNG}}$.

Table 3.2: Values of crucial parameters

Parameter	Values
Δ_E	500, 700, 900, 1100, 1119.333, 1300, 1500
U_{MDO}	800, 900, 950, 1000, 1100, 1200
$\hat{U}_{\text{LNG}}$	700, 750, 800, 850, 900, 950, 1000
$\tilde{U}_{\text{LNG}}$	550, 600, 650, 700, 750
$C_{\mathcal{P}}^i$ (average value)	3285000, 3650000, 4015000, 4380000, 4745000
$C_{\mathcal{V}}^j$	$[305700, 509500)$, $[509500, 1019000)$, $[1019000, 1528500)$, $[1528500, 2038000)$, $[2038000, 2547500)$

For each crucial parameter, a group of numerical experiments was conducted to analyze the influence of this parameter on $OptG$. For example, in $Group\Delta_E$, there were seven cases with different values of Δ_E, namely $C\Delta_E1$ to $C\Delta_E7$. All of the other parameters of cases in $Group\Delta_E$ were the same as in the basic case $CBasic$. The optimal objective values of the six groups of cases are listed in Figure 3.5.

From Figure 3.5(a), 3.5(b), and 3.5(f) we can see that $OptG$ decreases with $C_{\mathcal{P}}^i$, $C_{\mathcal{V}}^j$, and $\tilde{U}_{LNG}$. This is reasonable because a higher bunkering station construction

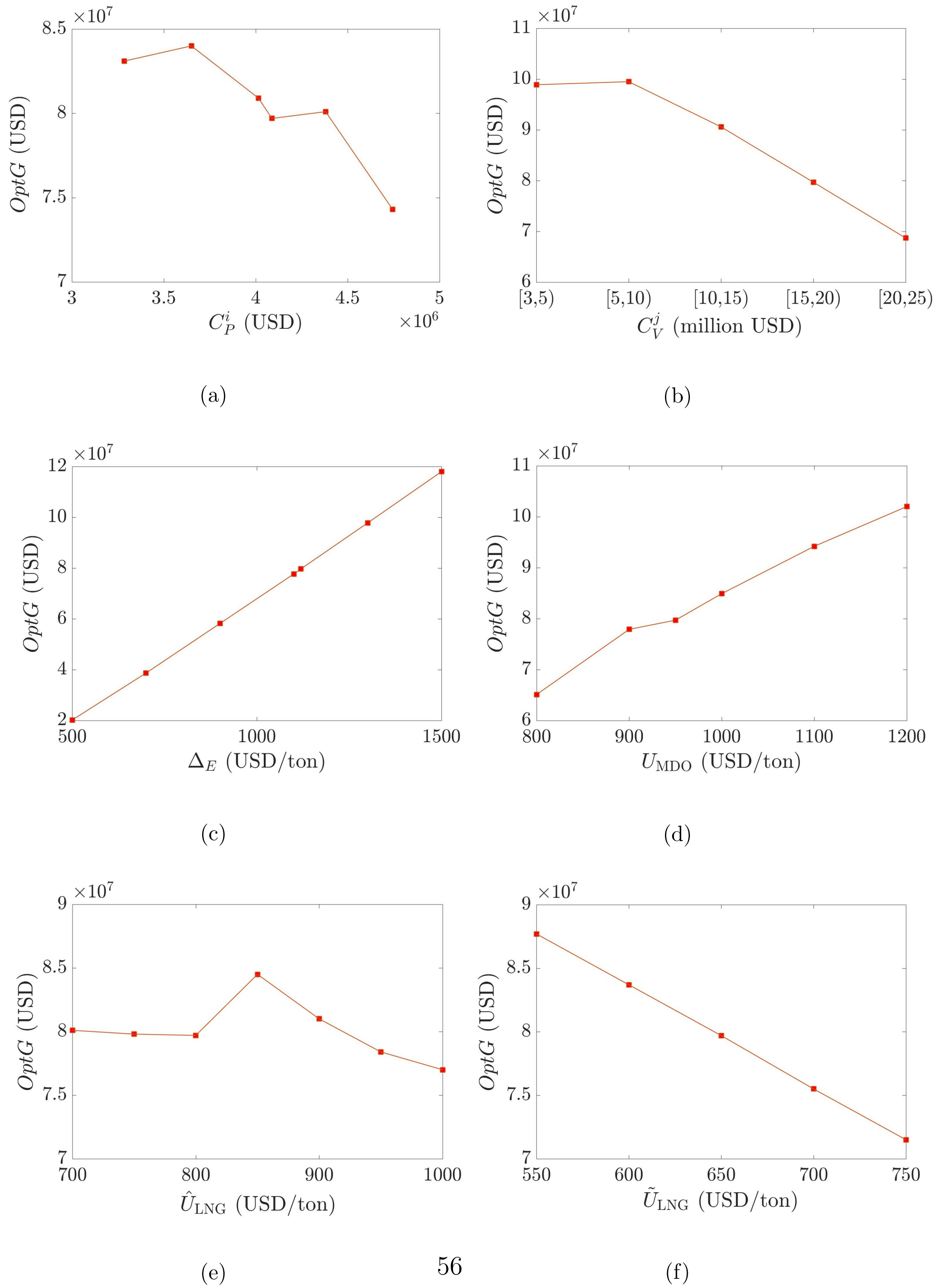

Figure 3.5: Results of numerical experiments with different values of critical parameters

cost, ship retrofitting cost, and LNG purchasing cost will discourage ports and ships from adopting LNG, so the government needs to provide more generous subsidies in response. Figure 3.5(c) and 3.5(d) show that *OptG* increases with Δ_E, and U_{MDO}. Regarding Δ_E, the result is intuitive, because a larger value of Δ_E leads to higher environmental revenue with the same LNG consumption volume. As for U_{MDO}, the higher the MDO price, the greater the bunker cost that ship operators can save by retrofitting their ships, and the lower the subsidy required to encourage them to do so. The relationship between *OptG* and $\hat{U}_{\text{LNG}}$ is slightly more complicated, as shown in Figure 3.5(e), because the value of $\hat{U}_{\text{LNG}}$ influences the bunker cost savings of ship operators and the LNG selling profit of ports in opposite ways. Thus, the subsidies required by ports and ships change in opposite directions.

3.5 Conclusions

LNG is a promising alternative fuel for the maritime transportation industry, as it can reduce ship emissions and alleviate environmental problems. However, the application of LNG as marine fuel is still in its infancy and is impeded by various factors, such as the "chicken and egg" problem that arises in any transition to alternative fuels. To break the deadlock, the government can provide subsidies for ports and ships to cover part of the costs of constructing LNG bunkering stations and retrofitting ships. Considering the environmental revenue resulting from the use of LNG as marine fuel and the subsidy expenditure, the government needs to select a subsidy rate that will maximize the total profit. Therefore, this study has investigated the government subsidy plan optimization problem for LNG as marine fuel. Three parties are involved in the problem, namely the government, the ports in the area under consideration, and the ships sailing in the area; each party acts in its own interests. Based on this structure, a trilevel programming model was proposed, and then the bilevel problem (port level and ship level) was converted into an equivalent single-level problem. Next, after linearization, the problem becomes a mixed-integer linear problem that can be solved by CPLEX. Finally, an enumeration algorithm was applied to determine the optimal subsidy rates.

Two series of numerical experiments were conducted. First, to determine how subsidy rates influence the net government profit and environmental revenue, numerical experiments with given values of $\alpha_{\mathcal{P}}$ and $\alpha_{\mathcal{V}}$ were carried out. The results showed that a government subsidy can significantly promote the application of LNG as marine fuel, but that there exist complex relationships between subsidy rates and net government profit, and between subsidy rates and environmental revenue. In extreme cases, the government net profit may become negative. It is therefore necessary to investigate the government subsidy plan optimization problem. Second, numerical experiments were conducted to analyze the impact of various crucial parameters on the optimal solution. The values of $C_{\mathcal{P}}^{i}$, $C_{\mathcal{V}}^{j}$, and $\tilde{U}_{\text{LNG}}$ are negatively related to the government's net profit. Meanwhile, higher values of Δ_E and U_{USD} lead to higher net government profit. However, the influence of $\hat{U}_{\text{LNG}}$ is more complicated, because $\hat{U}_{\text{LNG}}$ impacts the profit of ports and ships in opposite ways.

Chapter 4

LNG Bunkering Station Deployment Problem in Maritime Transportation

4.1 Introduction

Maritime transportation is indispensable for both international and domestic trade (UNCTAD 2020). With the transportation volume continuously increasing and reaching a record high, maritime emissions have become a common concern of the whole society (Deng et al. 2021, Ytreberg et al. 2021). Sofiev et al. (2018) estimated that pollutants from the maritime industry leads to more than 400,000 premature deaths annually. Therefore, sustainable shipping, decarbonization and ship pollution control remain priorities of the future development of the industry UNCTAD (2020). To alleviate problems caused by maritime emissions, the International Maritime Organization (IMO) as well as governments of various countries and regions have conducted regulations and rules that restrict ship emissions (International Maritime Organization 2013, Ministry of Transport of the People's Republic of China 2018, International Maritime Organization 2020, Commission 2021). Ships sailing through areas that are covered by certain restrictions have to obey those rules, and the carriers need to maintain service levels and reduce costs at the same time. Currently, there are two main types of methods that can be adopted by ship operators to reduce ship emissions, one includes technologies that can reduce impurity content in the marine fuel oil, or reduce the generation of pollutants, or clean exhaust gases before emit them (Deng et al. 2021). The other type is to use alternative fuels including bio-diesel, methanol, MGO and LNG to generate power.

LNG is one of the cleanest fossil fuels in the world and also a promising alternative fuel for marine transportation. LNG-fueled ships can dramatically reduce ship emissions compare to traditional ships, nearly 100% of SO_X and PM, up to 85–90% of NO_X, and 15–20% of CO_2 (Wang and Notteboom 2014, New South Wales Environment Protection Authority of Australia 2015). However, various areas lack the LNG bunkering system, which is necessary for the application of LNG-fueled ships. Therefore, to popularize LNG-fueled ships, the government needs to build a complete LNG bunkering system and construct bunkering stations at some critical ports located in the area. Considering the limited annual budget, the construction work has to be finished in a planning period that usually last for several years. Although the outcome of the construction work is fixed, namely all the predetermined ports will be equipped with bunkering stations, the construction sequence will influence the ship emission volume in the planning period. In this chapter, we focus on the LNG bunkering station deployment problem and try to find the optimal solution to the question that at which period should each bunkering station be constructed. In addition to the government decisions, the reaction of different shipping lines will also be considered. In another word, at shipping lines make operational decisions at each period on their own interests. According to the report of Schinas and Butler (2020), ships that powered purely by LNG are always an LNG carrier and use natural gas produced during transportation for power. Therefore, we focus on the dual-fueled ships, which are equipped with dual-fuel engines that can switch between traditional bunker fuel oil and LNG during a trip (Fokkema et al. 2017).

The deployment problem of port facilities for emission reduction has recently been proposed. Wu and Wang (2020) explore the deployment problem of port-side shore power facilities in a container shipping network. Although both this chapter and

Wu and Wang (2020) study the deployment problem and have multilevel structures, there are essential differences between them. The first difference is in the ship level model, it roots in how these two technologies work. In Wu and Wang (2020), the only decision for the ship operator is whether to install the onboard shore power facilities. In this chapter more operational decisions of shipping lines are considered, including the ship type and ship number to deploy on the route and the sailing speed of ships, because these factors impact on the ship emission related to the use of LNG. Second, due to the difference in ship level, the method proposed by Wu and Wang (2020) becomes not applicable. Therefore, we propose a tailored two-stage method to solve our model. In conclusion, this chapter is essentially different from Wu and Wang (2020) in both the model and solution method.

The academic contribution of this paper is threefold.

- As far as the authors are concerned, this is the first paper that investigates the LNG bunkering station deployment problem and aims to minimize the ship emission through the planning period.
- A bilevel model is originally proposed to describe the problem. Not only the government decisions but also the shipping lines' operational decisions, including ship type, ship number, and sailing speed, are considered simultaneously.
- A tailored two-stage solution method is designed to solve the model. In the first stage we reduce the range of potential optimal solutions of each ship route, and we handle the bilevel structure by using a matrix to indicate the decision shipping lines in the second stage. Also, the numerical experiment results and analysis validate the model and solution method we propose.

The remainder of the paper is organized as follows: Section 4.2 describes the problem and gives the mathematical model. Section 4.3 displays the two-stage method originally proposed to solve the model. Numerical experiments based on data from previous studies and the results we obtained are presented in Section 4.4. Last, Section 4.5 set the conclusions.

4.2 Model Formulation

4.2.1 Problem Description

In this chapter, we consider an inland river area that has a set of ports along it, denoted by $\mathcal{P} = \{1, 2, ..., |\mathcal{P}|\}$ from downstream to upstream. A set of shipping routes, denoted by $\mathcal{R} = \{1, 2, ..., |\mathcal{R}|\}$, are operated by different shipping lines to satisfy transportation demand among ports in $\mathcal{P}$. The number of homogeneous ships that are chartered in and deployed on route j is denoted by η_j. Each ship deployed in route $j, j \in \mathcal{R}$, sails along a closed loop, from the most downstream physical port of the route, which is denoted by D_j, to the most upstream one, which is denoted by U_j, and then sails back to D_j. The set of ports covered by route j is denoted by $\mathcal{P}'_j$, and $k \in \mathcal{P}'_j$ represents the k^{th} one, and different ports may refer to the same physical port. Here we define a binary variable T_{jki} that equals 1 if the k^{th} port of route j corresponds to physical port $i \in \mathcal{P}$, and 0 otherwise. In Figure 4.1 is an example of route j on a river with 5 different physical ports.

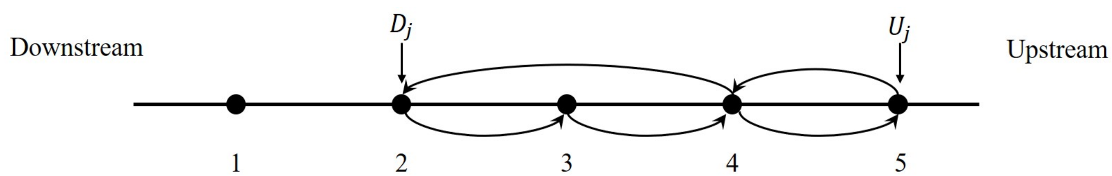

Figure 4.1: An example of route j

As shown in Figure 4.1, to finish route j, a ship has to visit port 2, port 3, port 4, port 5, and port 4, in sequence and then go back to port 2. In this example, we have $\mathcal{P}'_j = \{1, 2, 3, 4, 5\}$. Meanwhile, we have $T_{j12} = T_{j23} = T_{j34} = T_{j45} = T_{j54} = 1$, and all other T_{jki} equal to 0. From the example we can see that route j does not visit all physical ports that the ship passes by, and the route can be divided into $\left|\mathcal{P}'_j\right|$ voyages with the sailing distance of L_{jk}. Ships sailing on voyage j berth at port k for m_{jk} hours for cargo handling, and sail at a speed of μ_j knots (nautical mile per hour). The sailing speed of ships on route j, μ_j, is directly related to the ship number and meet the constraint of weekly service frequency.

Currently, there is no LNG bunkering station at any port in the area, and therefore all ships deployed in the area are traditional diesel ships that use MDO as the main bunker fuel for power. Since the service is provided with a weekly frequency, in this chapter we set the minimization of the weekly operating cost as the objective of the shipping line. In this chapter, the operating cost includes two parts, namely the ship chartering cost and the bunker cost. The weekly chartering cost of a traditional diesel ship is denoted by C^j_{MDO}.

The bunker cost depends on MDO price as well as MDO consumption rate. The market bunkering price of MDO, O_{MDO} USD/ton, is assumed to be the same for all ships, but the consumption rates varies from vessel to vessel.The MDO consumption of ship j to sail one nautical mile, $g^j_{\text{MDO}}(\mu_j)$ ton/n mile, is also closely related to the sailing speed. However the MDO consumption rate while berthing, ${g'}^j_{\text{MDO}}$ does not depend on the sailing speed. The government incurs the emission costs of E_{MDO} USD when a ton of MDO is consumed as the bunker fuel.

In addition to traditional diesel ships, shipping lines can charter in and deploy dual-fueled ships on the route at the weekly price of C^j_{Dual} for each. A dual-fueled ship is able to switch between MDO and LNG during any voyage. Due to the limited LNG tank capacity, which is denoted by W_j, MDO would be used if and only if LNG is in short. Ships can get refueled at LNG bunkering stations that are available, and the bunkering operation of MDO is not considered in this chapter. When ships on route j rely on LNG for power, $g^j_{\text{LNG}}(\mu_j)$ tons of LNG would be consumed to sail one nautical mile, and ${g'}^j_{\text{LNG}}$ tons of LNG to berth for one hour. For MDO consumption rates of dual-fueled ships, we consider they are the same as those of traditional diesel ships that can be deployed on the same route. We further assume that ${g'}^j_{\text{MDO}}/{g'}^j_{\text{LNG}} = g^j_{\text{MDO}}(\mu_j)/g^j_{\text{LNG}}(\mu_j) = Q$, $j \in \mathcal{V}$, in which Q is a coefficient. This assumption means that for route j, Q tons of MDO will be saved if one ton of LNG is consumed as the bunker fuel.

Compared with MDO, LNG has a much lower emission cost E_{LNG}. With the aim to reduce emission costs, the government, which operates all physical ports in $\mathcal{P}$, has decided to promote the application of LNG as bunker fuel in this area. To achieve the goal, the government will construct LNG bunkering stations at various ports.

Constructing a bunkering station at port $i, i \in \mathcal{P}$, will cost the government $\bar{C}_i^{\mathcal{P}}$ USD. Due to the limited financial budget, it is not possible to construct LNG bunkering stations at all ports at one time. Therefore, the government needs to make an LNG bunkering station deployment plan to schedule the construction sequence. The deployment plan covers T years, and in each year $t = 1, ..., T$, a given budget of B_t USD is allocated to the construction of LNG bunkering stations. Then, the problem becomes a multi-stage LNG bunkering station deployment problem, in which year t represents stage t, and the government aims to minimize the total ship emission costs at all stages.

Considering that the government and shipping lines act on their own interests, this problem can be described by a bilevel model. In the upper-level model, with the constraint of financial budget B_t, the government decides at which port to construct LNG bunkering stations at each stage t. The objective is to minimize the total environment costs in all stages. In the lower-level model, given the LNG bunkering station availability, the objective of each shipping line is to minimize the weekly operating cost of the route that they operate at each stage. The shipping line has to decide the ship type chartered and deployed on the route, the number of ships deployed, the sailing speed of deployed ships, and the LNG bunkering operations if dual-fueled ships are deployed. The route operation, in turn, influences the LNG bunkering station construction. Stage-by-stage, the LNG bunkering system will be developed in the area, and dual-fueled ships would be extensively adopted.

4.2.2 Upper-level Model

The government makes decisions at the upper-level to minimize total emission costs in all stages. The decision is denoted by $\vec{y}_t := (y_{ti} \in \{0, 1\}, i \in \mathcal{P})$, and we have $y_{ti} = 0$ if LNG bunkering station at physical port i will be constructed at stage t, otherwise we have $y_{ti} = 0$. For convenience, we further denote the LNG bunkering stations that are available at stage t as $\vec{z}_t := \vec{z}_{t-1} + \vec{y}_t$. Since there is no LNG bunkering station at the beginning, we have $\vec{z}_0 = \vec{0}$. To be specific, $\vec{z}_t := (z_{ti} \in \{0, 1\}, i \in \mathcal{P})$, and $z_{ti} = 1$ represents that LNG bunkering station is available at port i at stage

t. Since the objective of the government is to minimized emission costs, the LNG bunkering station will be set to just cover the cost of providing it, denoted by O_{LNG}.

4.2.3 Lower-level Model

At stage $t, t \in T$, given the LNG bunkering station availability, $\vec{z}_t$, decided by the government at stage shipping lines minimize the total operating cost of their routes. The type of ships that will be charted in and deployed on route $j, j \in \mathcal{R}$ is denoted by a binary variable x_j. The number of ships deployed on route j, η_j, and their sailing speed, μ_j, should meet the weekly service requirement. If $x_j = 0$, namely traditional diesel ships are deployed on route j, the weekly bunker cost can be calculated as $O_{\text{MDO}}\left[g^j_{\text{MDO}}(\mu_j)\sum_{k\in\mathcal{P}'_j} L_{jk} + g'^j_{\text{MDO}}\sum_{k\in\mathcal{P}'_j} m_{jk}\right]$.

If dual-fueled ships are chartered in and deployed on route j, namely $x_j = 1$, the bunker cost would be consist of the MDO cost and the LNG cost. As the LNG bunkering price, O_{LNG}, is the same at different ports, the LNG tank of dual-fueled ships will be filled up at every port with LNG bunkering stations. For simplicity, it is assumed that the dual-fueled ships would get refueled when the cargo handling is finished if the port has a LNG bunkering station, and then leave the port. To calculate the LNG and MDO usage, we introduce a series of decision variables: π^{Finish}_{jk} and π^{Leave}_{jk}. For port $k, k \in \mathcal{P}'_j$, π^{Finish}_{jk} represents the LNG remaining volume of ships deployed on route j when the cargo handling at the port k is just finished (before refueling, if any), and π^{Leave}_{jk} represents the LNG remaining volume when ships leave the k^{th} port (after refueling, if any). If ships get refueled at this port, then we have $0 \le \pi^{Finish}_{jk} < \pi^{Leave}_{jk} = W_j$; otherwise we have $\pi^{Finish}_{jk} = \pi^{Leave}_{jk}$.

4.2.4 Mathematical model

Here we list the notations that will be used before representing the mathematical model.

Parameters

$\mathcal{P}$	the set of physical ports along the river, $\mathcal{P} = \{1, 2, ..., \lvert\mathcal{P}\rvert\}$, indexed by i;

$\mathcal{R}$	the set of shipping routes that are operated to satisfy transport demand along the river, $\mathcal{R} = \{1, 2, ..., \lvert\mathcal{R}\rvert\}$, indexed by j;
$\mathcal{P'}_j$	the set of ports covered by route j, $\forall j \in \mathcal{R}$, indexed by k;
D_j	the most downstream physical port covered by route j, $\forall j \in \mathcal{R}$;
U_j	the most upstream physical port covered by route j, $\forall j \in \mathcal{R}$;
T_{jki}	binary parameter, equal to 1 if the k^{th} port of route j refers to physical port i, 0 otherwise, $\forall j \in \mathcal{R}, \forall k \in \mathcal{P'}_j, \forall i \in \mathcal{P}$;
L_{jk}	the sailing distance (nm) from the k^{th} port on route j to the $k+1^{\text{th}}$ port, $\forall j \in \mathcal{R}, k = 1, ..., \lvert\mathcal{P'}_j\rvert - 1$;
$L_{j\lvert\mathcal{P'}_j\rvert}$	the sailing distance (nm) from the $\lvert\mathcal{P'}_j\rvert^{\text{th}}$ port on route j to the 1^{st} port, $\forall j \in \mathcal{R}$;
$\bar{\mu}_j$	the upper limit of sailing speed (knot) of ships deployed on route j, $\forall j \in \mathcal{R}$;
$\underline{\mu}_j$	the lower limit of sailing speed (knot) of ships deployed on route j, $\forall j \in \mathcal{R}$;
C^j_{MDO}	the weekly chartering cost of traditional diesel ships deployed on route j, $\forall j \in \mathcal{R}$;
C^j_{Dual}	the weekly chartering cost of dual-fueled ships deployed on route j, $\forall j \in \mathcal{R}$;
O_{MDO}	the bunkering price of MDO (USD/ton);
O_{LNG}	the bunkering price of LNG (USD/ton);
$\bar{C}^{\mathcal{P}}_i$	the construction cost (USD) of LNG bunkering station at port i;
T	the number of LNG bunkering station deployment plan stages;
B_t	the given budget (USD) that is allocated to LNG bunkering station construction at stage t, $t = 1, ..., T$;
Q	the coefficient that represents the relationship between the consumption rate of MDO and LNG;
E_{MDO}	the emission cost of one ton of MDO (USD/ton);
E_{LNG}	the emission cost of one ton of LNG (USD/ton);

W_j the LNG tank capacity of dual-fueled ships that are deployed on route j, $\forall j \in \mathcal{R}$;

m_{jk} the berthing time (hour) at the k^{th} port of call on route j, $\forall j \in \mathcal{R}, \forall k \in \mathcal{P'}_j$.

Decision variables

x_j binary variable, equal to 0 if traditional diesel ships are deployed on route j, equal to 1 if dual-fueled ships are deployed on route j, $\forall j \in \mathcal{R}$;

y_{ti} binary variable, equal to 1 if LNG bunkering station at physical port i will be constructed at stage t, 0 otherwise, $\forall i \in \mathcal{P}, t = 1, ..., T$;

z_{ti} binary variable, equal to 1 if LNG bunkering station at physical port i is available at stage t, 0 otherwise, $\forall i \in \mathcal{P}, t = 0, ..., T$;

η_j integer variable, the number of ships chartered in and deployed on route j, $\forall j \in \mathcal{R}$;

μ_j integer variable, the number of ships chartered in and deployed on route j, $\forall j \in \mathcal{R}$;

$g^j_{\text{MDO}}(\mu_j)$ the MDO consumption rate (ton/n mile) of ships deployed on route j while sailing, $\forall j \in \mathcal{R}$;

g'^j_{MDO} the MDO consumption rate (ton/hour) of ships deployed on route j while berthing, $\forall j \in \mathcal{R}$;

$g^j_{\text{LNG}}(\mu_j)$ the LNG consumption rate (ton/n mile) of dual-fueled ships deployed on route j while sailing, $\forall j \in \mathcal{R}$;

g'^j_{LNG} the LNG consumption rate (ton/hour) of dual-fueled ships deployed on route j while berthing, $\forall j \in \mathcal{R}$;

θ_{jk} binary variable, equal to 1 if port k on route j has LNG bunkering station, 0 otherwise, $\forall j \in \mathcal{R}, \forall k \in \mathcal{P'}_j$;

π^{Leave}_{jk} the LNG remaining volume of when ships leave port k on route j (after refueling, if any), $\forall j \in \mathcal{R}, \forall k \in \mathcal{P'}_j$;

π^{Finish}_{jk} the LNG remaining volume of when the cargo handling at port k on route j is just finished (before refueling, if any), $\forall j \in \mathcal{R}, \forall k \in \mathcal{P'}_j$;

$\hat{\rho}^j_{\text{LNG}}$ the weekly LNG consumption volume (ton) of route j, $\forall j \in \mathcal{R}$;

$\hat{\rho}^{j}_{\text{MDO}}$ the weekly MDO consumption volume (ton) of route j, $\forall j \in \mathcal{R}$.

Vectors

$\vec{y}_t$ the vector of y_{ti}, $\vec{y}_t = \left(y_{t1}, ..., y_{t|\mathcal{P}|}\right)$, $t = 1, ..., T$;

$\vec{z}_t$ the vector of z_{ti}, $\vec{z}_t = \left(z_{t1}, ..., z_{t|\mathcal{P}|}\right)$, $t = 0, ..., T$;

$\vec{\theta}_j$ the vector of θ_{jk}, $\vec{\theta}_{jk} = \left(\theta_{j1}, ..., \theta_{j|\mathcal{P'}_j|}\right)$, $\forall j \in \mathcal{R}$.

Then the LNG bunkering station deployment problem faced by the government can be described by the following bilevel model $[MG]$:

$$[\boldsymbol{MG}] \quad \underset{\vec{y}_1,...,\vec{y}_T,\vec{z}_1,...,\vec{z}_T}{\text{minimize}} \sum_{t=1}^{T} \sum_{j \in \mathcal{R}} 52 \left(E_{\text{LNG}} \hat{\rho}^{tj*}_{\text{LNG}} + E_{\text{MDO}} \hat{\rho}^{tj*}_{\text{MDO}}\right) \tag{4.1}$$

subject to

$$\sum_{i \in \mathcal{P}} \bar{C}^{\mathcal{P}}_i y_{ti} \leq B_t, t = 1, ..., T \tag{4.2}$$

$$\vec{z}_t = \vec{z}_{t-1} + \vec{y}_t, t = 2, ..., T \tag{4.3}$$

$$\vec{z}_0 = \vec{y}_0 \tag{4.4}$$

$$\sum_{t=1}^{T} y_{ti} = 1, \forall i \in \mathcal{P} \tag{4.5}$$

$$y_{ti} = 0, 1, t = 1, ..., T, \forall i \in \mathcal{P} \tag{4.6}$$

$$z_{ti} = 0, 1, t = 1, ..., T, \forall i \in \mathcal{P} \tag{4.7}$$

and

$$\left(\hat{\rho}^{tj*}_{\text{LNG}}, \hat{\rho}^{tj*}_{\text{MDO}}\right) \in \Psi_j \left(\vec{z}_t\right), t = 1, ..., T \tag{4.8}$$

where $\Psi_j \left(\vec{z}_t\right)$ are determined by the following lower-level model:

$$
[\boldsymbol{MR_j}] \quad \hat{\Psi}_j\left(\vec{z}_t\right) = \underset{x_j,\eta_j,\mu_j,\hat{\rho}^j_{\text{LNG}},\hat{\rho}^j_{\text{MDO}},\vec{\theta}_j}{\arg\min} \left(1-x_j\right) C^j_{\text{MDO}}\eta_j + x_j C^j_{\text{Dual}}\eta_j + O_{\text{LNG}}\hat{\rho}^j_{\text{LNG}} + O_{\text{MDO}}\hat{\rho}^j_{\text{MDO}} \tag{4.9}
$$

subject to

$$
\pi^{Leave}_{jk} = \pi^{Finish}_{jk} + \theta_{jk}\left(W_j - \pi^{Finish}_{jk}\right), \forall k \in \mathcal{P}'_j \tag{4.10}
$$

$$
\pi^{Finish}_{jk} = \max\left\{0, \pi^{Leave}_{j,k-1} - L_{j,k-1} g^j_{\text{LNG}}(\mu_j) - m_{jk} {g'}^j_{\text{LNG}}\right\}, k = 2, 3, ..., \left|\mathcal{P}'_j\right| \tag{4.11}
$$

$$
\pi^{Finish}_{j1} = \max\left\{0, \pi^{Leave}_{j\left|\mathcal{P}'_j\right|} - L_{j\left|\mathcal{P}'_j\right|} g^j_{\text{LNG}}(\mu_j) - m_{j1} {g'}^j_{\text{LNG}}\right\} \tag{4.12}
$$

$$
\theta_{jk} = \sum_{i \in \mathcal{P}} z_{ti} T_{jki}, \forall k \in \mathcal{P}'_j \tag{4.13}
$$

$$
\frac{\sum\limits_{k \in \mathcal{P}'_j} L_{jk}}{\mu_j} + \sum_{k \in \mathcal{P}'_j} m_{jk} \leq 168\eta_j \tag{4.14}
$$

$$
\hat{\rho}^j_{\text{LNG}} = x_j \sum_{k \in \mathcal{P}'_j} \left(\pi^{Leave}_{jk} - \pi^{Finish}_{jk}\right) \tag{4.15}
$$

$$
\begin{aligned}
\hat{\rho}^j_{\text{MDO}} = \left(1-x_j\right) \left[g^j_{\text{MDO}}(\mu_j) \sum_{k \in \mathcal{P}'_j} L_{jk} + {g'}^j_{\text{MDO}} \sum_{k \in \mathcal{P}'_j} m_{jk}\right] \\
+ Q x_j \left[g^j_{\text{LNG}}(\mu_j) \sum_{k \in \mathcal{P}'_j} L_{jk} + {g'}^j_{\text{LNG}} \sum_{k \in \mathcal{P}'_j} m_{jk} - \sum_{k \in \mathcal{P}'_j} \left(\pi^{Leave}_{jk} - \pi^{Finish}_{jk}\right)\right]
\end{aligned} \tag{4.16}
$$

$$
\underline{\mu}_j \leq \mu_j \leq \bar{\mu}_j \tag{4.17}
$$

$$
\theta_{jk} = 0, 1, \forall k \in \mathcal{P}'_j \tag{4.18}
$$

$$
x_j = 0, 1 \tag{4.19}
$$

$$\eta_j \in \mathbb{Z}^+ \tag{4.20}$$

$$0 \leq \pi_{jk}^{Finish} \leq \max\left\{0, W_j - L_{j,k-1} g_{\text{LNG}}^{j}(\mu_j) - m_{jk} {g'}_{\text{LNG}}^{j}\right\}, k = 2, ..., \left|\mathcal{P}_j'\right| \tag{4.21}$$

$$0 \leq \pi_{j1}^{Finish} \leq \max\left\{0, W_j - L_{j,\left|\mathcal{P}_j'\right|} g_{\text{LNG}}^{j}(\mu_j) - m_{j1} {g'}_{\text{LNG}}^{j}\right\} \tag{4.22}$$

$$0 \leq \pi_{jk}^{Leave} \leq W_j, \forall k \in \mathcal{P}_j'. \tag{4.23}$$

In the upper-level model $[MG]$, the objective function (4.1) minimizes the emission costs in all stages, and 52 represents that there are 52 weeks in a year. Constraints (4.2) are the budget constraints in each stage. The relationship between $\vec{z}_t$ and $\vec{y}_t$ is explained by constraints (4.3). Constraints (4.5) assure that all physical port will be equipped with an LNG bunkering station at the end of period T. Constraints (4.6) and (4.7) are the domains of z_{ti} and y_{ti}. In the lower-level, different shipping lines make their decisions independently, we build $[MR_j]$ for route j. The objective function (4.9) minimizes the weekly operating cost of route j, which consists of the ship chartering cost and the bunker cost. Constraints (4.10) explain the relationship between the LNG remaining volume when dual-fueled ships finish the cargo handling at port k along the route and the remaining volume when they leave the port. Constraints (4.11) and (4.12) state that dual-fueled ships mainly rely on LNG for power to sail and berth, and MDO will be used if and only if LNG is in short. Constraints (4.13) show that the LNG tank of dual-fueled ships will be filled up at every port with LNG bunkering station. Constraint (4.14) guarantees the weekly service frequency, and 168 represents there are 168 hours in a week. Constraints (4.15) and (4.16) calculate the weekly MDO and LNG consumption volume of route j. Constraints (4.17) to (4.23) are the domains of variables. For constrains (4.21) and (4.22), the upper limit of π_{jk}^{Finish} will be reached only if dual-fueled ships get refueled at the last port along the route before port k.

4.3 Solution Method

In this section, we present the method of addressing the bilevel model proposed. The lower-level model is linearized and a set of possible optimal solutions are generated for each $[MR_j]$. Next, with a series of binary variables, the bilevel linear model is converted as an equivalent single-level one.

4.3.1 Potential Optimal Solution Reduction

The lower-level model for ship j is a mix-integer nonlinear model, which contains nonlinear factors in both the objective function and constraints. Next, we show how to handle the nonlinear elements caused by the ship sailing speed, namely L_{jk}/μ_j in constraint (4.14) and the bunkering fuel consumption rate function $g^j_{\text{MDO}}(\mu_j)$, $g^j_{\text{LNG}}(\mu_j)$. Following previous studies that consider ship sailing speed optimization, the function of MDO consumption is described as $g^j_{\text{MDO}}(\mu_j) = a_j\mu_j^{b_j}$. According to the estimate of Wang and Meng (2012), the value of a_j ranges from 0.004 to 0.006 and the value of b_j ranges from 1.9 to 2.0.

To avoid the nonlinear elements caused by fuel consumption rate, we investigate the relationship between the sailing speed μ_j and ship umber η_j. For $[MR_j]$, $j \in \mathcal{R}$, have the following property.

Proposition 4.1. *Denote the optimal values of μ_j and η_j as μ_j^* and η_j^*, we have $\sum\limits_{k\in\mathcal{P}'_j} L_{jk}/\mu_j^* + \sum\limits_{k\in\mathcal{P}'_j} m_{jk} = 168\eta_j^*$.*

Proof. *Suppose that the optimal solution satisfy $\sum\limits_{k\in\mathcal{P}'_j} L_{jk}/\mu_j^* + \sum\limits_{k\in\mathcal{P}'_j} m_{jk} < 168\eta_j^*$. Then we have $\mu_j > \sum\limits_{k\in\mathcal{P}'_j} L_{jk}/\left(168\eta_j^* - \sum\limits_{k\in\mathcal{P}'_j} m_{jk}\right)$. We can replace μ_j^* by $\tilde{\mu}_j = \sum\limits_{k\in\mathcal{P}'_j} L_{jk}/\left(168\eta_j^* - \sum\limits_{k\in\mathcal{P}'_j} m_{jk}\right)$. The new solution remains feasible and the objective function decreases because $\tilde{\mu}_j < \mu_j^*$ and the fuel consumption rate $g^j_{\text{LNG}}(\mu_j)$ and $g^j_{\text{MDO}}(\mu_j)$ increase with μ_j. Therefore, μ_j^* is not the optimal value of μ_j.*

With the limited sailing speed range $\left[\underline{\mu}_j, \bar{\mu}_j\right]$, the possible ship numbers deployed on route j can be enumerated, in which the smallest and largest possible ship number are denoted by $\underline{\eta_j}$ and $\overline{\eta_j}$. According to Property 4.1, the optimal solution of $[MR_j]$ can be obtained by enumerating all combinations of possible ship types and ship numbers with the corresponding optimal sailing speed. However, the number of combinations are still large, so we narrow the range of possible optimal solutions for $[MR_j]$ under different LNG bunkering station deployment situations.

With the set of physical ports $\mathcal{P}$, there are $2^{|\mathcal{P}|}$ LNG bunkering station deployment situations. Under each situation, $[MR_j]$ yields a corresponding optimal solution. Considering 4.1, the optimal solution can be represented by the values of η_j and x_j. Denote the set of optimal values of η_j and x_j under different deployment situations as η_{js}^* and x_{js}^*, $s = 1, 2, ..., 2^{|\mathcal{P}|}$, in which $s = 1$ represents the situation that no LNG bunkering station is available and $s = 2^{|\mathcal{P}|}$ represents the situation that all physical ports are equipped with LNG bunkering station. Next we prove the following two properties.

Proposition 4.2. *For $[MR_j]$, we have $\eta_{j1}^* = \max\left\{\eta_{j1}^*, \eta_{j2}^*, ..., \eta_{j2^{|\mathcal{P}|}}^*\right\}$ and $\eta_{j2^{|\mathcal{P}|}}^* = \min\left\{\eta_{j1}^*, \eta_{j2}^*, ..., \eta_{j2^{|\mathcal{P}|}}^*\right\}$.*

Proof. *For route j, the LNG consumption volume is non-decreasing with the number of LNG bunkering stations available along the route, because dual-fueled ships get their LNG tanks fueled up at every available LNG bunkering stations. With the same ship number, the more LNG is consumed, the more bunker cost savings can be achieved. For $s = 1$, the traditional ships must be deployed, because there is no LNG bunkering stations available. As more LNG bunkering stations are constructed, more LNG is consumed and the average bunker cost decreases. In addition, since the weekly ship chartering cost keeps the same, the optimal ship number when dual-fueled ships are deployed will decrease too. Following this logic, for $s = 2^{|\mathcal{P}|}$, namely all ports are equipped with LNG bunkering station, the optimal ship number when dual-fueled ships are deployed reaches the lowest value.*

According to Property 4.2, for route j, the range of potential optimal ship number is narrowed down to $\eta_{j2^{|\mathcal{P}|}}^*, \eta_{j2^{|\mathcal{P}|}}^* + 1, ..., \eta_{j1}^*$.

Proposition 4.3. *For route j, dual-fueled ship is the optimal ship type of all cases whose optimal ship number is less than η^*_{j1}.*

Proof. *Suppose that in a case, the optimal ship type is traditional ship and the optimal ship number is less than η^*_{j1}. Apparently, the operation of traditional ships is not affected by LNG bunkering station deployment. Therefore, the optimal solution in this case is the same as in case $s = 1$, which is deploying η^*_{j1} traditional ships on the route. This conflicts whit the assumption that the optimal ship number is less than η^*_{j1}.*

Combining Property 4.2 and Property 4.3, we can obtain $\left(x^*_{j1}, \eta^*_{j1}\right)$ by enumerating the following solutions $\left(x_j = 0, \underline{\eta_j}\right), \left(x_j = 0, \underline{\eta_j} + 1\right), ..., (x_j = 0, \overline{\eta_j})$ under the situation $s = 1$. And $\left(x^*_{j2^{|\mathcal{P}|}}, \eta^*_{j2^{|\mathcal{P}|}}\right)$ can be obtained by enumerating $\left(x_j = 0, \underline{\eta_j}\right)$, $\left(x_j = 1, \underline{\eta_j}\right), \left(x_j = 1, \underline{\eta_j} + 1\right), ..., (x_j = 1, \overline{\eta_j})$ under the situation $s = 2^{|\mathcal{P}|}$.

Therefore, the range of potential optimal values of x_j and η_j of $[MR_j]$ under situation s, $s = 1, 2, ..., 2^{|\mathcal{P}|}$, can be narrowed down to a set as follows.

Set

$\mathcal{S}_j$ — the set of candidate for optimal solution of $[MR_j]$, if $x^*_{j2^{|\mathcal{P}|}} = 0$ and $\eta^*_{j2^{|\mathcal{P}|}} = \eta^*_{j1}$, $\mathcal{S}_j = \left\{\left(0, \eta^*_{j1}\right)\right\}$, if $x^*_{j2^{|\mathcal{P}|}} = 1$ and $\eta^*_{j2^{|\mathcal{P}|}} = \eta^*_{j1}$, $\mathcal{S}_j = \left\{\left(0, \eta^*_{j1}\right), \left(1, \eta^*_{j1}\right)\right\}$, if $x^*_{j2^{|\mathcal{P}|}} = 1$ and $\eta^*_{j2^{|\mathcal{P}|}} < \eta^*_{j1}$, $\mathcal{S}_j = \left\{\left(0, \eta^*_{j1}\right), \left(1, \eta^*_{j1}\right), \left(1, \eta^*_{j1} - 1\right), ..., \left(1, \eta^*_{j2^{|\mathcal{P}|}}\right)\right\}$, $\forall j \in \mathcal{R}$.

For simplicity, we denote the following parameters for each potential optimal solution as follows.

Parameters

$\tilde{\eta}_{js}$ — the value of η_j in candidate s of $[MR_j]$, $\forall s \in \mathcal{S}_j$, $\forall j \in \mathcal{R}$;

$\tilde{\mu}_{js}$ — the value of μ_j in candidate s of $[MR_j]$, equal to $\sum_{k \in \mathcal{P}'_j} L_{jk} / \left(168\tilde{\eta}_{js} - \sum_{k \in \mathcal{P}'_j} m_{jk}\right)$, $\forall s \in \mathcal{S}_j$, $\forall j \in \mathcal{R}$;

$\tilde{g}^{js}_{\text{MDO}}$ — the MDO consumption rate of ν_j in candidate s of $[MR_j]$, equal to $a_j \tilde{\mu}^{b_j}_{js}$, $\forall s \in \mathcal{S}_j$, $\forall j \in \mathcal{R}$;

$\tilde{g}^{js}_{\text{LNG}}$ — the LNG consumption rate of ν_j in candidate s of $[MR_j]$, equal to $\frac{1}{Q} a_j \tilde{\mu}^{b_j}_{js}$, $\forall s \in \mathcal{S}_j$, $\forall j \in \mathcal{R}$.

We assume that $|S_j| > 1$, $j \in \mathcal{R}$, because otherwise the route's operation is not influenced by the LNG bunkering station deployment situation and can be excluded from this problem. Therefore, $[MR_j]$ can be rewritten as follows.

Decision variables

$\tilde{x}_{js}$ equal to 1 if candidate s of $[MR_j]$ is applied, 0 otherwise, $\forall j \in \mathcal{R}, \forall k \in \mathcal{P}'_j, \forall s \in \mathcal{S}_j$;

π_{jks}^{Leave} the LNG remaining volume of when ships leave port k on route j (after refueling, if any) when candidate s is applied, $\forall j \in \mathcal{R}, \forall k \in \mathcal{P}'_j, s = 2, ... |\mathcal{S}_j|$;

π_{jks}^{Finish} the LNG remaining volume of when the cargo handling at port k on route j is just finished (before refueling, if any) when candidate s is applied, $\forall j \in \mathcal{R}, \forall k \in \mathcal{P}'_j, s = 2, ... |\mathcal{S}_j|$;

$\hat{\rho}_{\text{LNG}}^{js}$ the weekly LNG consumption volume (ton) of route j when candidate s is applied, $\forall j \in \mathcal{R}, s = 2, ..., |\mathcal{S}_j|$;

$\hat{\rho}_{\text{MDO}}^{js}$ the weekly MDO consumption volume (ton) of route j when candidate s is applied, $\forall j \in \mathcal{R}, \forall s \in \mathcal{S}_j$;

θ_{jkt} binary variable, equal to 1 when ships of route j get refueled for LNG at the k port of call at period t, 0 otherwise, $\forall j \in \mathcal{R}, \forall k \in \mathcal{P}'_j t = 1, ..., T$.

Then the lower-level model $[MR_j]$ is converted into the following model.

$$\begin{aligned}[\boldsymbol{MR'_j}] \quad \hat{\Psi}'_j(\vec{z}_t) = \arg\min_{\tilde{x}_{js}} \tilde{x}_{j1}\left[C_{\text{MDO}}^j \tilde{\eta}_{j1} + O_{\text{MDO}} \hat{\rho}_{\text{MDO}}^{j1}\right] \\ + \sum_{s=2}^{|\mathcal{S}_j|} \tilde{x}_{js}\left\{C_{\text{Dual}}^j \tilde{\eta}_{js} + O_{\text{LNG}} \hat{\rho}_{\text{LNG}}^{js} + O_{\text{MDO}} Q \hat{\rho}_{\text{MDO}}^{js}\right\}\end{aligned} \tag{4.24}$$

subject to

$$\pi_{jks}^{Leave} = \pi_{jks}^{Finish} + \theta_{jkt}\left(W_j - \pi_{jks}^{Finish}\right), s = 2, ..., |\mathcal{S}_j|, \forall k \in \mathcal{P}'_j \tag{4.25}$$

$$\begin{aligned}\pi_{jks}^{Finish} = \max\left\{0, \pi_{j,k-1,s}^{Leave} - L_{j,k-1} \tilde{g}_{\text{LNG}}^{js} - m_{jk} g'^{j}_{\text{LNG}}\right\} \\ s = 2, ..., |\mathcal{S}_j|, k = 2, ..., \left|\mathcal{P}'_j\right|\end{aligned} \tag{4.26}$$

$$\pi_{j1s}^{Finish} = \max\left\{0, \pi_{j|\mathcal{P}'_j|s}^{Leave} - L_{j|\mathcal{P}'_j|}\tilde{g}_{\text{LNG}}^{js} - m_{j1}{g'}_{\text{LNG}}^{j}\right\}, s = 2, ..., |S_j| \tag{4.27}$$

$$\theta_{jkt} = \sum_{i\in\mathcal{P}} z_{ti}T_{jki}, \forall j \in \mathcal{R}, \forall k \in \mathcal{P}'_j, t = 1, ...T \tag{4.28}$$

$$\sum_{s\in\mathcal{S}_j} \tilde{x}_{js} = 1 \tag{4.29}$$

$$\hat{\rho}_{\text{LNG}}^{js} = \sum_{k\in\mathcal{P}'_j} \pi_{jks}^{Leave} - \pi_{jks}^{Finish}, s = 2, ..., |\mathcal{S}_j| \tag{4.30}$$

$$\hat{\rho}_{\text{MDO}}^{j1} = \tilde{g}_{\text{MDO}}^{j1} \sum_{k\in\mathcal{P}'_j} L_{jk} + {g'}_{\text{MDO}}^{j} \sum_{k\in\mathcal{P}'_j} m_{jk} \tag{4.31}$$

$$\hat{\rho}_{\text{MDO}}^{js} = Q\left[\tilde{g}_{\text{LNG}}^{js} \sum_{k\in\mathcal{P}'_j} L_{jk} + {g'}_{\text{LNG}}^{j} \sum_{k\in\mathcal{P}'_j} m_{jk} - \sum_{k\in\mathcal{P}'_j} \left(\pi_{jks}^{Leave} - \pi_{jks}^{Finish}\right)\right]$$
$$s = 2, ..., |\mathcal{S}_j| \tag{4.32}$$

$$\tilde{x}_{js} = 0, 1. \tag{4.33}$$

Objective function (4.24) consists of $|S_j|$ parts and each part represents the operating cost when one of the candidates is applied. Constraints (4.25)–(4.27) calculate the LNG remaining volume at each port of call. Constraint (4.29) shows that only one candidate can be applied. Constraints (4.28) calculate the value of θ_{jkt}. Constraints (4.30)–(4.32) calculate the weekly consumption volume of LNG and MDO when each candidate is adopted. Constraint (4.33) is the range of $\tilde{x}_{js}$. The rewritten model is a mixed integer nonlinear model, in which nonlinear factors exist in both the objective function and constraints. The nonlinear elements in constraints (4.25)–(4.27) can be easily linearized as shown in the Appendix B.

4.3.2 Model conversion

In this subsection, based on the reduced potential optimal solutions for each route $|\mathcal{S}_j|$, we convert the original bilevel model into a single level model $[MGS]$.

We list the new notations used in $[MGS]$ as follows.

Decision variables

β_{jtsm} equal to 1 if solution m of route j is more economical than solution s, at period t, 0 otherwise, $\forall j \in \mathcal{R}, t = 1, ..., T, \forall s \in \mathcal{S}_j, \forall m \in \mathcal{S}_j$;

α_{jts} equal to 1 if solution s of route j is adopted at period t, 0 otherwise, $\forall j \in \mathcal{R}, t = 1, ..., T, \forall s \in \mathcal{S}_j$;

π^{Leave}_{jkts} the LNG remaining volume of when ships leave port k on route j (after refueling, if any) at period t when candidate solution s is applied, $\forall j \in \mathcal{R}, \forall k \in \mathcal{P}'_j, t = 1, ..., T, s = 2, ... |\mathcal{S}_j|$;

π^{Finish}_{jkts} the LNG remaining volume of when the cargo handling at port k on route j is just finished (before refueling, if any) at period t when candidate solution s is applied, $\forall j \in \mathcal{R}, \forall k \in \mathcal{P}'_j, t = 1, ..., T, s = 2, ... |\mathcal{S}_j|$;

Em_{jts} the weekly emission cost candidate solution s of route j at period t, equal to 0 when candidate solution s is not adopted, $\forall j \in \mathcal{R}, t = 1, ..., T, s = 2, ... |\mathcal{S}_j|$;

The model $[MGS]$ is listed as follows.

$$[\boldsymbol{MGS}] \quad \text{minimize} \sum_{j \in \mathcal{R}} \sum_{t=1}^{T} 52 \left\{ \sum_{s=2}^{|\mathcal{S}_j|} Em_{jts} + \sum_{k \in \mathcal{P}'_j} L_{jk} \tilde{g}^{j1}_{\text{MDO}} + m_{jk} g'^{j}_{\text{MDO}} \alpha_{jt1} \right\} \tag{4.34}$$

subject to constraints (4.2)–(4.7), constraints (4.25)–(4.27) for $t = 1, ..., T$, constraint (4.28) and the following constraints:

$$Em_{jts} = \alpha_{jts} \sum_{k \in \mathcal{P}'_j} (E_{\text{LNG}} - QE_{\text{MDO}}) \left(\pi^{Leave}_{jkts} - \pi^{Finish}_{jkts}\right) + QE_{\text{MDO}} \left(L_{jk} \tilde{g}^{js}_{LNG} + m_{jk} g'^{j}_{\text{LNG}}\right)$$
$$\forall j \in \mathcal{R}, t = 1, ..., T, s = 2, ..., |\mathcal{S}_j| \tag{4.35}$$

$$\alpha_{jts} \geq 1 - \sum_{m \in \mathcal{S}_j} \beta_{jtsm}, \forall j \in \mathcal{R}, t = 1, ..., T \tag{4.36}$$

$$\sum_{s \in \mathcal{S}_j} \alpha_{jts} = 1, \forall j \in \mathcal{R}, t = 1, ..., T \tag{4.37}$$

$$\beta_{jtsm} = 0, \forall s \in \mathcal{S}_j, m = s \tag{4.38}$$

$$\beta_{jtsm} = 1 - \beta_{jtms}, s = 2, ..., |\mathcal{S}_j|, m = 1, ..., s-1 \tag{4.39}$$

$$\begin{aligned} &\eta_{j1} C^j_{\text{MDO}} - \eta_{jm} C^j_{\text{Dual}} + \sum_{k \in \mathcal{P}'_j} \left[O_{\text{MDO}} L_{jk} \left(\tilde{g}^{j1}_{\text{MDO}} - Q \tilde{g}^{jm}_{\text{LNG}} \right) \right. \\ &\left. + \left(Q O_{\text{MDO}} - O_{\text{LNG}} \right) \left(\pi^{Leave}_{jktm} - \pi^{Finish}_{jktm} \right) \right] \leq M^B_{jm} \beta_{jt1m}, m = 2, ..., |\mathcal{S}_j| \end{aligned} \tag{4.40}$$

$$\begin{aligned} &-\eta_{j1} C^j_{\text{MDO}} + \eta_{jm} C^j_{\text{Dual}} - \sum_{k \in \mathcal{P}'_j} \left[O_{\text{MDO}} L_{jk} \left(\tilde{g}^{j1}_{\text{MDO}} - Q \tilde{g}^{jm}_{\text{LNG}} \right) \right. \\ &\left. + \left(Q O_{\text{MDO}} - O_{\text{LNG}} \right) \left(\pi^{Leave}_{jktm} - \pi^{Finish}_{jktm} \right) \right] \leq M^B_{jm} \left(1 - \beta_{jt1m} \right), m = 2, ..., |\mathcal{S}_j| \end{aligned} \tag{4.41}$$

$$\begin{aligned} &\left(\eta_{js} - \eta_{jm} \right) C^j_{\text{Dual}} + O_{\text{MDO}} Q \sum_{k \in \mathcal{P}'_j} L_{jk} \left(\tilde{g}^{js}_{\text{LNG}} - \tilde{g}^{jm}_{\text{LNG}} \right) \\ &+ \left(O_{\text{LNG}} - O_{\text{MDO}} Q \right) \sum_{k \in \mathcal{P}'_j} \left[\left(\pi^{Leave}_{jkts} - \pi^{Finish}_{jkts} \right) - \left(\pi^{Finish}_{jktm} - \pi^{Finish}_{jktm} \right) \right] \leq M^B_{jm} \beta_{jtsm} \\ &\forall j \in \mathcal{P}'_j, t = 1, ..., T, s = 2, ..., |\mathcal{S}_j| - 1, m = s+1, ..., |\mathcal{S}_j| \end{aligned} \tag{4.42}$$

$$\begin{aligned} &\left(\eta_{jm} - \eta_{js} \right) C^j_{\text{Dual}} - O_{\text{MDO}} Q \sum_{k \in \mathcal{P}'_j} L_{jk} \left(\tilde{g}^{js}_{\text{LNG}} - \tilde{g}^{jm}_{\text{LNG}} \right) \\ &- \left(O_{\text{LNG}} - O_{\text{MDO}} Q \right) \sum_{k \in \mathcal{P}'_j} \left[\left(\pi^{Leave}_{jkts} - \pi^{Finish}_{jkts} \right) - \left(\pi^{Finish}_{jktm} - \pi^{Finish}_{jktm} \right) \right] \leq M^B_{jm} \left(1 - \beta_{jtsm} \right) \\ &\forall j \in \mathcal{P}'_j, t = 1, ..., T, s = 2, ..., |\mathcal{S}_j| - 1, m = s+1, ..., |\mathcal{S}_j|. \end{aligned} \tag{4.43}$$

Constraints (4.35) calculate the emission cost of route j at period t of candidate solution s. Constraints (4.36)–(4.39) construct the matrix indicating the choice of ship route $j, j \in \mathcal{R}$ at period $t, t = 1, ..., T$, and requiring that the solution with the lowest cost will be adopted. An example of such a matrix is shown as follows:

$$matrix_{jt} = \begin{bmatrix} 0 & 0 & 0 \\ 1 & 0 & 1 \\ 1 & 0 & 0 \end{bmatrix}_{m \times s.} \tag{4.44}$$

From 4.44 we can see that at period t, route j should choose the second solution, because no other solution is more economical. Constraints (4.40)–(4.43) indicate that candidate solution s is more preferable than solution m when the operating cost of solution s is lower than the cost of solution m.

After the model conversion, the problem can be described as the single level model $[MGS]$, which is still nonlinear. The linearization of constraints (4.35), as shown in Appendix C, is similar to that of constraints (4.25). Then, the model becomes a mix integer linear programming model $[MGSL]$, and can be solved by an off-the-shelf CPLEX solver.

4.4 Numerical Experiments

The algorithm is programmed in C++ with Visual Studio 2019, and we used CPLEX 12.10 to solve $[MGSL]$. Multiple numerical experiments were conducted to validate the model and the algorithm. Computational experiments were conducted on a HP ENVY x360 Convertible 15-dr1xx laptop with i7-10510U CPU, 2.30 GHz processing speed and 16 GB of memory.

4.4.1 Parameter settings

Data from previous studies and technical reports were collected and used in the numerical experiments. Consider the stringent quality restrictions on bunker fuels used by vessels in inland river areas, e.g., the Law of the People's Republic of China on the Prevention and Control of Atmospheric Pollution (The National People's Congress of the People's Republic of China 2018) regulates that ships sailing along China's inland rivers must use regular diesel oil available on the market, which contains no more than 0.005% sulfur, we assume traditional ships consume diesel that contains 0.005% sulfur in mass. The emission cost of LNG and MDO are estimated as the weighted average of environmental damage of main pollutants in ship emissions. which include SO_X, NO_X, CO_2, and $PM_{2.5}$. More than 99% of ship emissions consist of these four pollutants, which have been proved to be harmful to social welfare. The IMO has released the Fourth Greenhouse Gas Study (Faber et al. 2020) and concluded that a traditional ship will emit 0.0001 ton of SO_X, 0.167 ton of NO_X, 3.206 tons of CO_2, and 0.00203 ton of $PM_{2.5}$ while consuming one ton of regular diesel, meanwhile a dual-fueled ship will emit 3.17×10^{-5} ton of SO_X, 0.0466 ton of NO_X, 2.75 tons of CO_2, and 1.26×10^{-4} ton of $PM_{2.5}$ while consuming one ton of LNG. Ivestigations of Nunes et al. (2019) and Song (2014) summarized that the social costs associated with these four main components of ships emissions, namely SO_X, NO_X, CO_2, and $PM_{2.5}$ are 11,123 USD/ton, 6,282 USD/ton, 33 USD/ton, and 61,179 USD/ton, respectively. As a result, we obtained $E_{\text{MDO}} = 1,280.31$ USD/ton, $E_{\text{LNG}} = 391.43$ USD/ton. Considering the marine fuel market fluctuations, the bunkering price of regular diesel is set at 950 USD/ton and the bunkering price of LNG, $\hat{U}_{\text{LNG}}$, is about 800 USD/ton. Therefore, $\Delta_U = 321$ USD/ton. The LNG purchasing cost of bunkering stations is around 500 USD/ton.

To numerically validate the model and solution method proposed in this chapter, we generated a port set of 10 ports, a route set of 25 routes, and consider a 5 period construction plan with $1,800,000$ USD budget per year. According to the International Maritime Organization (2016), the annualized construction cost of an LNG bunkering station is about $650,000$ USD. On this basis, we randomly generated the values of $C_i^{\mathcal{P}}$, $i \in \mathcal{P}$, between $520,000$ USD $(= 0.8 \times 650,000)$ and $780,000$ USD $(= 1.2 \times 650,000)$.

For ship route operators, the ship chartering cost and maintenance cost is randomly generated between $54,000\,(= 0.9 \times 60,000)$ to $66,000\,(= 1.1 \times 60,000)$ USD per week for traditional ships, and for each route, dual-fueled ships have the cost 1.3 times (between $70,200$ to $85,800$ USD per week) of traditional ships'. The LNG tank capacity of dual-fueled ships for route j ranges from 60 to 80 m^3, namely 25.56 to 34.08 tons. As mentioned in Subsection 4.3.1, the value of a_j and b_j are randomly generated between 0.004 to 0.006 and between 1.9 to 2.0. The fuel consumption rate at berth is between $0.01215\,(= 0.9 \times 0.0135)$ to $0.01485\,(= 1.1 \times 0.0135)$ tons per hour of LNG, and the regular diesel consumption rate ${g'}^j_{\text{MDO}} = Q{g'}^j_{\text{LNG}}$. The lower bound of sailing speed $\underline{\mu_j}$ of route $j, j \in \mathcal{R}$ is set at 2 knots, while the upper limit is related to the ports the route covers. Consider that the upstream of a inland river tends to be narrower, we set $\overline{\mu_j} = 22$ knots if $U_j \leq 8$, $\overline{\mu_j} = 20$ knots if $U_j = 8$, and $\overline{\mu_j} = 16$ knots if $U_j = 9, 10$. Considering the small capacity of container ships sailing along the inland river, the berthing time at each port varies from two to five hours.

4.4.2 Results and Analysis

Based on the parameters collected, a numerical experiment was conducted. At the potential optimal solution reduction stage, the number of solutions for different routes has been reduced from up to 8 to no more than 4. This reduction obviously improve the solution speed. For comparison, we also design a greedy algorithm to solve the bilevel problem. Decisions in period 1 to period T were made sequentially, and the goal of each period is to cover as much as new port of calls. For period $t, t = 1, ..., T$, the following model was solved.

Parameters

$\bar{y}_{ti}$ integer parameter, equal to 0 if y_{ti} is fixed to be equal to 0, 1 if y_{ti} is fixed to be equal to 1, $t = 1, ...T, \forall i \in \mathcal{P}$;

$$[\boldsymbol{MG_t}] \quad \underset{\vec{y}_t}{\text{maximize}} \sum_{i \in \mathcal{P}} y_{ti} \sum_{j \in \mathcal{R}} \sum_{k \in \mathcal{P}'_j} T_{jki} \tag{4.45}$$

subject to

$$\sum_{t'=1}^{t-1} \bar{y}_{t'i} + y_{ti} \leq 1, \forall i \in \mathcal{P} \tag{4.46}$$

$$(4.2), (4.6).$$

As shown in Algorithm 2, we can get a upper bound of a node by solving $[MG_t]$ for $t = 1, ..., T$ sequentially.

Then, by solving $[MGSL]$, we obtained the optimal solution. Although the scale of $[MGSL]$ is relatively large, CPLEX solves the model in $2,000$ seconds. Optimal ship emission costs and LNG bunkering station construction plan of the two methods are listed in Table 4.1.

The result shows that the optimal plan is to construct the LNG bunkering station

Algorithm 2 Greedy algorithm for upper bound at a node

Input: $\bar{C}_P^i$, T_{jkt}, and $\bar{y}_t i$.
Output: EmG, the ship emission cost through the planning period.
1: Initialization: initial variables $UpE = 0$, $\bar{y}_{ti} = 0$, $t = 1, ..., T, i \in \mathcal{P}$, initial solution $EmG = 0$.
2: **for** $t = 1$ to T **do**
3: Solve $[MG_t]$
4: Update $\bar{y}_{ti} = 0, \forall(t,i) \in \{(t,i)\,|y_{ti} = 0\}, \bar{y}_{ti} = 1, \forall(t,i) \in \{(t,i)\,|y_{ti} = 1\}$
5: Solve $\left[MR'_j\right], \forall j \in \mathcal{R}$
6: Update EmG
7: **end for**
8: **return** $\bar{y}_{ti}$ and EmG.

Table 4.1: Optimal solutions of $[MGSL]$ and greedy method

Method	Constructed stations p1	p2	p3	p4	p5	Ship emission cost (USD)	gap
$[MGSL]$	p6, p7	p2, p4, p8	p5, p9	p1, p3	p10	$833,799,200$	NA
Greedy method	p4, p5, p8	p6, p7	p3, p9	p1, p3	p10	$987,859,600$	15.6%

of port 6, port 7 at period 1, port 2, port 4, and port 8, at period 2, port 5, port 9 at period 3, port 1, port 3 at period 4, and port 10 at period 5, and a total emission cost of $833,799,200$ USD can be achieved in the whole planning. Meanwhile, the total ship emission cost of $987,859,600$ USD can be achieved by applying Algorithm 2, and the greedy method suggests to construct the LNG bunkering station of port 4, port 5, and port 8 at period 1, port 6, port 7 at period 2, port 3, port 9 at period 3, port 1, port 2 at period 4, and port 10 at period 5. Comparing the two results, $[MGSL]$ yields a superior solution than the greedy method, and the gap reaches up to 15.6%.

To show how ship route operators react to the LNG bunkering station, the candidate solutions that different routes adopt at each period are listed in Table 4.2.

As suggested by Table 4.2, compared with the greedy method, $[MGSL]$ better considers the reaction of ship route operators, namely the lower level of the problem, and that is the reason why it can reduce an extra amount of ship emission than the greedy method.

Table 4.2: Solutions adopted at different periods

Route	[$MGSL$]					Greedy method				
	p1	p2	p3	p4	p5	p1	p2	p3	p4	p5
r1	0	2	3	3	3	0	0	0	3	3
r2	0	0	2	2	2	0	0	0	2	2
r3	0	0	2	2	2	0	0	2	2	2
r4	0	0	2	2	2	0	0	0	2	2
r5	0	2	2	2	2	0	2	2	2	2
r6	0	0	2	2	2	0	0	0	2	2
r7	0	2	2	2	2	0	0	2	2	2
r8	0	2	2	2	2	0	0	2	2	2
r9	0	2	2	2	2	0	0	0	2	2
r10	0	0	0	2	2	0	0	0	2	2
r11	0	2	2	2	2	0	2	2	2	2
r12	0	0	0	1	1	0	0	0	1	1
r13	0	2	2	2	2	0	0	0	2	2
r14	0	2	2	2	2	0	0	0	2	2
r15	0	2	2	2	2	0	0	0	2	2
r16	0	0	2	2	2	0	0	0	2	2
r17	0	0	2	2	2	0	0	0	2	2
r18	0	0	0	2	2	0	0	0	2	2
r19	0	0	1	1	1	0	0	0	1	1
r20	0	0	2	2	2	0	0	2	2	2
r21	0	0	2	2	2	0	0	0	2	2
r22	0	0	2	2	2	0	2	2	2	2
r23	0	0	2	2	2	0	0	0	2	2
r24	0	2	2	2	2	0	0	0	2	2
r25	0	2	2	2	2	0	0	0	2	2

4.5 Conclusions

Ship emission has become one of the main concerns of maritime transportation and study on approaches to ship emission reduction attracts a lot of attention from both academia and industry. Compared with traditional ships that consume MDO, LNG-fueled ships that can be switch between MDO and LNG for fuel have much lower ship emission level. Due to the limited LNG bunker volume, a complete LNG bunkering system is indispensable for promoting the application of dual-fueled ships. Given the annual budget, the LNG bunkering stations have to be constructed through a planning period of several years, and construction sequence influences the ship emission in the planning period. In this chapter, considering the ship route operations including the ship type, ship number and sailing speed, we investigate the LNG bunkering station deployment problem and determine the construction sequence.

A bilevel programming model was built to describe the problem. To solve the problem, we proposed a two-stage solution method, which reduces the number of potential optimal solution for each route in the first, and then use a matrix to handle the bilevel structure in the second stage. After the conversion, the problem became a mixed integer linear problem and was solved by CPLEX. To demonstrate the necessity of the study and validate the model and solution method presented, numerical experiments for the two-stage method with $[MGSL]$ and a greedy method were conducted and analyzed. The comparison shows that the two-stage method with $[MGSL]$ can reduce another 15.6% ship emission costs in the planning period. The two-stage method with $[MGSL]$ is superior to the greedy method because it considers the ship route operations at different periods simultaneously, while the greedy method focus on each period at a time.

Chapter 5

Summary and Future Research

5.1 Conclusions

This thesis focused on the government act on the promotion of the two emission reduction technologies adopted in maritime transportation: shore power and LNG as marine fuel. The main body of this thesis consists of three parts. The first part considered a port authority that aims to improve the utilization rate of the shore-side shore power system. With such target, the port decides to provide a favorable shore power price and subsidy for each time shore power is used. Given the shore power price and subsidy amount, ship operators decide whether to use shore power or not. With the help of historical data of ship visits, we made an closer approximation of ship visits in a coming year than previous studies. Faced with the great number of scenarios of ship visits in a year, we reformulated the model and made the model tractable by taking advantage of knowledge of mathematical statistics and binomial distributions. Summarizing the results of extensive numerical experiments, we have come up with useful managerial insights for port authorities to maximize their net benefits, which equals the environmental benefits achieved by the using of shore power and the subsidy expenditure.

The second part investigated the government subsidy plan optimization for LNG as marine fuel. In this part, considering that a complete LNG bunkering system and plenty of LNG-fueled ships are indispensable for achieving an obvious ship emission reduction through using LNG as marine fuel, the government decides to provide subsidies for both parties. In specific, part of the LNG bunkering station construction cost and the ship retrofitting cost will be covered by the government in the form of subsidies. To balance between the subsidy expenditure and the environmental benefits of emission reduction, the subsidy rates need to be set wisely. A trilevel model was developed to describe the problem and capture the interrelationships between decisions of different parties. On the basis of the special problem structure, the bilevel problem that consists of the port level and ship level was converted into an equivalent single-level problem. Then the optimal subsidy rates were identified by an enumeration algorithm. Comparisons between numerical experiments under different subsidy rates show the sophisticated relationship between subsidy expenditure and environmental benefits. It is also suggested that optimal solution varies with multiple parameters, and the government should make decisions taking the situation it confronts into consideration.

The third part explored the optimal LNG bunkering station deployment problem, given the ports that needs to be equipped with LNG bunkering stations. Owing to the limited annual budget, the LNG bunkering station construction works have to be done in several years. Therefore, the ship emission volume in the construction period will be influenced by the specific construction sequence. The operational decisions of shipping lines were integrated with decisions on the construction sequence through a bilevel model. We proposed a two-stage method to first reduce the candidate strategies that each shipping line may adopt and then convert the problem into a single-level problem. Comparing the results of the two-stage method and a greedy method, we proved the effectiveness of our model and solution method.

5.2 Future Research

Based on the above studies, there are several future research directions that can be explored.

In the first study, we assumed that the availability at the port does not influence the decision of ship operators on whether to install onboard shore power facilities, and therefore only considered the visits by ships equipped with shore power system. However, in some cases, for example in an inland river area, the subsidy plan of multiple ports may have the ability to influence the decision of ship operators whose vessels stick to the area. The collaborative optimization among ports will explore the impact of such cooperation and obtain the optimal subsidy plan for the port group to further reduce ship emissions in the area.

In the second study, we assumed that all ports are controlled by the same port group and therefore sell LNG to ships at the same price. In practice, different ports act on their own benefits and compete for the share of the LNG bunkering market. In that case, game theory will be applied in the port level to capture the competition among ports. Then a new solution method that can solve the more sophisticated model will be deeded.

The third study demonstrated that the two-stage method we proposed are able to solve cases with 10 ports and 25 routes, which is near to the practical size. However, it might be very time consuming for CPLEX to solve cases larger than that, for instance an inland river area with more ports and more shipping routes operating on it. On the other hand, large problem size may also influence the reliability of the results yielded by the solver. Therefore, future research can try to develop more efficient algorithms to solve the problem in a shorter computational time.

Appendix A

Model Linearization of $[SP]$ in Chapter 3

In the objective function (3.20), there is one nonlinear part, namely the product of $y_j\ \omega_{ji}$. The product of θ_{jk} and π_{jk}^{Finish} in constraints (3.9) and the maximum calculations in constraints (3.10) and (3.11) also need to be linearized. The following variables are introduced to linearize the model.

Decision variables

$\hat{\omega}_{ji}$	variable introduced to linearize the objective function (3.20), $\forall j \in \mathcal{V}, \forall i \in \mathcal{P}$;
γ_{jk}^1	introduced to linearize constraints (3.9), $\forall j \in \mathcal{V}, \forall k \in \mathcal{P}_j'$;
γ_{jk}^2	binary variable introduced to linearize constraints (3.10) and (3.11), $\forall j \in \mathcal{V}, \forall k \in \mathcal{P}_j'$;

To linearize the objective function (3.20), we replace $y_j\theta_{jk}$ with $\hat{\theta}_{jk}$, and replace $y_j\omega_{ji}$ with $\hat{\omega}_{ji}$. Then the objective function can be rewritten as:

$$[\boldsymbol{SP}] \quad \max \sum_{i\in\mathcal{P}} \left[-(1-\alpha_{\mathcal{P}})\, C_i^{\mathcal{P}} x_i + \sum_{j\in\mathcal{V}} \left(\hat{U}_{\text{LNG}} - \tilde{U}_{\text{LNG}} \right) \hat{\omega}_{ji} \right] - \sum_{j\in\mathcal{V}} \hat{M}_j \xi_j \qquad \text{(A.1)}$$

Meanwhile, following constraints should be added:

$$\hat{\omega}_{ji} \leq M_{ji} y_j, \forall i \in \mathcal{P}, \forall j \in \mathcal{V} \tag{A.2}$$

$$\hat{\omega}_{ji} \leq \omega_{ji}, \forall i \in \mathcal{P}, \forall j \in \mathcal{V} \tag{A.3}$$

$$\hat{\omega}_{ji} \geq \omega_{ji} - M_{ji} \left(1 - y_j\right), \forall i \in \mathcal{P}, \forall j \in \mathcal{V} \tag{A.4}$$

$$\hat{\omega}_{ji} \leq M_{ji}, \forall i \in \mathcal{P}, \forall j \in \mathcal{V} \tag{A.5}$$

Constraints (3.9) can be replaced by the following constraints:

$$\pi_{jk}^{Leave} = \pi_{jk}^{Finish} + \theta_{jk} q_j - \gamma_{jk}^1, \forall k \in \mathcal{P}'_j, \forall j \in \mathcal{V} \tag{A.6}$$

$$\gamma_{jk}^1 \leq q_j \theta_{jk}, \forall k \in \mathcal{P}'_j, \forall j \in \mathcal{V} \tag{A.7}$$

$$\pi_{jk}^{Finish} - q_j \left(1 - \theta_{jk}\right) \leq \gamma_{jk}^1, \forall k \in \mathcal{P}'_j, \forall j \in \mathcal{V} \tag{A.8}$$

$$\gamma_{jk}^1 \leq \pi_{jk}^{Finish}, \forall k \in \mathcal{P}'_j, \forall j \in \mathcal{V} \tag{A.9}$$

$$0 \leq \gamma_{jk}^1 \leq q_j, \forall k \in \mathcal{P}'_j, \forall j \in \mathcal{V} \tag{A.10}$$

Constraints (3.10) and (3.11) can be replaced by the following constraints:

$$\pi_{jk}^{Finish} \geq 0, \forall k \in \mathcal{P}'_j, \forall j \in \mathcal{V} \tag{A.11}$$

$$\begin{gathered} \pi_{jk}^{Finish} \leq \pi_{j,k-1}^{Leave} - L_{j,k-1} R_{\text{LNG}}^j - m_{jk} R_{\text{LNG}}'^j + M_{jk} \left(1 - \gamma_{jk}^2\right) \\ k = 2, 3, ..., \left|\mathcal{P}'_j\right|, \forall j \in \mathcal{V} \end{gathered} \tag{A.12}$$

$$\pi_{j1}^{Finish} \leq \pi_{j,\left|\mathcal{P}'_j\right|}^{Leave} - L_{j,\left|\mathcal{P}'_j\right|} R_{\text{LNG}}^j - m_{j1} R_{\text{LNG}}'^j + M_{j1} \left(1 - \gamma_{j1}^2\right), \forall j \in \mathcal{V} \tag{A.13}$$

$$\pi_{jk}^{Finish} \leq M_{jk} \gamma_{jk}^2, \forall k \in \mathcal{P}'_j, \forall j \in \mathcal{V} \tag{A.14}$$

$$\begin{gathered} \pi_{jk}^{Finish} \geq \pi_{j,k-1}^{Leave} - L_{j,k-1} R_{\text{LNG}}^j - m_{jk} R_{\text{LNG}}'^j - M_{jk} \left(1 - \gamma_{jk}^2\right) \\ k = 2, 3, ..., \left|\mathcal{P}'_j\right|, \forall j \in \mathcal{V} \end{gathered} \tag{A.15}$$

$$\pi_{j1}^{Finish} \geq \pi_{j,\left|\mathcal{P}'_j\right|}^{Leave} - L_{j,\left|\mathcal{P}'_j\right|} R_{\text{LNG}}^j - m_{j1} R_{\text{LNG}}'^j - M_{j1} \left(1 - \gamma_{j1}^2\right), \forall j \in \mathcal{V} \tag{A.16}$$

$$\begin{gathered} \pi_{j,k-1}^{Leave} - L_{j,k-1} R_{\text{LNG}}^j - m_{jk} R_{\text{LNG}}'^j \geq -M_{jk} \left(1 - \gamma_{jk}^2\right) \\ k = 2, 3, ..., \left|\mathcal{P}'_j\right|, \forall j \in \mathcal{V} \end{gathered} \tag{A.17}$$

$$\pi_{j,\left|\mathcal{P}'_j\right|}^{Leave} - L_{j,\left|\mathcal{P}'_j\right|} R_{\text{LNG}}^{j} - m_{j1} R_{\text{LNG}}'^{j} \geq -M_{j1}\left(1-\gamma_{j1}^{2}\right), \forall j \in \mathcal{V} \tag{A.18}$$

$$\pi_{j,k-1}^{Leave} - L_{j,k-1} R_{\text{LNG}}^{j} - m_{jk} R_{\text{LNG}}'^{j} \leq M_{jk}\gamma_{jk}^{2}, k = 2, 3, ..., \left|\mathcal{P}'_j\right|, \forall j \in \mathcal{V} \tag{A.19}$$

$$\pi_{j,\left|\mathcal{P}'_j\right|}^{Leave} - L_{j,\left|\mathcal{P}'_j\right|} R_{\text{LNG}}^{j} - m_{j1} R_{\text{LNG}}'^{j} \leq M_{j1}\gamma_{j1}^{2}, \forall j \in \mathcal{V} \tag{A.20}$$

$$\gamma_{jk}^{2} = 0, 1, \forall k \in \mathcal{P}'_j, \forall j \in \mathcal{V}. \tag{A.21}$$

In these constraints, $M_{jk}, j \in \mathcal{V}, k \in \mathcal{P}'_j$ are numbers that are large enough, and the specific values are as follows.

Parameters

M_{jk}	parameter used in constraints (A.15), equals $q_j + L_{j,k-1} R_{\text{LNG}}^{j} + m_{jk} R_{\text{LNG}}'^{j}, \forall j \in \mathcal{V}, k = 2, 3, ..., \left|\mathcal{P}'_j\right|$;
M_{j1}	parameter used in constraints (A.16), equals $q_j + L_{j,\left|\mathcal{P}'_j\right|} R_{\text{LNG}}^{j} + m_{j1} R_{\text{LNG}}'^{j}, \forall j \in \mathcal{V}$.

Appendix B

Model Linearization of $\left[MR'_j\right]$ in Chapter 4

In constraints (4.25) the product of θ_{jkt} and π_{jkt}^{Finish} is nonlinear and it can be replaced by $\hat{\pi}_{jkt}^{Finish}$. Meanwhile, the following constraints should be added.

$$\hat{\pi}_{jkt}^{Finish} \leq M_{jk}\theta_{jkt}, \forall j \in \mathcal{R}, \forall k \in \mathcal{P'}_j, t = 1, ..., T \tag{B.1}$$

$$\hat{\pi}_{jkt}^{Finish} \leq \pi_{jkt}^{Finish}, \forall j \in \mathcal{R}, \forall k \in \mathcal{P'}_j, t = 1, ..., T \tag{B.2}$$

$$\hat{\pi}_{jkt}^{Finish} \geq \pi_{jkt}^{Finish} - M_{jk}\left(1 - \theta_{jkt}\right), \forall j \in \mathcal{R}, \forall k \in \mathcal{P'}_j, t = 1, ..., T \tag{B.3}$$

$$\hat{\pi}_{jkt}^{Finish} \leq M_{jk}, \forall j \in \mathcal{R}, \forall k \in \mathcal{P'}_j, t = 1, ..., T \tag{B.4}$$

In these constraints, $\hat{\pi}_{jkt}^{Finish}$ is used to replace $\theta_{jkt}\pi_{jkt}^{Finish}$, and M_{jk} is a parameter, the definition of them are listed as follows.

Decision variable

$\hat{\pi}_{jkt}^{Finish}$	variable used to replace $\theta_{jkt}\pi_{jkt}^{Finish}$, $\forall j \in \mathcal{R}, \forall k \in \mathcal{P'}_j, t = 1, ..., T$.

Parameter

M_{jk}	the upper limit of π_{jkt}^{Finish}, equal to $W_j + L_{j,k-1}\tilde{g}_{\mathrm{LNG}}^{j2} + m_{jk}{g'}_{\mathrm{LNG}}^{j}$, $\forall j \in \mathcal{R}, k = 2, ..., \lvert\mathcal{P'}_j\rvert$;
M_{j1}	the upper limit of π_{j1t}^{Finish}, equal to $W_j + L_{j,\lvert\mathcal{P'}_j\rvert}\tilde{g}_{\mathrm{LNG}}^{j2} + m_{j1}{g'}_{\mathrm{LNG}}^{j}$, $\forall j \in \mathcal{R}$.

Constraints (4.26) and (4.27) can be replaced by the following constraints:

$$\pi_{jks}^{Finish} \geq 0, \forall k \in \mathcal{P}'_j, s = 2, ..., |\mathcal{S}_j| \tag{B.5}$$

$$\pi_{jks}^{Finish} \leq \pi_{j,k-1,s}^{Leave} - L_{j,k-1}\tilde{g}_{\text{LNG}}^{js} - m_{jk}{g'}_{\text{LNG}}^{j} + M_{jks}\left(1 - \gamma_{jks}^{1}\right)$$
$$k = 2, 3, ..., \left|\mathcal{P}'_j\right|, s = 2, ..., |\mathcal{S}_j| \tag{B.6}$$

$$\pi_{j1s}^{Finish} \leq \pi_{j\left|\mathcal{P}'_j\right|s}^{Leave} - L_{j\left|\mathcal{P}'_j\right|}\tilde{g}_{\text{LNG}}^{js} - m_{j1}{g'}_{\text{LNG}}^{j} + M_{j1s}\left(1 - \gamma_{j1s}^{1}\right) s = 2, ..., |\mathcal{S}_j| \tag{B.7}$$

$$\pi_{jks}^{Finish} \leq M_{jks}\gamma_{jks}^{1}, \forall j \in \mathcal{R}, \forall k \in \mathcal{P}'_j, s = 2, ..., |\mathcal{S}_j| \tag{B.8}$$

$$\pi_{jks}^{Finish} \geq \pi_{j,k-1,s}^{Leave} - L_{j,k-1}\tilde{g}_{\text{LNG}}^{js} - m_{jk}{g'}_{\text{LNG}}^{j} - M_{jks}\left(1 - \gamma_{jks}^{1}\right)$$
$$\forall j \in \mathcal{R}, k = 2, 3, ..., \left|\mathcal{P}'_j\right|, s = 2, ..., |\mathcal{S}_j| \tag{B.9}$$

$$\pi_{j1s}^{Finish} \geq \pi_{j\left|\mathcal{P}'_j\right|s}^{Leave} - L_{j\left|\mathcal{P}'_j\right|}\tilde{g}_{\text{LNG}}^{js} - m_{j1}{g'}_{\text{LNG}}^{j} - M_{j1s}\left(1 - \gamma_{j1s}^{1}\right)$$
$$\forall j \in \mathcal{R}, s = 2, ..., |\mathcal{S}_j| \tag{B.10}$$

$$\pi_{j,k-1,s}^{Leave} - L_{j,k-1}\tilde{g}_{\text{LNG}}^{js} - m_{jk}{g'}_{\text{LNG}}^{j} \geq -M_{jks}\left(1 - \gamma_{jks}^{1}\right)$$
$$\forall j \in \mathcal{R}, k = 2, 3, ..., \left|\mathcal{P}'_j\right|, s = 2, ..., |\mathcal{S}_j| \tag{B.11}$$

$$\pi_{j\left|\mathcal{P}'_j\right|s}^{Leave} - L_{j\left|\mathcal{P}'_j\right|}\tilde{g}_{\text{LNG}}^{js} - m_{j1}{g'}_{\text{LNG}}^{j} \geq -M_{j1s}\left(1 - \gamma_{j1s}^{1}\right), \forall j \in \mathcal{R}, s = 2, ..., |\mathcal{S}_j| \tag{B.12}$$

$$\pi_{j,k-1,s}^{Leave} - L_{j,k-1}\tilde{g}_{\text{LNG}}^{js} - m_{jk}{g'}_{\text{LNG}}^{j} \leq M_{jks}\gamma_{jks}^{1}$$
$$\forall j \in \mathcal{R}, k = 2, 3, ..., \left|\mathcal{P}'_j\right|, s = 2, ..., |\mathcal{S}_j| \tag{B.13}$$

$$\pi_{j\left|\mathcal{P}'_j\right|s}^{Leave} - L_{j\left|\mathcal{P}'_j\right|}\tilde{g}_{\text{LNG}}^{js} - m_{j1}{g'}_{\text{LNG}}^{j} \leq M_{j1s}\gamma_{j1s}^{1}, \forall j \in \mathcal{R}, s = 2, ..., |\mathcal{S}_j| \tag{B.14}$$

$$\gamma_{jks}^{1} = 0, 1, \forall k \in \mathcal{P}'_j, \forall j \in \mathcal{R}, s = 2, ..., |\mathcal{S}_j|. \tag{B.15}$$

In these constraints, γ_{jks}^{1} is a binary variable and M_{jks} is a parameter, the definition of them are listed as follows.

Binary variable

γ_{jks}^{1} binary variable, equal to 1 if $\pi_{j,k-1,s}^{Leave} - L_{j,k-1}\tilde{g}_{\text{LNG}}^{js} - m_{jk}{g'}_{\text{LNG}}^{j} > 0$, 0 otherwise, $\forall j \in \mathcal{V}, s = 2, 3, ..., |\mathcal{S}_j|, \forall k \in \mathcal{P'}_j$;

Parameters

M_{jks} equal to $W_j + L_{j,k-1}\tilde{g}_{\text{LNG}}^{js} + m_{jk}{g'}_{\text{LNG}}^{j}, \forall j \in \mathcal{V}, k = 2, 3, ..., \left|\mathcal{P}'_j\right|, s = 2, 3, ..., |\mathcal{S}_j|$;

M_{j1s} equal to $W_j + L_{j|\mathcal{P}'_j|}\tilde{g}^{js}_{\mathrm{LNG}} + m_{j1}{g'}^{j}_{\mathrm{LNG}}, \forall j \in \mathcal{V}, s = 2, 3, ..., |\mathcal{S}_j|$.

Appendix C

Model Linearization of $[MGS]$ in Chapter 4

In constraints (4.36) the product of α_{jts} and $\sum_{k\in\mathcal{P'}_j}(E_{\text{LNG}} - QE_{\text{MDO}})\left(\pi_{jkts}^{Leave} - \pi_{jkts}^{Finish}\right) + QE_{\text{MDO}}\left(L_{jk}\tilde{g}_{LNG}^{js} + m_{jk}{g'}_{\text{LNG}}^{j}\right)$ is nonlinear and constraints (4.36) can be replaced by the following linear constraints.

$$Em_{jts} \leq M_{js}^{E}\alpha_{jts}, \forall j \in \mathcal{R}, t = 1, ..., T, s = 2, ..., |\mathcal{S}_j| \tag{C.1}$$

$$Em_{jts} \leq \sum_{k\in\mathcal{P'}_j}(E_{\text{LNG}} - QE_{\text{MDO}})\left(\pi_{jkts}^{Leave} - \pi_{jkts}^{Finish}\right) + QE_{\text{MDO}}\left(L_{jk}\tilde{g}_{LNG}^{js} + m_{jk}{g'}_{\text{LNG}}^{j}\right)$$
$$\forall j \in \mathcal{R}, t = 1, ..., T, s = 2, ..., |\mathcal{S}_j| \tag{C.2}$$

$$Em_{jts} \geq \forall j \in \mathcal{R}, t = 1, ..., T, s = 2, ..., |\mathcal{S}_j| - M_{js}^{E}(1 - \alpha_{jts})$$
$$\forall j \in \mathcal{R}, \forall j \in \mathcal{R}, t = 1, ..., T, s = 2, ..., |\mathcal{S}_j| \tag{C.3}$$

$$Em_{jts} \leq M_{js}^{E}, \forall j \in \mathcal{R}, t = 1, ..., T, s = 2, ..., |\mathcal{S}_j|. \tag{C.4}$$

In these constraints, M_{js}^{E} is a parameter, the value of them are listed as follows.

Parameter

M_{js}^{E} the upper limit of Em_{jts}, equal to $QE_{MDO}\sum_{k\in\mathcal{P'}_j} L_{jk}tildeg_{\text{LNG}}^{js} + m_{jk}{g'}_{\text{LNG}}^{j}$, $\forall j \in \mathcal{R}, s = 2, ..., |\mathcal{S}_j|$;

References

Acciaro, M., 2014. Real option analysis for environmental compliance: LNG and emission control areas. Transportation Research Part D 28, 41–50.

Altosole, M., Campora, U., Savio, S., 2018. Improvements of the ship energy efficiency by a steam powered turbogenerator in LNG propulsion applications. 2018 International Symposium on Power Electronics, Electrical Drives, Automation and Motion, IEEE , 449–455.

Aneziris, O., Koromila, I., Nivolianitou, Z., 2020. A systematic literature review on LNG safety at ports. Safety Science 124, 104595.

Ballini, F., Bozzo, R., 2015. Air pollution from ships in ports: The socio-economic benefit of cold-ironing technology. Research in Transportation Business & Management 17, 92–98.

California Air Resources Board, 2020. Final regulation order airborne toxic control measure for auxiliary diesel engines operated on ocean-going vessels at berth in a California port. URL: https://ww3.arb.ca.gov/ports/shorepower/finalregulation.pdf.

Chen, J., Zheng, T., Garg, A., Xu, L., Li, S., Fei, Y., 2019. Alternative maritime power application as a green port strategy: Barriers in China. Journal of Cleaner Production 213, 825–837.

CMA CGM Group, 2020. The CMA CGM JACQUES SAADE, the world's first 23,000 TEU powered by LNG. URL: https://cmacgm-group.com/en/launching-cmacgm-jacques-saad%25C3%25A9-world%2527s-first-ultra-large-vessel-powered-by-lng.

Commission, E., 2021. Air emissions from maritime transport. URL: https://ec.europa.eu/environment/air/sources/maritime.htm.

Cooper, D., Gustafsson, T., 2004. Methodology for calculating emissions from ships: 1. update of emission factors. URL: https://www.diva-portal.org/smash/get/diva2:1117198/FULLTEXT01.pdf.

Dai, L., Hu, H., Wang, Z., Shi, Y., Ding, W., 2019. An environmental and techno-economic analysis of shore side electricity. Transportation Research Part D 75, 223–235.

Deng, J., Wang, X., Wei, z., Wang, L., Wang, C., Chen, Z., 2021. A review of nox and sox emission reduction technologies for marine diesel engines and the potential evaluation of liquefied natural gas fuelled vessels. Science of the Total Environment 766, 144319.

Department of Transport, 2019. Clean maritime plan. URL: https://assets.publishing.service.gov.uk/government/uploads/system/uploads/attachment_data/file/815664/clean-maritime-plan.pdf.

European Commission, 2002. Quantification of emissions from ships associated with ship movements between ports in the European Community. URL: https://ec.europa.eu/environment/air/pdf/chapter1_ship_emissions.pdf.

European Commission, 2019. Energy tax report. URL: https://ec.europa.eu/taxation_customs/sites/taxation/files/energy-tax-report-2019.pdf.

European Executive Agency for Competitiveness and Innovation, 2009. Lightening the load - Marco Polo leads the way, office for official publications of the European Communities. URL: http://ec.europa.eu/inea/sites/inea/files/download/MoS/mp_projectbrochure_en_web_final.pdf.

European Union, 2016. Directive (EU) 2016/802 of the European Parliament and of the council of 11 May 2016 relating to a reduction in the sulphur content of certain liquid fuels. URL: https://eur-lex.europa.eu/legal-content/EN/TXT/PDF/?uri=CELEX:32016L0802&from=EN.

Faber, J., Hanayama, S., Zhang, S., Pereda, P., Comer, B., Hauerhof, E., Smith, T., Zhang, Y., Kosaka, H., Adachi, M., Bonello, J.M., 2020. Reduction of GHG emissions from ships: Fourth IMO GHG study 2020–Final report.

Fokkema, J.E., Buijs, P., Vis, I., 2017. An investment appraisal method to compare LNG-fueled and conventional vessels. Transportation Research Part D 56, 229–240.

Freight Waves, 2019. Hapag-Lloyd to retrofit 15,000 TEU ship for LNG. URL: https://www.freightwaves.com/news/hapag-lloyd-to-retrofit-15000-teu-ship-for-lng.

Guan, G., Lin, Y., Chen, Y., 2017. An optimisation design method for cryogenic pipe support layout of LNG-powered ships. Journal of Marine Engineering & Technology 16, 45–50.

Innes, A., Monios, J., 2018. Identifying the unique challenges of installing cold ironing at small and medium ports – The case of Aberdeen. Transportation Research Part D 62, 298–313.

International Maritime Organization, 2012. Guidelines on the method of calculation of the attained energy efficiency design index (EEDI) for new ships, MEPC 63/23, annex 8. URL: http://www.imo.org/en/KnowledgeCentre/IndexofIMOResolutions/Marine-Environment-Protection-Committee-%28MEPC%29/Documents/MEPC.212%2863%29.pdf.

International Maritime Organization, 2013. Prevention of air pollution from ships. URL: http://www.imo.org/en/OurWork/Environment/PollutionPrevention/AirPollution/Pages/Air-Pollution.aspx.

International Maritime Organization, 2016. Studies on the feasibility and use of LNG as a fuel for shipping. URL: http://www.imo.org/en/OurWork/Environment/PollutionPrevention/AirPollution/Documents/LNG%20Study.pdf.

International Maritime Organization, 2018. Sulphur oxides (SOx) and particulate matter (PM)—regulation 14. URL: http://www.imo.org/en/OurWork/Environment/PollutionPrevention/AirPollution/Pages/Sulphur-oxides-(SOx)-\OT1\textendash-Regulation-14.aspx.

International Maritime Organization, 2019. Marine environment. URL: http://www.imo.org/en/OurWork/Environment/Pages/Default.aspx.

International Maritime Organization, 2020. Sulphur 2020–cutting sulphur oxide emissions. URL: https://www.imo.org/en/MediaCentre/HotTopics/Pages/Sulphur-2020.aspx.

Kana, A.A., Harrison, B.M., 2017. A Monte Carlo approach to the ship-centric Markov decision process for analyzing decisions over converting a containership to LNG power. Ocean Engineering 130, 40–48.

Kana, A.A., Knight, J., Sypniewski, M.J., Singer, D.J., 2015. A Markov decision process framework for analyzing LNG as fuel in the face of uncertainty. 12th International Marine Design Conference 2015 .

Ko, J., Gim, T.H.T., Guensler, R., 2017. Locating refuelling stations for alternative fuel vehicles: a review on models and applications. Transport Reviews 37, 551–570.

Li, H., 2019. Benefit analysis of using shore power and low sulfur oil when ships approach port. URL: https://www.wti.ac.cn/zjgd/4288.jhtml.

Lim, S., Kuby, M., . Heuristic algorithms for siting alternative-fuel stations using the Flow-Refueling Location Model. European Journal of Operational Research 204, 51–61.

Lim, T.W., Choi, Y.S., 2020. Thermal design and performance evaluation of a shell-and-tube heat exchanger using LNG cold energy in LNG fuelled ship. Applied Thermal Engineering 171, 115120.

McArthur, D.P., Osland, L., 2013. Ships in a city harbour: An economic valuation of atmospheric emissions. Transportation Research Part D 21, 47–52.

Milioulis, K., Bolbot, V., Theotokatos, G., 2021. Model-based safety analysis and design enhancement of a marine LNG fuel feeding system. Marine Science and Engineering 9, 1–25.

Ministry of Transport of the People's Republic of China, 2017. Guidelines for the application of incentive funds for 2016–2018 shore power projects for berthing ships. URL: http://xxgk.mot.gov.cn/jigou/haishi/201702/t20170228_2979907.html.

Ministry of Transport of the People's Republic of China, 2018. Adjustment plan of ship emission control area. URL: http://xxgk.mot.gov.cn/jigou/haishi/201807/P020180724575874820285.pdf.

New South Wales Environment Protection Authority of Australia, 2015. Transport and environment comments to New South Wales Environment Protection Authority of Australia consultation regarding stricter sulphur fuel requirement for cruise ships in Sydney harbor. URL: https://www.transportenvironment.org/.

Ng, S.K.W., Zheng, A.J., Li, C., Jiamin, O., Fan, X., 2016. Pearl river delta ship emission inventory study technical report en. URL: https://civic-exchange.org/report/pearl-river-delta-ship-emission-inventory-study/.

Nunes, R., Alvim-Ferraz, M., Martins, F., Sousa, S., 2019. Environmental and social valuation of shipping emissions on four ports of Portugal. Journal of Environmental Management 235, 62–69.

Offshore Energy, 2018. EU Parliament supports tax exemption for ships using onshore power supply. URL: https://www.offshore-energy.biz/eu-parliament-supports-tax-exemption-for-ships-using-onshore-power-supply/.

Oxford Institute for Energy Studies, 2018. A review of demand prospects for LNG as a marine transport fuel. URL: https://www.oxfordenergy.org/wpcms/wp-content/uploads/2018/07/A-review-of-demand-prospects-for-LNG-as-a-marine-fuel-NG-133.pdf.

Park, S., Jeong, B., Yoon, J., Paik, K., 2018. A study on factors affecting the safety zone in ship-to-ship LNG bunkering. Ships and Offshore Structures 13, S312–S321.

Peng, Y., Zhao, X., Zuo, T., Wang, W., 2021. A systematic literature review on port LNG bunkering station. Transportation Research Part D 91, 102704.

Qi, J., Wang, S., Peng, C., 2020. Shore power management for maritime transportation: Status and perspectives. Maritime Transport Research 1.

Radwan, M.E., Chen, J., Wan, Z., Zheng, T., Hua, C., Huang, X., 2019. Critical barriers to the introduction of shore power supply for green port development: case of Djibouti container terminals. Clean Technologies and Environmental Policy 21, 1293–1306.

Sascha, S., 2017. The social costs of electricity generation—categorising different types of costs and evaluating their respective relevance. Energies 10, 356.

Schinas, O., Butler, M., 2020. Feasibility and commercial considerations of LNG-fueled ships. Ocean Engineering 122, 84–96.

Sciberras, E.A., Zahawi, B., Atkinson, D., 2015. Electrical characteristics of cold ironing energy supply for berthed ships. Transportation Research Part D 39, 31–43.

Shanghai Government, 2019. Measures for the administration of special funds for pilot subsidy of shore-based power supply for berthing international ships in Shanghai Port. URL: http://www.shanghai.gov.cn/Attach/Attaches/202002/202002041121211315.pdf.

Shenzhen Municipal Committee of Communication, 2019. Detailed rules for the implementation of the interim measures of Shenzhen municipality on the administration of subsidies for the construction of green and low carbon ports. URL: http://jtys.sz.gov.cn/zwgk/xxgkml/zcfgjjd/zcfg/ghjy/201909/t20190902_18190492.htm.

Shenzhen Transportation Commission, 2014. Interim measures of Shenzhen municipality on the administration of subsidies for port, ship shore power facilities and ship low sulfur oil. URL: http://www.gd.gov.cn/zwgk/zcfgk/content/post_2531480.html.

Ship Technology, 2017. Shore-side power: a key role to play in greener shipping. URL: http://www.ship-technology.com/features/featureshore-side-power-a-key-role-to-play-in-greener-shipping-4750332/.

Smith, T., Jalkanen, J., Anderson, B., Corbett, J., Faber, J., Hanayama, S., O'Keeffe, E., Parker, S., Johansson, L., Aldous, L., Raucci, C., Traut, M., Ettinger, S., Nelissen, D., Lee, D., Ng, S., Agrawal, A., Winebrake, J., Hoen, M., Chesworth, S., Pandey, A., 2014. Third international maritime organization greenhouse gas study. URL: http://www.imo.org/en/OurWork/Environment/PollutionPrevention/AirPollution/Documents/Third%20Greenhouse%20Gas%20Study/GHG3%20Executive%20Summary%20and%20Report.pdf.

Sofiev, M., Winebrake, J.J., Johansson, L., Carr, E.W., Prank, M., Soares, J., Vira, J., Kouznetsov, R., Jalkanen, J.P., Corbett, J.J., 2018. Cleaner fuels for ships provide public health benefits with climate tradeoffs. Nature Communications 9, 406.

Song, S., 2014. Ship emissions inventory, social cost and eco-efficiency in Shanghai Yangshan port. Atmospheric Environment 82, 288–297.

Song, T., Li, Y., 2017. Cost-effective optimization analysis of shore-to-ship power system construction and operation. IEEE Conference on Energy Internet and Energy System Integration (EI2) , 1–6.

Starcrest Consulting Group, 2019. Inventory of air emissions for calendar year 2017. URL: https://kentico.portoflosangeles.org/getmedia/0e10199c-173e-4c70-9d1d-c87b9f3738b1/2018_Air_Emissions_Inventory.

Tam, J.H., 2020. Overview of performing shore-to-ship and ship-to-ship compatibility studies for LNG bunker vessels. Journal of Marine Engineering & Technology 19, 1–14.

The Government of Canada, 2017. The shore power technology for ports program (SPTP) has funded the following projects, by province. URL: https://www.tc.gc.ca/en/programs-policies/programs/shore-power-technology-ports-program/sptp-projects.html.

The National People's Congress of the People's Republic of China, 2018. Law of the People's Republic of China on the prevention and control of atmospheric pollution. URL: http://www.npc.gov.cn/npc/sjxflfg/201906/daae57a178344d39985dcfc563cd4b9b.shtml.

UNCTAD, 2019. Review of maritime transport 2019. URL: https://unctad.org/en/PublicationsLibrary/rmt2019_en.pdf.

UNCTAD, 2020. Review of maritime transport 2020. URL: https://unctad.org/system/files/official-document/rmt2020_en.pdf.

Ursavas, E., Zhu, S.X., Savelsbergh, M., 2020. LNG bunkering network design in inland waterways. Transportation Research Part C 120, 102779.

Vaishnav, P., Fischbeck, P.S., Morgan, M.G., Corbett, J.J., 2016. Shore power for vessels calling at U.S. ports: Benefits and costs. Environmental Science & Technology 50, 1102–1110.

Viana, M., Hammingh, P., Colette, A., Querol, X., Degraeuwe, B., Vlieger, I.d., Aardenne, John, v., 2014. Impact of maritime transport emissions on coastal air quality in europe. Atmospheric Environment 90, 96–105.

Wan, C., Yan, X., Zhang, D., Yang, Z., 2019. A novel policy making aid model for the development of LNG fuelled ships. Transportation Research Part A 119, 29–44.

Wang, H., Mao, X., Rutherford, D., 2015. Costs and benefits of shore power at the Port of Shenzhen. URL: https://www.wilsoncenter.org/sites/default/files/costs_and_benefits_of_shore_power_at_the_port_of_shenzhen.pdf.

Wang, S., Meng, Q., 2012. Sailing speed optimization for container ships in a liner shipping network. Transportation Research Part E 48.

Wang, S., Notteboom, T., 2014. The Adoption of Liquefied Natural Gas as a Ship Fuel: A Systematic Review of Perspectives and Challenges. Transport Reviews 34, 749–774.

Winkel, R., Weddige, U., Johnsen, D., Hoen, V., Papaefthimiou, S., 2016. Shore-side electricity in Europe: Potential and environmental benefits. Energy Policy 88, 584–593.

Winkel, R., Weddige, U., Johnsen, D., Hoen, V., Papaefthymiou, G., 2015. Potential for shore-side electricity in Europe. URL: http://www.ecofys.com/files/files/ecofys-2014-potential-for-shore-side-electricity-in-europe.pdf.

Wu, L., Wang, S., 2020. The shore power deployment problem for maritime transportation. Transportation Research Part E 135, 1–12.

Xu, H., Yang, D., 2020. LNG-fuelled container ship sailing on the Arctic Sea: Economic and emission assessment. Transportation Research Part D 87, 102566.

Yoo, B.Y., 2017. Economic assessment of liquefied natural gas (LNG) as a marine fuel for CO_2 carriers compared to marine gas oil (MGO). Energy 121, 772–780.

Ytreberg, E., Astrom, S., Fridell, E., 2021. Valuating environmental impacts from ship emissions–the marine perspective. Journal of Environmental Management 282, 111958.

Zheng, W., Jian, D., Shi, H., 2017. The risk research of inland river LNG filling barge based on Spill simulation. 2017 4th International Conference on Transportation Information and Safety (ICTIS), August 8-10, 2017, Banff, Canada .

Zhuge, D., Wang, S., Zhen, L., Laporte, G., 2019. Schedule design for liner services under vessel speed reduction incentive programs. Naval Research Logistics 67, 45–62.

Zhuge, D., Wang, S., Zhen, L., Laporte, G., 2020. Subsidy design in a vessel speed reduction incentive program under government policies. Naval Research Logistics , 1–15.